Osteoarthritis: the role and mechanisms of the chondroprotective peptide Urocortin I

Omeco Bianco White

School of Life Sciences

OSTEOARTHRITIS: THE ROLE AND MECHANISMS OF THE CHONDROPROTECTIVE PEPTIDE UROCORTIN I

Omeco Bianco White

A thesis submitted in partial fulfilment of the requirements of the University of Westminster for the degree of Doctor of Philosophy

September 2011

AUTHOR'S DECLARATION

I declare that the present work was carried out in accordance with the Guidelines and Regulations of the University of Westminster. The work is original except where indicated by special reference in the text.

The submission as a whole or part is not substantially the same as any that I previously or am currently making, whether in published or unpublished form, for a degree, diploma or similar qualification at any university or similar institution.

Until the outcome of the current application to the University of Westminster is known, the work will not be submitted for any such qualification at another university or similar institution.

Any views expressed in this work are those of the author and in no way represent those of the University of Westminster.

Signed: Date

Abstract

Osteoarthritis (OA), a chronic degenerative condition of the diarthrodial joints is most predominant amongst the middle aged and elderly population, where it is associated with progressive disability and deformity of the joints. Whilst the exact mechanism of OA pathogenesis is currently unknown, chondrocyte death by apoptosis is seen as one of the main contributors to the disease process. It is increasingly recognised that the overproduction of mediators such as Nitric Oxide (NO) in Osteoarthritic cartilage contributes to the disease pathology partly by inducing chondrocyte apoptosis. Therefore, agents, which protect against NO-induced mitochondrial injury, may have therapeutic potential in Osteoarthritis.

The *CRF* related peptide, Urocortin I (UCNI), has been shown to protect the human chondrocyte cell line, C-20/A4, from SNAP/NO induced apoptotic death, but little is yet known about its mechanism of action. Therefore the aim of this project is to investigate the potential mechanism through which *UCNI* exerts its observed protective effects. The studies documented here, have demonstrated the endogenous expression of this cytoprotective peptide, UCNI, by C-20/A4 chondrocytes and have shown that treatment of chondrocytes with SNAP (a NO donor) resulted in a significant increase in apoptosis which was abrogated by the addition of exogenous UCNI. Therefore, an investigation into the potential mechanism for UCNI mediated protection against apoptosis in chondrocytes (i.e. chondroprotection) detected the mRNA expression of both *CRFR1* and *CRFR2* receptors specifically the *CRFR1*α and *CRFR2*β splice variants by the C-20/A4 chondrocytes. However the CRFR antagonist, α–helical CRH failed to induce apoptosis or abrogate the protective effects of UCNI against SNAP/NO induced apoptosis. RT-PCR studies have also demonstrated C-20/A4 mRNA expression of the *Kir6.1*, *Kir6.2*, *SUR1* and *SUR2B* subunits of the K_{ATP} channels suggesting that functional K_{ATP} channels are also present in these cells, which represent a further putative mechanism of action for UCNI.

Quantitative PCR studies were performed to determine regulation of *CRFR* and *Kir6.1* expression by UCNI. These studies showed that treatment of chondrocytes with UCNI and SNAP alone and concurrently resulted in no significant change in mRNA expression of either *CRF* receptors or *kir6.1* (the pore forming subunit of the mitochondrial K_{ATP} channel). Treatment of chondrocytes with Diazoxide, a mitochondrial K_{ATP} channel opener, resulted in a reduction in SNAP induced apoptosis, mimicking that seen for UCNI, suggesting a similar protective role for these channels in chondrocytes, to that proposed in other cell types and supporting these channels as potential targets for UCNI in chondroprotection.

“All things are possible to him that believeth”

St Mark 9:23

Dedication:

For my grandmother and late grandfather (Mrs Gertrude White and Mr Gilbert White), the White Family and Mr Lewis D. Barrett; thank you for always believing in me, with all my love

Acknowledgement

There is so much to be thankful for and so many people to thank for the completion of such an immense achievement. First and foremost thanks to the almighty God - “to him be the Glory”. To my family, who have always been there for me, for believing in me, for your prayers, and endless support along the way. Specifically, my grandmother, Mrs Gertrude White, thank you for investing so much in me; and my aunts Mrs Dorisette White-Harrison and Miss Avis White - your sacrifices were not in vain. I also wish to thank Mr Lewis Barrett, for his continued unconditional love, encouragement and support especially through such a demanding, sometimes stressful and difficult time in my life; thank you for standing by me - I am indebted to you. To my dad, Mr Glenton White and mother Ms Rose Marie Jackson; thank you.

To my supervisory team, Dr Ian Locke (director of studies), Professor Chas Chowdrey and Dr Richard Knight; and also Dr Kevin Lawrence, a huge thank you for all your informed advice, input, direction and support. I thoroughly enjoyed embarking on this PhD opportunity. My sincere thanks also go to Professor Tajali Keshavarz, Dr Martin Parry and Dr Pamela Greenwell for their endless support, encouragement and inspiration. To Dr Miriam Dwek, thanks for the opportunity of undertaking a brief but truly productive job role within cancer research and to Dr Mark Clements for his guidance and help with flow cytometry.

I also wish to extend my gratitude to my friends and colleagues of which there are many, but in particular, Kasia Vossers-Wietsma, Maryam Safari, Dr Daniel Gyamfi, Dr Neela Gaungoo, Karima, Dr Diluka Peirs, Dr Madhuri Shamana, and Dr Shameem Fawdar and many others, without whom this journey would have sometimes been impossible to complete. The technical staff at the University of Westminster (specially Mr Thakor Tandel, Ms Vanita Amin, Ms Kim Storey, Mr Joe Oneill and Mr Glen Wotherspoon), stores department (Sylvia Anani, Ewa Joachimiak and Alrick Stewart), the staff in Research Degrees department (particularly, Mr Mike Fisher and Ms Shila Panchasara) and the security staff at the Cavendish campus all deserve my appreciation; thank you.

Table of Contents

List of Tables

List of figures

List of Abbreviations

α-helical CRH or αhCRH$_{(9-41)}$	alpha- helical corticotrophin releasing hormone$_{(9-41)}$
ADP	adenosine di-phosphate
ANOVA	Analysis of Variance
ΔC_q	Delta C_q
$\Delta\Delta C_q$	Delta delta C_q
AGE	Agarose gel electrophoresis
ATP	adenosine triphosphate
Bak	Bcl-2 Homologous killer
Bax	Bcl-2 associated protein X
Bcl-2	B cell leukaemia/lymphoma 2
Bcl-XL	B cell lymphoma- extra large
Bid	BH3 interacting domain death agonist
bp	base pairs
cAMP	cyclic adenosine monophosphate
C/EBP	CCAAT enhancer-binding protein
Ca^{2+}	calcium
Caspase	Cysteine aspartate protease
cDNA	complementary deoxyribonucleic acid
CLIP	Cartilage intermediate layer protein

CRE	c-AMP responsive Element
CRF	Corticotropin Releasing Factor
CRFR	Corticotropin Releasing Factor Receptor
CRFR1	Corticotropin Releasing Factor Receptor type 1
CRFR2	Corticotropin Releasing Factor Receptor type 2
C_q	quantification cycle
Cyt c	Cytochrome C
DD	Death Domain
DED	Death Effector Domain
DISC	Death Inducing Signalling Complex
DMEM	Dulbecco's Modified Eagles Medium
dNTP's	deoxynucleotide triphosphates
DPBS	Dulbecco's phosphate buffered saline
ECM	extracellular matrix
EDTA	ethylenediaminetetraacetic acid
ER	Endoplasmic Reticulum
FADD	Fas associated Death Domain
Fas-L	Fas- Ligand
FCS	Foetal calf serum
FITC	Fluorescein isothiocyanate
FSC	forward scatter
GAPDH	Glyceraldehyde-3-phosphate dehydrogenase
GOI	gene of Interest

GPCR	G-Coupled Protein Receptor
IL-1β	Interleukin 1- beta
K^+	potassium
K_{ATP}	ATP sensitive potassium channel
Kir	Inwardly rectifying potassium
LDH	Lactate Dehydrogenase
M	molar
MAPK	Mitogen Activated Protein kinases
Mg^{2+}	magnesium
mitoK_{ATP} channel	mitochondrial ATP sensitive potassium channel
ml	millilitre
mRNA	messenger ribonucleic acid
Na^+	sodium
NDB1	Nucleotide binding domain 1
NO	nitric oxide
OA	Osteoarthritis
Oligo-dT	oligo-dexoythymidine
PCD	Programmed Cell Death
PI	Propidium Iodide
PI3	Phosphatidylinositol 3 kinase
PKA	Protein Kinase A
PKC	Protein Kinase C
PT pore	Permeability Transition pore

PS	phosphatidylserine phospholipid
qPCR	quantitative-PCR
RNA	Ribonucleic acid
RT-PCR	Reverse Transcriptase-Polymerase chain reaction
RT-PCR	Reverse Transcriptase-Polymerase chain reaction
RT-qPCR	Reverse transcriptase-qPCR
sarcK_{ATP} channel	Sarcolemmal ATP sensitive potassium channel
SEM	standard error of mean
Smac/Diablo	Second mitochondrial-derived activator of caspase/direct IAP (inhibitory of apoptosis protein) protein binding protein with low pI
SNAP	S-nitroso-N-acetyl-L-penicillamine
SSC	side scatter
SUR	Sulfonylurea receptor
SUR1	Sulfonylurea Receptor type 1
SUR2	Sulfonylurea Receptor type 2
TAE	tris –acetate-EDTA
Taq polymerase	*Thermophilus aquaticus* polymerase
tBid	truncated Bid
TMD1	Transmembrane domain 1
TM6-11	Transmembrane domain segments 6-11
TNFα	Tumour necrosis factor- alpha
TRAIL	Tumour necrosis factor (TNF) –related apoptosis inducing ligand

TUNEL	Terminal deoxynucleotidyl transferase (TdT)-mediated deoxyuridine triphosphate (dUTP) nick end labelling
UCNI	Urocortin I
UCNII	Urocortin II
UCNIII	Urocortin III

Chapter 1: Introduction

1 INTRODUCTION

1.1 Chondrocyte and the Articular cartilage environment

The diarthrodial (synovial) joints are freely movable joints within the skeletal system that permit repetitive movement that is smooth, pain-free and frictionless (Roach *et al*, 2007). These properties are attributed to a thin, whitish layer of connective tissue derived from a hyaline cartilage temple, which covers the interosseous surface known as articular cartilage (figure 1.1A).

Articular cartilage is a connective tissue, devoid of neuronal connections and has no blood or lymphatic vessels (Roach *et al*, 2007; Poole, 1997); it therefore essentially relies on solutes diffusing through the synovial fluid and to and from the underlying subchondral bone for its source of nutrients and oxygen supply, as well as waste exchange(Chubinskaya and Kuettner, 2003; Coimbra *et al*, 2004).
It is composed of a single highly differentiated mesenchymal cell type, the chondrocyte, which is found, embedded in matrix cavities or spaces called lacunae and surrounded by an extensive extracellular matrix (ECM) (Poole, 1997; Lin *et al*, 2006). The nature of these cartilage specific cells and their surrounding ECM, divide the articular cartilage horizontally into four well defined layers or zones namely: tangential (or superficial), transitional (middle or intermediate), radial (or deep), and calcified (Poole, 1997; Chi *et al*, 2004) (figure 1.1B-C).

In each layer, the chondrocytes differ in morphology, distribution, metabolic activity, expression of genes and responsiveness to stimuli (Chi *et al*, 2004; Chubinskaya and Kuettner, 2003). For instance, the chondrocytes located in the tangential layer are flat, disc-shaped cells that are arranged with their long axis parallel to the articular cartilage surface. In the transitional, radial and calcified layers, the chondrocytes are rounded. The cells located in the transitional layer are randomly distributed throughout the ECM. The Deep layer constitutes about 30% of the total cartilage thickness and contains chondrocytes, which are arranged in columns that are oriented perpendicular to the “tidemark” – a demarcation that segregates the upper three cartilage layers (the tangential, transitional and radial) from the calcified layer (figure 1.1.C and D) (Hayes *et al*, 2003; Buckwalter and Mankin, 1998; Poole, 1997).

The joint and structure of articular cartilage

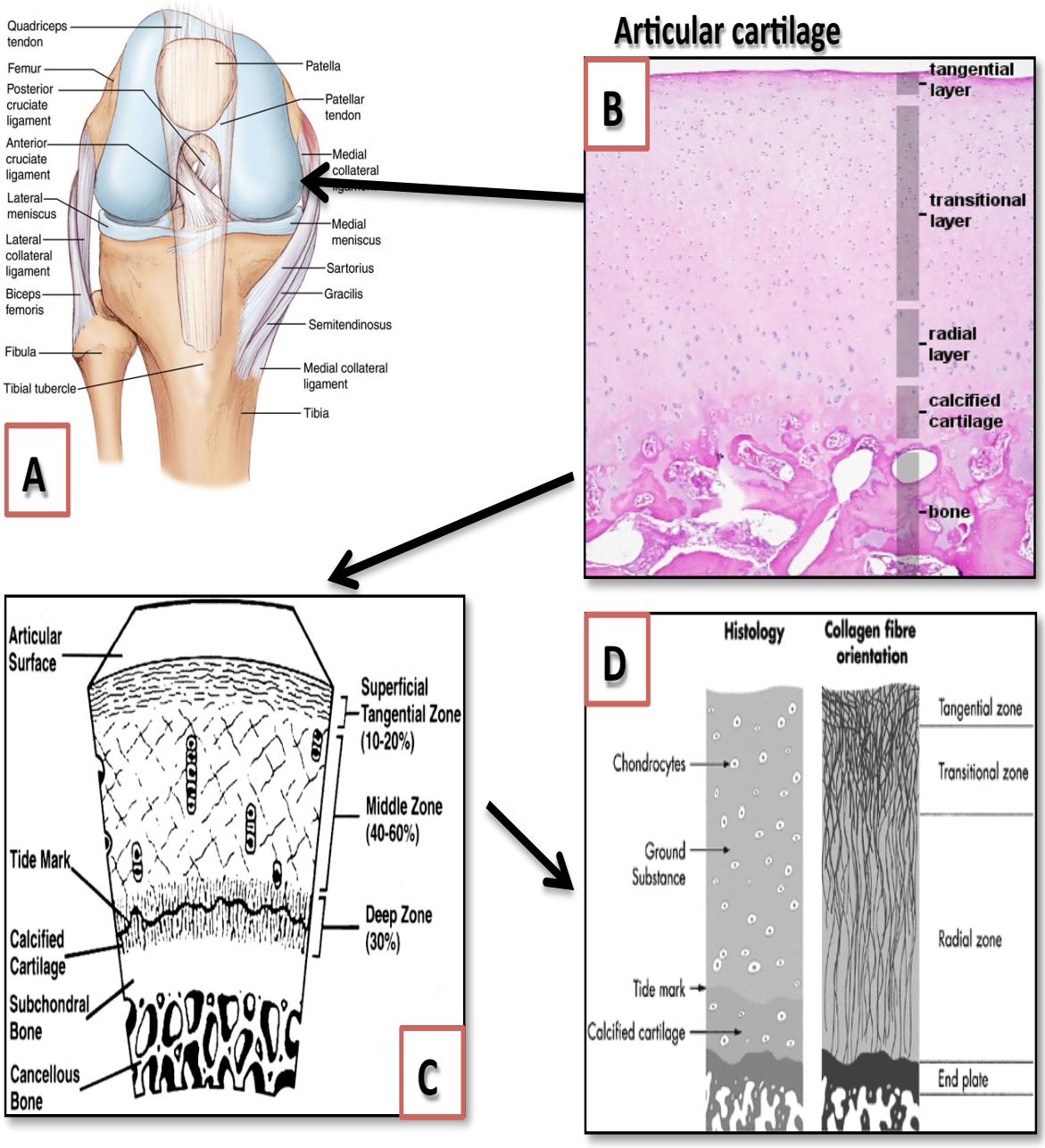

Figure 1.1: A schematic representation of the articular cartilage structure
A: shows the location of the articular cartilage within the knee joint. **B**: A Haemotxylin and Eosin (H&E) staining showing the histology of articular cartilage with its four defined zones. **C**: A diagrammatic representation of the structure of the articular cartilage and the subchondral bone as depicted in the previous H&E satin (C). **D**: The articular cartilage cell and collagen organisation within different zones of the ECM. Images were adapted from the following web pages: (http://www.ismoc.net/images/knee_rev.jpg,http://php.med.unsw.edu.au/embryology/images/0/07/Articular_cartilage.jpg,http://www.kneejointsurgery.com/pics/articular-cartilage-zones.gifhttp://ajs.sagepub.com/content/26/6/853/F3.large.jpg)

In addition to its horizontal subdivisions, the articular cartilage matrix can be divided circumferentially to the chondrocyte where three layers are described based on its structure and morphology; the pericellular, territorial (or capsular) and interterritorial matrices (Chubinskaya and Kuettner, 2003; Poole, 1997) (see figure 1.2). The chondrocyte is encircled by the pericellular matrix, which, in conjunction with the cell is referred to as a chondron. These chondrons are the basic functional units of the cartilage and may contain a single, two or multiple chondrocytes, which are surrounded by collagen fibrils (the territorial matrix). Finally, the ECM environment is composed of many of these territories enclosed in the interterritorial matrix, which represents the largest portion of the cartilage matrix constituting about 90% of the cartilage volume (Poole, 1997; Chubinskaya and Kuettner, 2003; Chi *et al*, 2004). The chondrons of the tangential and transitional layers contain a single chondrocyte, whilst the radial zone is composed of between five to eight chondrocytes per chondron (Hunziker *et al*, 2002).

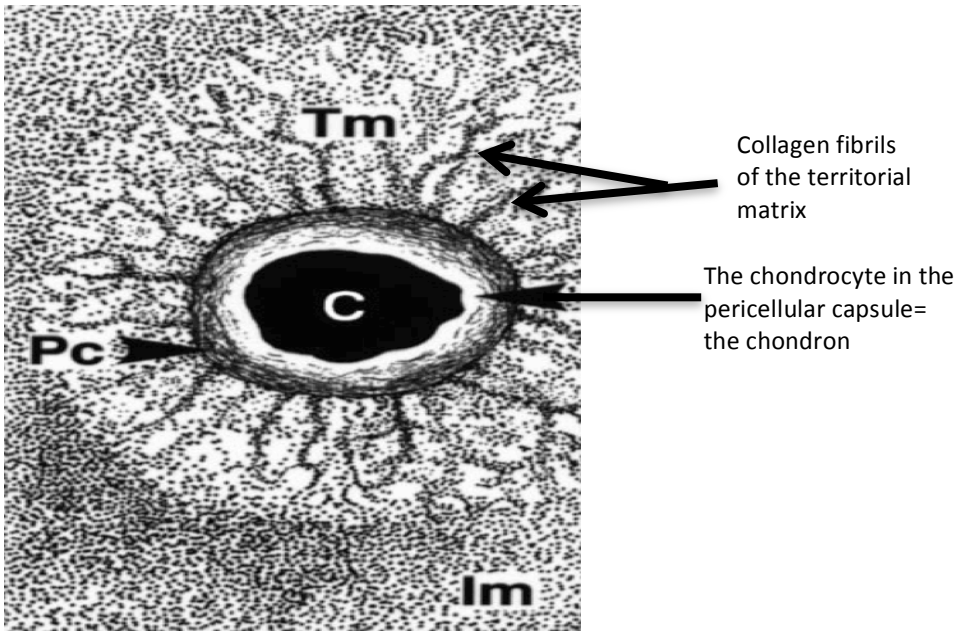

Figure 1.2: The three layers of the ECM the Pericellular matrix, Territorial matrix and Interterritorial matrix.
The diagram shows the chondrocyte (C) encapsulated in the pericellular matrix (PC) to form the chondron, surrounding the chondron is the territorial matrix (TM) with its extending collagen fibrils embedded in the extensive interterritorial matrix (IM), which represents the ECM). Adapted from (Poole, 1997).

The ECM is chiefly composed of water (75%), proteoglycans (mostly aggrecan) (20%) and type II collagen fibres (5%) (Ruiz-Romero *et al*, 2005; Chubinskaya and Kuettner, 2003). Other ECM macromolecules include: type VI, IX, X, and XI collagen fibres, non-collagenous proteins (such as fibronectin, and cartilage intermediate layer protein (CLIP)) and lipids (Goldring, 2000; Aigner *et al*, 2006; Roughley, 2001). The proteoglycans characterize the elastic properties of the tissue endowing the cartilage with its compressive strength, whilst the collagen fibres confer its tensile strength; collectively, they disperse mechanical pressure imposed on localised joint areas to avoid damage to the cartilage tissue (Roach *et al*, 2007; Aigner *et al*, 2006).

Chondrocytes in the superficial layer synthesize large amounts of densely packed thin collagen fibres (hence the capacity of the cartilage to resist tension) but low amounts of proteoglycans. The presence of abundant collagen in this zone gives the cartilage its characteristic opaque appearance (Chi *et al*, 2004; Hayes *et al*, 2003; Poole, 1997). In the transitional layer, chondrocytes increase their proteoglycan production (Poole, 1997; Hayes *et al*, 2003). The deep zone contains the highest proteoglycan content in contrast to the calcified layer, which lacks proteoglycans. The calcified layer separates the hyaline cartilage from the underlying subchondral bone and serves to anchor the articular cartilage to the subchondral bone. The small population of hypertrophic chondrocytes in the calcified layer are embedded in uncalcified lacunae (Poole, 1997; Martel-Pelletier *et al*, 2008).

The chondrocytes are sparsely distributed throughout the ECM of the cartilage and although they constitute only approximately 5-10% of its total volume, they ensure that the structural integrity and functionality of the tissue is regulated and maintained. The roles of the chondrocyte include: synthesis, secretion, organization and degradation of the distinct repertoire of ECM macromolecules such as proteoglycans, collagen, non-collagenous and membrane protein synthesis, the production of cartilage metabolic enzymes and maintenance of cartilage tissue homeostasis (Goldring, 2000; Chubinskaya and Kuettner, 2003; Poole, 1997; Ruiz-Romero *et al*, 2005).

Generally, the chondrocytes sustain cartilage homeostasis by maintaining a state of equilibrium between the production of the ECM macromolecules (anabolic activities) and their subsequent degradation and loss (catabolic activities) via interaction with the pericellular matrix (Aigner *et al*, 2006; Chubinskaya and Kuettner, 2003; Lin *et al*, 2006; Magne *et al*, 2005).

The anabolic program is initiated in response to matrix degradation and involves: secretion of cytokines that are antagonists of catabolism, synthesis of ECM components and protease inhibitors, and chondrocyte replication. The cytokines involved in this process include: Bone Morphogenetic proteins (BMPs), Insulin-like Growth Factor (IGF) and Transforming Growth Factor beta (TGFβ), (Aigner *et al*, 2006; Chubinskaya and Kuettner, 2003; Ruiz-Romero *et al*, 2005; Goldring, 2000).

Conversely, the catabolic phenotype may be induced by stimuli such as proinflammatory cytokines and involves: suppression of ECM synthesis, promotion of the production of proteases, oxidants and other catabolic mediators, inhibition of cell proliferation and the induction of chondrocyte apoptosis. Such cytokines include: interleukin-1β (IL-1β), tumour necrosis factor alpha (TNFα), and interleukin-17 (IL-17), which are responsible for maintaining the catabolic phenotype of the cartilage (Abramson and Yazici, 2006; Ruiz-Romero *et al*, 2005; Lotz *et al*, 1995). A diagrammatic representation of this balance in cartilage metabolism is shown in figure 1.3.

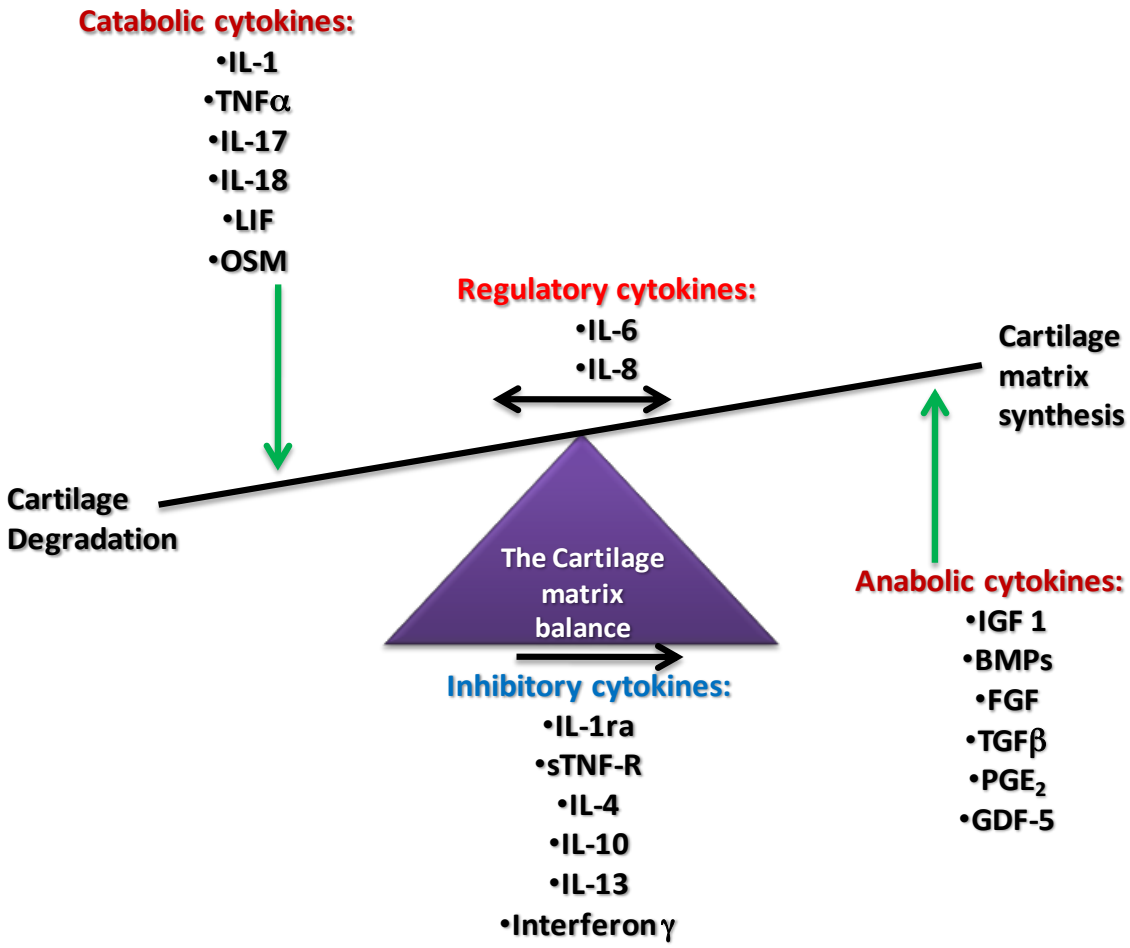

Figure 1.3: A diagrammatic representation of the cytokines involved in balancing the anabolic and catabolic activities in articular cartilage
IL-1 =Interleukin-1, IL-17 =Interleukin-17, LIF= Leukaemia Inhibitory Factor, OSM= Oncostatin M, sTNF-R= soluble Tumour Necrosis Factor Receptor, GDF-5= Growth Differentiation Factor, IL-1ra = Interleukin-1 receptor antagonist, TGFβ=Transforming Growth Factor β, FGF=Fibroblast Growth Factors, PGE_2= Prostaglandin E_2. The anabolic cytokines promote matrix synthesis, whilst the catabolic cytokines promote matrix degradation. The inhibitory cytokines inhibit the catabolic cytokines, which cause matrix degradation for e.g. IL-4 and IL-10 promote chondroprotection *in vivo*. Regulatory cytokines modulate the catabolic and anabolic activities. Adapted from: (Goldring, 2000)

Consequently, in normal, healthy tissue the chondrocytes maintain the composition and structural integrity of articular cartilage to provide a substance which functions synergistically as a biomechanical shock absorber which dissipates compressive and shearing forces evenly over the joint surface to reduce stress on the joint, a lubricant reducing friction and wearing of the cartilage surfaces and a load bearing surface that essential for smooth and free joint movements (Chubinskaya and Kuettner, 2003; Poole, 1997).

Numerous studies have attested that the ECM environment is a rich source of information in which cell-matrix interactions are vital in controlling biological processes such as: chondrocyte growth, migration, differentiation and survival (Loeser *et al*, 2000; Lin *et al*, 2006; Lukashev and Werb, 1998). In particular, the interaction between the chondrocyte and its' pericellular matrix have been shown to be of great importance in regulating the biochemical, biophysical and biomechanical transduction mechanisms of the chondrocyte response to mechanical stimuli. Essentially, normal loading of the joints coupled with enzymatic activity degrades ECM components, which are compensated for by an increased synthesis of matrix components to maintain the homeostatic balance of the matrix (Lin *et al*, 2006; Aigner *et al*, 2006).

Whilst articular cartilage is a resilient substance, a number of mechanical and biological events can disturb the normal homeostatic processes within the tissue resulting in an imbalance in the anabolic and catabolic events in favour of catabolism, as the cell-ECM interaction is misregulated and metabolic responses are altered. Consequently, the increased catabolic processes result in matrix degradation and ultimately, tissue damage (Lin *et al*, 2006; Aigner *et al*, 2006; Lukashev and Werb, 1998). This degeneration of the cartilage tissue is referred to as Osteoarthritis (OA) (Aigner *et al*, 2006).

1.2 Osteoarthritis

Osteoarthritis (OA) is a chronic degenerative condition characterised by cartilage degradation leading to joint dysfunction. The disease is prevalent in older individuals worldwide (affecting >50% of the population over 60 yrs) and is frequently associated with significant pain, deformity and disability, especially of the hips and knees (Haq *et al*, 2003; Felson *et al*, 2000; Poole *et al*, 2002).

There is currently no preventative treatment or cure available for OA. In the early stages, treatment is currently limited to analgesics (such as paracetamol and non-steroidal anti-inflammatory drugs, NSAID's) and intra-articular injections of hyaluronic acid and corticosteroids, which provide symptomatic relief. In the latter stages surgical intervention by endoprosthetic surgery is the only treatment and thus this disease and its' treatment carries huge socio-economic burden (Abramson and Yazici, 2006; Roach *et al*, 2007). The current treatment options available for OA treatment are shown in figure 1.4.

The clinical features of swelling, stiffness and loss of joint function are a result of the metabolic and biochemical changes which occur in the articular cartilage of the affected joints in the course of the disease process (Poole *et al*, 2002; Birchfield, 2001).

Whilst the exact pathology of OA is not fully understood, it seems likely that disease progression is multi–factorial and may occur as a consequence of a complex system of interacting factors including: abnormal biomechanical forces, environmental and biochemical factors (Goldring, 2000; Haq *et al*, 2003) and genetic predisposition (Haq *et al*, 2003; Fernandez-Moreno *et al*, 2008). These factors continue to result in an alteration in the normal functioning of the chondrocytes with the resulting abnormalities leading to the clinical features observed, of which joint pain is the cardinal feature (figure1.5) (Goldring, 2000; Martel-Pelletier *et al*, 2008; Haq *et al*, 2003).

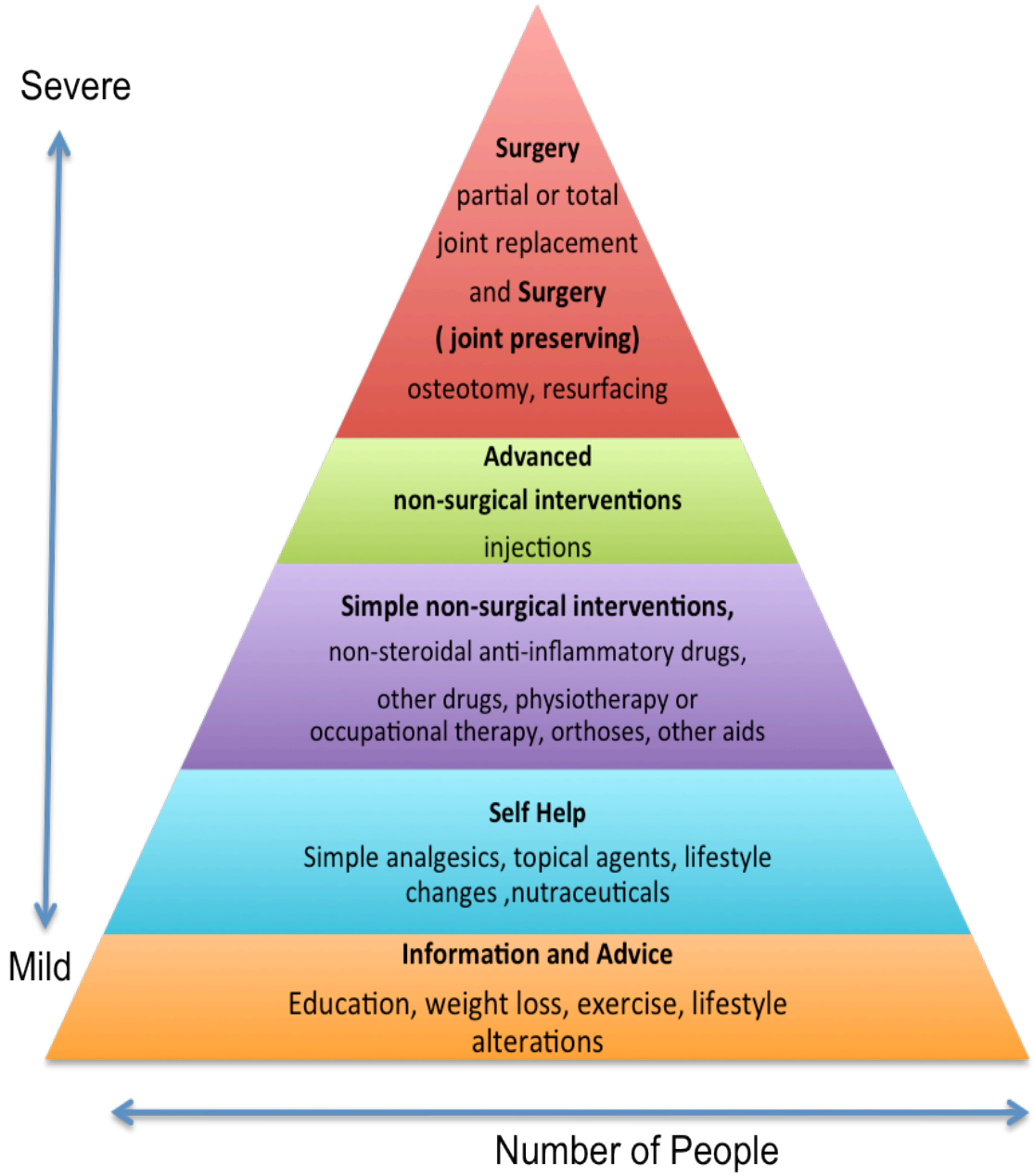

Figure 1.4: A representation of the current treatment strategies available for the treatment of OA patients
As the severity of the disease process increases so does the treatment. Supervision of treatment begins at simple non-surgical interventions however, before this stage treatment is largely unsupervised by a medical practitioner. Adapted from (Dieppe and Lohmander, 2005).

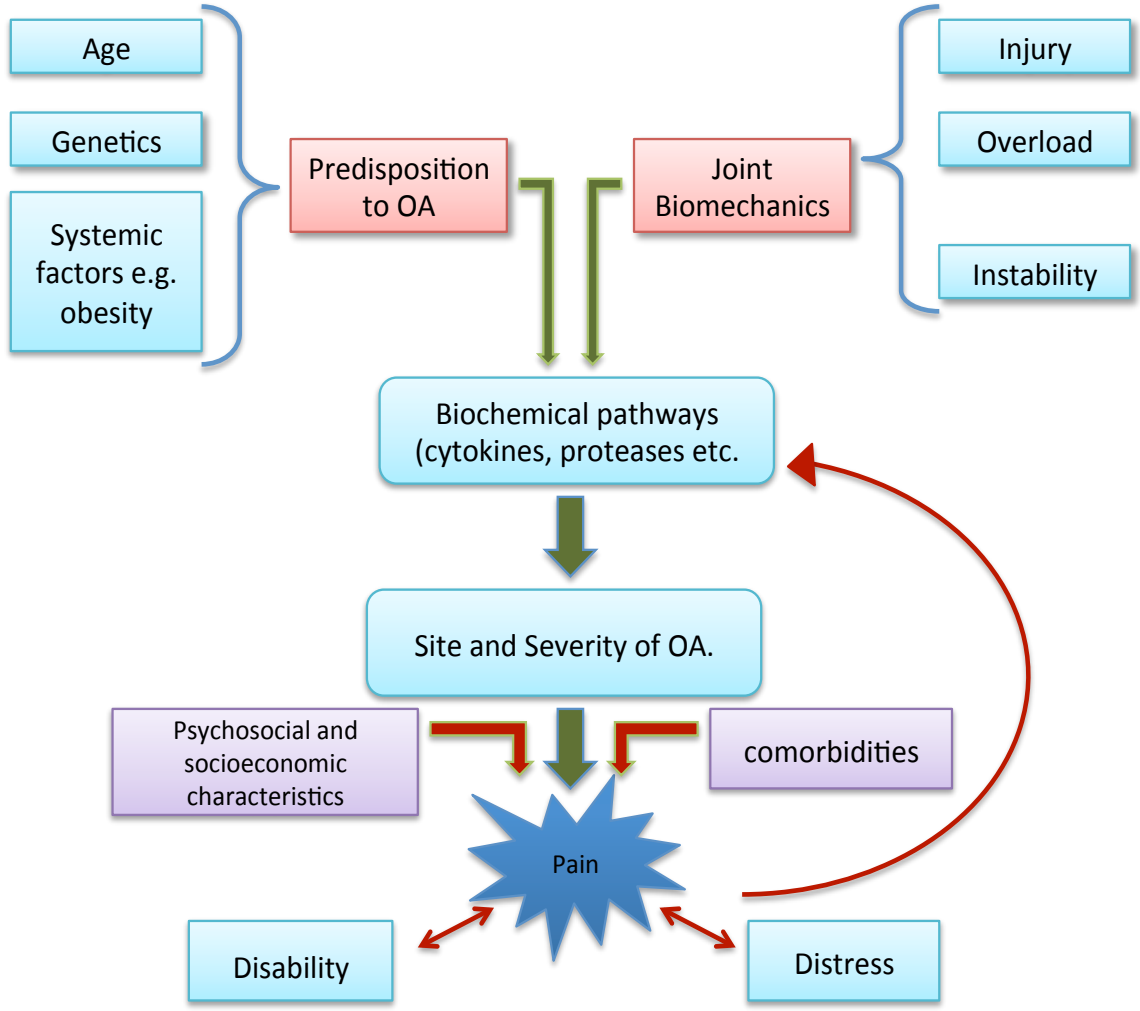

Figure 1.5: A schematic presentation of the interaction between environmental and endogenous risk factors for joint damage, OA development, joint pain and their consequences. Adapted from (Dieppe and Lohmander, 2005).

There is evidence to suggest that during the early stages of OA the chondrocytes up-regulate their anabolic events producing chondrons and synthesising ECM molecules such as proteoglycans and collagen, in an attempt to repair the cartilage and regain tissue homeostasis following the increased production of the catabolic cytokines and degrading enzymes. Increased synthesis and deposition of the CLIP protein into the interterritorial matrix has also been observed. However, with time, the catabolic activities increase and the chondrocyte lose their ability to sustain the anabolic activities necessary for maintaining matrix repair and tissue homeostasis.

Ultimately, the imbalance between the anabolic and catabolic activities in the articular cartilage in favour of catabolism results in the degradation of collagen fibres and proteoglycans from the matrix. This final pathway culminates in articular cartilage degradation characterised by reduced ECM water content and pericellular matrix volume and loss of cartilage tensile strength (Aigner *et al*, 2006; Goldring, 2000; Chubinskaya and Kuettner, 2003; Lorenzo *et al*, 1998).

Some of the key factors proposed are the overproduction of chemokines and proinflammatory cytokines such as TNFα and IL-1β, stimulated by the increased catabolic program, which in turn promotes the increased synthesis of proteinases such as: matrix metalloproteinases (MMPs), aggrecanases, plasmogen activators (PA) and cathepsins. Activity of these proteases, along with Nitric Oxide (NO) and other catabolic mediators, results in the degradation of cartilage and promotion of chondrocyte death by apoptosis (Abramson and Yazici, 2006; Goldring, 2000; Ruiz-Romero *et al*, 2005). Thus, understanding the balance between the anabolic and catabolic phenotype of the chondrocytes are crucial for developing treatment strategies for OA as potential therapeutic interventions can target at, for instance, delaying or inhibiting the catabolic process which culminates in chondrocyte apoptosis and cartilage destruction (Aigner *et al*, 2006).

Chondrocyte death results in a reduced number of active cells in the articular cartilage and therefore a reduction in the capacity of the cartilage cells to repair existing cartilage and/or generate new cartilage components. The end results of such events are the progressive destruction of the articular cartilage matrix and formation of cysts. Osteophyte formation and subsequent remodelling and sclerosis of the subchondral bone are also pathological manifestations, (Sandell and Aigner, 2001; Buckwalter and Martin, 2006) that are considered to occur as a consequence of a compensation mechanism for lack of cartilage (Haq *et al*, 2003).

1.3 Cell Death

1.3.1 Apoptosis

Apoptosis is the term used to describe the innate, genetically controlled morphological and biochemical processes by which a cell responds to various stimuli to systematically inactivate, dissemble and degrade its' structural and functional constituents in order to complete its own demise (Kim and Blanco, 2007; Majno and Joris, 1995).

The word "apoptosis" is of Greek origin and was first used as an analogy to explain the "falling off" of the leaves from trees or the petals from flowers by Kerr *et al*, in 1972; emphasising that though this process of cellular destruction occurred in a very complicated but orderly fashion, it is an essential part of a living organisms life cycle (Gewies, 2003; McHugh and Turina, 2006).

In contrast to other forms of cell death, apoptosis occurs through cellular, chemical and molecular processes, which are controlled and regulated by cellular signalling systems (Kim and Blanco, 2007; Kuhn *et al*, 2004; Gewies, 2003). Thus, apoptotic cell death is a non-accidental programmed process in which the cells are actively involved and for this reason apoptosis is sometimes referred to as "cell suicide" (Majno and Joris, 1995).

Apoptosis can be considered as a universally critical event as it occurs in both physiological and pathological scenarios (Kim and Blanco, 2007; McHugh and Turina, 2006). With regards to its physiological benefits, apoptosis is essential for the normal development of multicellular organisms and for regulating and maintaining cell populations of adult tissues (Gewies, 2003; Kim and Blanco, 2007; Kuhn *et al*, 2004). Apoptosis is a fundamental part of many biological events including development and morphogenesis, proliferation and homeostasis, regulation and function of the immune system, and the elimination of harmful and damaged cells that would otherwise pose a threat to the organism (Kim and Blanco, 2007; Schultz and Harrington, 2003; Gewies, 2003). Apoptosis and Programmed Cell Death (PCD), are used interchangeably to refer to apoptosis; reflecting that the death of cells follows a sequential program of cellular, biochemical and molecular events (Kim and Blanco, 2007; Majno and Joris, 1995).

In relation to apoptosis as a pathological event, dysfunction or dysregulation of apoptosis has been implicated in many diseases. For example, inadequate levels of apoptosis have resulted in pathological conditions such as cancer, and autoimmune diseases (e.g. systemic lupus erythematosus (SLE) and rheumatoid arthritis); whilst excessive apoptosis promotes the initiation and development of neurodegenerative diseases (e.g. alzheimer's disease, spinal muscular atrophy, parkinson's disease), ischaemic disease (e.g. congestive heart failure and stroke), severe immunodeficiency syndrome and acquired immune deficiency syndrome (AIDS) (Kim and Blanco, 2007; Gewies, 2003).

Typically, the apoptotic process is divided into three stages and is characterised by a range of distinctive morphological changes. Thus, apoptosis can be divided into a commitment or initiation phase, an execution phase and a clearance phase with the structural changes associated with apoptotic cell death occurring in the execution phase (Kruidering and Evan, 2000; Kim and Blanco, 2007). In addition, apoptosis can be distinguished by the following: cell shrinkage, chromatin condensation and margination to the perimeter of the nuclear membrane, cytoplasmic condensation, externalisation of phosphatidylserine phospholipids from the inner to the outer membrane envelope, plasma membrane blebbing or budding and finally the formation of apoptotic bodies containing cell remnants (coalescent chromatin in well defined masses, organelles and cytosol) encircled by a cytoplasmic membrane. Clearance of the apoptotic bodies from the tissues is achieved by phagocytosis involving dendritic cells and macrophages. This process ensures that no inflammatory mediators are released to initiate an inflammatory response within the tissue, which is vital to maintain normal functioning of the tissues and immune system and the health of organisms during development (Kim and Blanco, 2007; Gewies, 2003; Kruidering and Evan, 2000; McHugh and Turina, 2006).

Apoptosis can occur through two distinct pathways extrinsic and intrinsic. These two pathways differ in their initiation and signalling mechanisms but eventually activate the same mechanisms signals resulting in the characteristic features associated with apoptotic cell death (Kim and Blanco, 2007; Gewies, 2003).

The intrinsic or mitochondrial pathway of apoptosis may be initiated by stimuli such as DNA damage, cellular stress (e.g. from exposure to ultraviolet irradiation, X-irradiation, viral infection or chemotherapeutic agents), growth factor deprivation and oxidative stress following free radical generation (Schultz and Harrington, 2003; Gewies, 2003; McHugh and Turina, 2006).

Following cellular damage, the pro-apoptotic members of the B cell leukaemia/ lymphoma 2 (Bcl-2) family, Bax and Bak, normally localised in the cytosol are relocated to the mitochondria where they integrate into the outer mitochondrial membrane and contribute to the formation of pores referred to as Permeability Transition pore (PT pore). Consequently, cytochrome C (Cyt C) and other pro-apoptotic factors (e.g. Smac/DIABLO and apoptosis-inducing factor (AIF)), located within the mitochondrial intermembrane space are released into the cytoplasm via the PT pore. In the cytosol, cytochrome C interacts with the adaptor protein, Apaf-1 (apoptotic protease activating factor-1) and subsequently recruits procaspase-9. These three proteins, along with deoxyadenosine triphosphate (dATP) form the Apoptosome complex, which activates procaspase-9 to its active form caspase-9, the initiator caspase of the intrinsic pathway. The released Smac/DIABLO inhibits IAP (Inhibitor of Apoptosis Protein), an anti-apoptotic protein that functions to block caspase activity and activation, permitting the activated caspase-9 to initiate the rest of the caspase cascade in which the effector caspases-3, -6 and -7 are activated (see figure 1.6) ultimately resulting in apoptosis (Gewies, 2003; Schultz and Harrington, 2003; Kim and Blanco, 2007).

The release of Cyt C and other pro-apoptotic mediators from the mitochondria is normally prevented by the anti-apoptotic proteins Bcl-2 and Bcl-XL, which are localised to the outer membrane of the mitochondria (see figure 1.6.). The Bcl-2 and Bcl-XL anti-apoptotic proteins, like Bax and Bak are members of the Bcl-2 family and function as inhibitors apoptosis by via blocking the formation of the PT pore. Consequently, an excess of Bcl-2 and Bcl-XL proteins at the mitochondria renders the cell less sensitive to apoptosis (McHugh and Turnia, 2006, Schultz and Harrington, 2003).

Conversely, the extrinsic pathway is defined by cell surface transmembrane receptors, which collectively are referred to as Death Receptors (DRs) and they transmit apoptotic signals following activation resulting from the binding of specific ligands.

Currently, six types of DRs are recognised:

- Fas (also known as CD95 or APO-1)
- TNF receptor 1 (TNFR1) also known as p55 or CD120a
- TNF-related apoptosis-inducing ligand receptor-1 (TRAIL-R1) also known as Death receptor 4 (DR4)
- TNF-related apoptosis-inducing ligand receptor-2 (TRAIL-R2) also known as Death receptor 5 (DR5)
- Death receptor 3 (DR3) also known as APO-3or TNF-receptor-related apoptosis mediated protein (TRAMP)
- Death receptor 6 (DR6).

These DRs are members of the Tumour Necrosis Factor Receptor (TNF-R) superfamily and so their ligands are chiefly Tumour Necrosis Factor (TNF), TRAIL and Fas Ligand (Fas-L/CD95L) (Kruidering and Evan, 2000; Schulze-Osthoff *et al*, 1998; Schultz and Harrington, 2003).

Activation of the extrinsic apoptotic pathway is achieved by ligation of Death Receptors with their cognate ligands (e.g. Fas-L binding to the Fas receptor). Interaction of the death receptor with its' ligand results in the recruitment of adaptor proteins by the cytoplasmic death domains (DD) of the death receptor. These recruited adaptor proteins (e.g. Fas associated Death Domain (FADD) in the case of the Fas-FasL interaction) also contain a DD and a protein-protein interaction domain referred to "Death Effector Domain (DED"). Once recruited, the DD of the adaptor protein interacts with the DD of the death receptor resulting in recruitment of procaspase -8 and binding of the DED of the adaptor protein with the DED of procaspase 8. The resulting receptor signalling complex consisting of the DD of the death receptor, adaptor protein and procaspase-8 is referred to as the "Death Inducing Signalling Complex"- DISC.

Following association of the DISC, procaspase -8 is activated to caspase 8, the initiator caspase of the extrinsic pathway. Capsase 8, in turn causes subsequent cleavage and activation of the effector procaspases -3, -6 and -7 to their active forms (caspase -3, -6 and -7), which execute apoptosis via cleavage of their substrates (e.g. structural and regulatory intracellular proteins) resulting in the biochemical and morphological features characteristic of apoptotic cell death (Gewies, 2003; Kuhn *et al*, 2004; Kim and Blanco, 2007; Schultz and Harrington, 2003).

In addition, apoptosis via the extrinsic pathway involving the Fas or TNFR1 death receptors can be mediated through a mitochondrial dependent apoptotic pathway. This cross talk between the intrinsic and extrinsic pathways of apoptosis is facilitated by the pro-apoptotic Bcl-2 family member, Bid. Initiation of this mitochondrial apoptotic pathway is said to be activated in response to low concentrations of procaspase -8 at the DISC. Subsequently, caspase -8 cleaves and activates Bid to its' truncated form termed "tBid" (truncated Bid). tBid is then translocated to the mitochondria where in concert with Bax and Bak results in the release of Cyt C, Smac/DIABLO and downstream activation of the effector caspases of the intrinsic apoptotic pathway. The Bid protein can also be inhibited by Bcl-2 and Bcl-XL (see figure 1.6) (Schultz and Harrington, 2003; Gewies, 2003; Scaffidi *et al*, 1998; Antonsson and Martinou, 2000).

More recently, a third apoptotic pathway involving the Endoplasmic Reticulum (ER) has also been implicated. Though its' exact downstream signalling pathways are not fully known, Caspase 12, localised to the Endoplasmic Reticulum is believed to be the initiator caspase for this intrinsic apoptotic pathway. Activation of caspase 12 may result from Endoplasmic Reticulum stress such as calcium homeostasis dysregulation and excess misfolded protein accumulation in the ER (Kim and Blanco, 2007; Kuhn *et al*, 2004). These three apoptotic pathways are illustrated in figure 1.6.

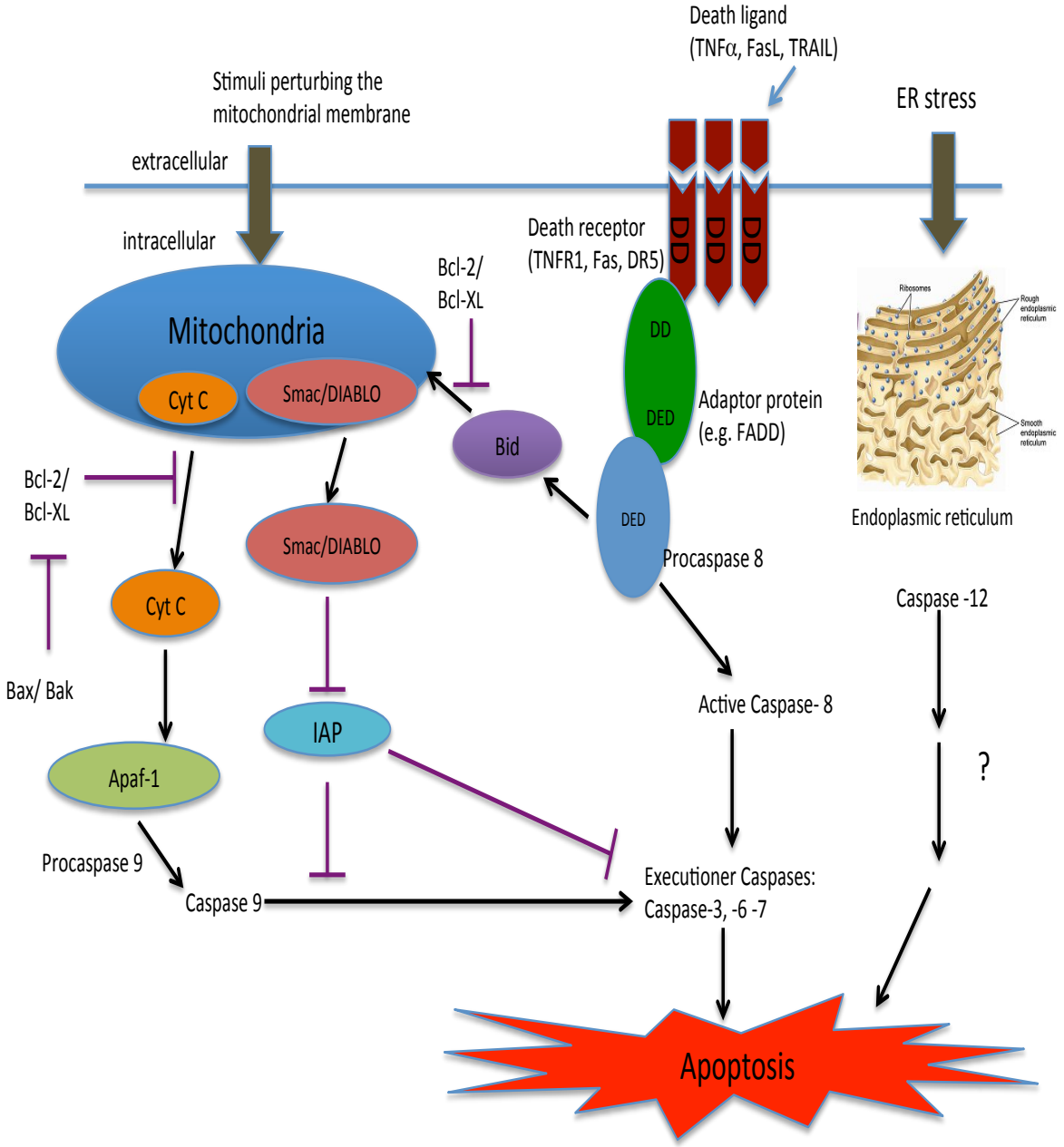

Figure 1.6: An overview of the extrinsic (death receptor mediated) and intrinsic (mitochondria and endoplasmic reticulum) pathways of apoptosis.
DD= death domains, DED= death effector domain, Cyt C= cytochrome C, IAP= inhibitor of apoptosis protein, Smac/DIABLO= Second mitochondria-derived activator of caspases, TNF- tumour necrosis factor, ER= endoplasmic reticulum, Apaf-1= apoptotic protease activating factor -1. FADD= Fas associated Death Domain. Adapted from (Kim and Blanco, 2007)

1.3.2 The Bcl-2 Family of Proteins

The Bcl-2 family members are essential signalling components, which play a central role in regulating apoptosis. These Bcl-2 proteins have been localised to the cytosol, outer nuclear envelop, endoplasmic reticulum and mitochondrial membranes and are regulated by cytokines and other death-survival signals at different stages of the apoptotic pathway (Antonsson and Martinou, 2000; Adams and Cory, 2001; Schultz and Harrington, 2003). Members of the Bcl-2 family share a very low homology in their amino acid sequence; however these proteins share homology in specific regions designated the Bcl-2 Homology (BH) domains of which there are four: BH1, BH2, BH3, and BH4.

The Bcl-2 proteins mediate protein interactions through these domains to exert their effects (Schultz and Harrington, 2003; Antonsson and Martinou, 2000). Consequently, the Bcl-2 family can be divided into two groups, those that are "anti-apoptotic" inhibiting apoptosis and "pro-apoptotic "promoting apoptosis and the survival or death of a cell is partly determined by the balance between the pro-apoptotic and anti-apoptotic Bcl-2 proteins. Additionally, mammalian cells contain at least 15 Bcl-2 proteins and they can be characterised based on their function and BH domain organisation as shown in table 1.1 (Schultz and Harrington, 2003; Gross *et al*, 1999).

Bcl-2 Family	Protein	Action on Apoptosis	Bcl-2 Homology (BH) Domains
Bcl-2 subfamily	Bcl-2, Bcl-XL, Mcl-1, A1, Bcl-w	Anti-apoptotic	BH1, BH2, BH3, BH4
Bax subfamily	Bax, Bak, Bok	Pro-apoptotic	BH1, BH2, BH3
BH3 only subfamily	Bik, Hrk, Bim, Blk, Bad, Bid	Pro-apoptotic	BH3

Table 1.1: The mammalian Bcl-2 family of anti-apoptotic and pro-apoptotic members. The Bcl-2 family members can be grouped according to their function to inhibit or promote apoptosis as well as their BH homology. The Bcl-2 subfamily proteins all bear resemblance to the first identified protein, Bcl-2 and have 4 conserved BH domains. The BH3 subfamily shares homology only in their BH3 domain. The Bax sub family constitutes the Bcl-2 family proteins with 3 domains BH1, BH2 and BH3. Adapted from: (Schultz and Harrington, 2003)

1.3.3 Necrosis

Necrosis is generally regarded as “accidental cell death or non-programmed” as it occurs unintentionally without the activation of a sequential program of intracellular signalling cascades (such as activation of caspases) (Kim and Blanco, 2007; Kuhn *et al*, 2004). Though apoptosis occurs in both physiological and pathological conditions, necrosis is predominantly seen in disease processes (Ziegler and Groscurth, 2004)and cells normally undergo necrosis following depletion of ATP (approximately 20-25% of baseline) (McHugh and Turina, 2006). Necrotic cell death can be induced by viruses (e.g. HIV), bacteria (e.g. *Mycobacterium avium*), defence components of the immune system (e.g. complement), heat stress, bacterial toxins, physical trauma and metabolic poisons as well as diseases such as Alzheimer’s and Epilepsy (Proskuryakov *et al*, 2003).

Many of the agents which trigger the apoptotic pathway have also been shown to initiate necrotic cell death, these include: cytokines released from affected tissues, which ligate TNF, Fas and TRAIL death receptors, increased production of reactive oxygen species and DNA damage (Proskuryakov *et al*, 2003). However, apoptosis can be distinguished from apoptosis by a variety of characteristic features (table 1.2).

Secondary necrosis is the mechanism by which the remnants of the apoptotic bodies that are not phagocytosed, undergo degradation similar to necrosis in which the cell swells and ruptures releasing their contents leading to inflammation and localised tissue damage (McHugh and Turina, 2006; Ziegler and Groscurth, 2004; Schultz and Harrington, 2003).

Distinguishing features	Apoptosis	Necrosis
Morphological	• Shrinking of cytoplasm and chromatin condensation • Nuclear fragmentation • Formation of apoptotic bodies	• Swelling of cytoplasm and mitochondria • Non-specific karyolysis • Total cellular disintegration without formation of vesicles
Physiological	• Induced by physiological stimuli • Tightly regulated signalling events • Energy dependent (i.e. ATP) • Enzymatically catalysed changes of cell membrane (annexin V binding) • Orderly fragmentation of chromosomal DNA (DNA laddering) • Activation of caspases • Late loss of membrane integrity	• Induced by non-physiological stimuli • Early loss of membrane integrity • No energy requirement • Random digestion of nuclear DNA (leading to smear in agarose gel electrophoresis) • DNA degradation following membrane permeabilisation
Consequences	• Affects individual cells • Phagocytosis by adjacent cells or macrophages • Typically not associated with an inflammatory response	• Affects groups of cells in a tissue • Disintegrating cells are phagocytosed by leukocytes • Associated with an inflammatory response

Table 1.2: The key distinguishing features between Apoptosis and Necrosis mechanisms of cell death.
Adapted from: (Kuhn *et al*, 2004)

1.3.4 Osteoarthritis (OA) and Apoptosis

For many years, there has been much debate concerning which of the underlying mechanisms of cell death is responsible for hypocelluarity in OA. Over the last decade however, several studies have documented apoptotic cell death as the main cause of cell depletion in OA (Blanco *et al*, 1998; Hashimoto *et al*, 1998; Kim *et al*, 2000; Lotz *et al*, 1999; Kim and Blanco, 2007). Heraud *et al*, in 2000, investigated the occurrence of apoptosis in OA cartilage compared to normal cartilage. Following quantification of chondrocytes isolated from OA and normal cartilage or chondrocytes present *in situ* in frozen cartilage sections, Heraud *et al* reported that approximately 18-21% of chondrocytes in osteoarthritic cartilage displayed apoptotic characteristics such as externalisation of phosphatidylserine phospholipids, compared with only 2-5% in healthy cartilage. This suggests that apoptosis increases in OA as compared to in normal cartilage (Heraud *et al*, 2000). There is also evidence to suggest that chondrocyte apoptosis increases with age, a factor that has also seen to contribute OA pathogenesis as a result of prolonged mechanical wear and tear causing alterations in the cartilage matrix components (Lorenz and Richter, 2006; Aigner *et al*, 2007).

Matrix degradation as a consequence of chondrocyte apoptosis has also been implicated as a major mechanism in the pathogenesis of OA (Kim and Blanco, 2007). The Fas death receptor and its ligand FasL has been implicated in promoting chondrocyte apoptosis in OA (Cheng *et al*, 2004; Goggs *et al*, 2003) and this pathway of apoptosis may possibly promote chondrocyte death in early OA as its expression was predominant in the superficial and transitional cartilage layer, where cartilage degeneration begins (Lotz *et al*, 1999; Hashimoto *et al*, 1997).

One of the main inducers of cell death in OA is the inflammatory mediator nitric oxide (NO) (Martel-Pelletier *et al*, 2008; Haq *et al*, 2003). NO can be generated in response to stimuli such as the pro-inflammatory cytokines IL-1β and TNFα and human chondrocytes were observed to produce large amounts of NO following stimulation with these cytokines (Goggs *et al*, 2003; Lotz *et al*, 1999; Abramson, 2008).

An increase in NO was observed in OA cartilage and it has been demonstrated to inhibit matrix synthesis, promote matrix catabolism and chondrocyte apoptosis (Martel-Pelletier *et al*, 2008; Heraud *et al*, 2000). Research by Intekhab-Alam in 2006, has also reported that apoptosis and not necrosis is the predominant cause of cell death in a human chondrocyte cell line, C-20/A4, following stimulation of cells with various pro-apoptotic stimuli: IL-1β, TNFα and a NO donor-SNAP (Intekhab-Alam, 2006). The duration of apoptosis in cells occurs rapidly, within minutes to hours, although the duration of chondrocyte apoptosis in cartilage is unknown (Heraud *et al*, 2000).

It is now widely accepted that chondrocyte death contributes to the pathogenesis of OA via cartilage degeneration. These cells maintain the integrity and functionality of the cartilage matrix and thus their loss ultimately results in matrix degeneration. If chondrocyte apoptosis is a major contributing factor to the development of OA, then reduction and/or prevention of this cell death would represent a possible target for therapeutic intervention in OA.

Intekhab-Alam, (2006) has also demonstrated that C-20/A4 chondrocytes express a Corticotropin releasing factor (CRF) family peptide, Urocortin I (UCNI), that is upregulated when the cells are subjected to stressors such as nitric oxide donors (SNAP) and pro-inflammatory cytokines previously mentioned. Selective depletion of endogenous Urocortin I by the addition of anti-UCNI antibody to C-20/A4 chondrocyte culture medium, or the addition of the competitive CRF antagonist, alpha helical corticotrophin releasing hormone $_{(9\text{-}41)}$ (αhCRH$_{(9\text{-}41)}$), resulted in an increased level of chondrocyte death even in the absence of pro-apoptotic stimuli. Conversely, addition of exogenous Urocortin I reduces the level of both NO and TNFα induced apoptosis indicating a possible 'chondroprotective' role for Urocortin I (Intekhab-Alam, 2006; Petsa, 2007). Since recent studies have suggested that *UCNI* exerts a greater degree of chondroprotection than other members of the Urocortin family, Urocortin II (UCNII) and Urocortin III (UCNIII) (Petsa, 2007), this research will focus on UCNI only.

1.4 Urocortin I (UCNI) and the CRF family of peptides

To date, the Corticotropin Releasing Factor (CRF) family of peptides consists of six members, namely: Corticotropin Releasing Factor (CRF), Urotensin I (Uro I), Sauvagine (Svg), and the Urocortin family comprised of Urocortin I (UCNI), Urocortin II (UCNII) or Stresscopin related peptide (SRP), and Urocortin III (UCNIII) or Stresscopin (SCP) (table 1.3) (Vale *et al*, 1997; Lederis *et al*, 1982; Okawara *et al*, 1988; Montecucchi and Henschen, 1981; Stenzel-Poore *et al*, 1992). These peptides are classified as the CRF family due to their structural and pharmacological homology to CRF, the first documented member (a hypothalamic peptide) isolated and characterised in 1981 by Vale *et al* (Vale *et al*, 1981; Kuizon *et al*, 2009).

CRF related peptide family member:	peptide amino acid length	species	References of descriptors
Corticotropin releasing factor (CRF)	41	• Human • Mouse • Rat • ovine	• Vale *et al*, 1981 • Vale *et al*, 1997
Urotensin I (Uro I)	41	• fish	• Lederis *et al*, 1982 • Okawara *et al*, 1988
Sauvagine (Svg)	40	• amphibian	• Montecucchi and Henschen, 1981 • Stenzel-Poore *et al*, 1992
Urocortin I (UCNI)	40	• human • rat • sheep • mouse	• Vaughn *et al*, 1995 • Donaldson *et al*, 1996 • Zhao *et al,* 1998 • Cepoi *et al*, 1999
Stresscopin related peptide (SRP) or Urocortin II (CNII)	38	• human • rat • mouse	• Reyes *et al*, 2001 • Hsu and Hsueh, 2001
Stresscopin (SCP) or Urocortin III (UCNIII)	38	• human • rat • mouse	• Lewis *et al*, 2001 • Hsu and Hsueh, 2001

Table 1.3: The mammalian and non-mammalian members of the CRF related peptide family. The non-mammalian CRF like peptides are: Sauvagine and Urotensin I, whilst the mammalian CRF like peptides are: CRF, UCNI, UCNII (SRP) and UCNIII (SCP). Adapted from: (Dautzenberg and Hauger, 2002; Hauger *et al*, 2003).

1.4.1 Urocortin I (UCNI)

Urocortin I (UCNI), the second member of this family to be identified, is a 40 amino acid peptide that was initially discovered by Vaughan *et al*, in 1995 following screening of a rat midbrain cDNA library with fish Urotensin I specific probe to isolate the cDNA which codes for the *UCNI* precursor (Cepoi *et al*, 1999; Vaughan *et al*, 1995; Fekete and Zorrilla, 2007). Shortly after, in 1996, the human gene for UCNI was isolated from a genomic library constructed from human placenta by Donaldson *et al*, (Takahashi *et al*, 1998; Donaldson *et al*, 1996). The human and rat *UCNI* shares a 95% amino acid sequence homology (Takahashi *et al*, 1998; Okosi *et al*, 1998) and since its discovery in rat and human the gene has also been identified in several other species including mouse, sheep, rhesus monkey and frog where the sequence remains highly conserved (Fekete and Zorrilla, 2007).

The human gene that encodes *UCNI* was localised to chromosome 2 (2p23-p21) and consists of two exons and one intron, with the mRNA sequence encoding the 122-124 amino acids precursor peptide residing in exon 2, analogous to the *CRF* peptide (Fekete and Zorrilla, 2007; Gysling *et al*, 2004; Huang *et al*, 2004). In addition to the mRNA coding region, also of importance on the *UCNI* gene are the multiple transcription factor binding sites in the *UCNI* promoter, some of which have been shown to regulate *UCNI* transcription. Such sites include: the TATA-like box, cyclic adenosine monophosphate (cAMP) responsive element (CRE) and GATA and CCAAT enhancer-binding protein (C/EBP) transcription factor-binding site (Fekete and Zorrilla, 2007; Zhao *et al*, 1998). For instance, augumented levels of cAMP are observed to stimulate UCNI production, which is facilitated via CRE binding sites on the promoter region of the UCNI gene increasing UCNI mRNA expression (Hauger *et al*, 2006; Slominski *et al*, 2001).

The UCNI peptide was originally known simply as Urocortin (UCN) and the name was derived from the fact that it displays a 63% amino acid sequence homology to fish Urotensin I (thus “Uro”) and a 45% homology to mammalian Corticotropin Releasing Factor (thus “cort”)(Koob and Heinrichs, 1999).

However, searching of the public human genome databases in 2001 identified two new members of the CRF family, the human homologues designated Stresscopin related peptide (SRP) and Stresscopin (SCP) and in mice are these are Urocortin II (UCN II) or Urocortin III (UCN III), both of which are composed of 38 amino acids (table 1.3) (Lewis *et al*, 2001; Reyes *et al*, 2001; Hsu and Hsueh, 2001; Suda *et al*, 2004; Chanalaris *et al*, 2003). UCN was consequently re-designated as UCNI by the International Union of Pharmacology so that it can be distinguished from UCNII and UCNIII (Suda *et al*, 2004; Hauger *et al*, 2003).

UCNII and UCNIII were noted to share sequence identity to CRF and UCNI, but were designated "Urocortins", as they predominantly bind to the Corticotropin Releasing Factor Receptor type 2 (CRFR2)(Fekete and Zorrilla, 2007). The human UCNII peptide shares a 31% homology to human UCNI whilst a 26% identity exists between human UCNIII and human UCNI. Moreover, a 37-40% sequence homology exists between UCNII and UCNIII (Takahashi *et al*, 2004; Imperatore *et al*, 2006; Hsu and Hsueh, 2001).

The UCNI mRNA is ubiquitously expressed in several tissues, notably, the skin and the reproductive, immune, digestive, cardiovascular and central nervous systems where it has a number of diverse physiological roles (Oki and Sasano, 2004; Slominski *et al*, 2000; Fekete and Zorrilla, 2007). In the cardiovascular system, *UCNI* production was observed to have a variety of physiological effects on cardiac function where a dose dependent administration resulted in an increase in heart rate, cardiac output and coronary blood plus a decrease in blood pressure in conscious rats (Parkes *et al*, 2001; Latchman, 2002). UCNI also exerted cardioprotective effects against cell death induced by hypoxia and *UCNI* mRNA levels were elevated following thermal injury in cultured cardiac cells (Okosi *et al*, 1998; Parkes *et al*, 2001). Furthermore, UCNI demonstrated protection against cell death following ischaemia/reperfusion injury in both cultured cardiac myocytes and the intact rat heart (Brar *et al*, 1999; Brar *et al*, 2000; Latchman, 2002). However, in the heart UCNI also appears to induce, and be involved in, cardiac hypertrophy (Latchman, 2002; Nishikimi *et al*, 2000; Chanalaris *et al*, 2005).

UCNI expression was also detected in the gastrointestinal tract and tissues of the immune system where expression was increased in diseases such as Gastritis and Rheumatoid arthritis; suggesting that *UCNI* may be involved in regulating immune responses(Oki and Sasano, 2004). Such roles of UCNI in the heart and gastrointestinal tract are postulated to be mediated via the GATA transcription factors which bind to the GATA regions of the *UCNI* promoter mediating *UCNI* expression therein (Zhao *et al*, 1998).

In relation to the Nervous system, *UCNI* expression was identified in many regions of the brain including the Edinger-Westphal nucleus, lateral superior olive, supraoptic nucleus, hypothalamus, and pituitary (Skelton *et al*, 2000; Zhao *et al*, 1998; Oki and Sasano, 2004). UCNI was reported to suppress appetite and regulate fluid homeostasis in rats (Oki and Sasano, 2004; Parkes *et al*, 2001; Spina *et al*, 1996). Studies by Zhao *et al,* 1998 demonstrated that the *UCNI* promoter region contains binding sites for the C/EBP transcription factor and it is suggested that the effects of UCNI in appetite suppression may potentially be mediated through activation of C/EBP transcription factors, which increase *UCNI* expression (Zhao *et al*, 1998). Other possible roles for UCNI in the CNS include the regulation of anxiety and activity (Oki and Sasano, 2004; Spina *et al*, 1996; Latchman, 2002).

UCNI expression in the reproductive system, notably the placenta implies a role for UCNI in labour, maintaining placenta function and regulation of sex hormone synthesis in the ovaries (Hillhouse and Grammatopoulos, 2002; Oki and Sasano, 2004). There is also increasing evidence suggesting that UCNI may play a role in regulating carcinogenesis. Several studies have identified *UCNI* expression in various cancers, for instance in pituitary adenoma, prostatic and endometrial carcinoma where it exerts numerous anti-cancer effects that are primarily mediated via activation of their receptors (Wang and Li 2007). UCNI inhibited the growth of tumour cells in a human neuroblastoma cell line (Schoeffter *et al*, 1999) as well as the proliferation of melanoma cells both *in vitro* and *in vivo*, these effects of UCNI were mediated through CRFR1 receptors (Carlson *et al*, 2001; Wang and Li, 2007).

Although *UCNI* has been identified in several different tissues, its' cytoprotective properties against cell death have thus far only been reported in cardiac myocytes, nerves cell and chondrocytes (Petsa, 2007; Brar *et al*, 1999; Abuirmeileh *et al*, 2007; Intekhab-Alam, 2006).

UCNI and other peptides of the CRF family are believed to exert their physiological actions primarily via two different types of stimulatory G-protein (G_s) coupled, seven transmembrane domain receptors: Corticotropin Releasing Factor Receptor 1 (CRFR1) and Corticotropin Releasing Factor Receptor 2 (CRFR2) (Grammatopoulos and Chrousos, 2002; Koob and Heinrichs, 1999).

1.5 The Corticotropin Releasing Factor Receptors (CRFR)

The Corticotropin Releasing Factor Receptors: CRFR1 and CRFR2, are members of the class II/ B1 subtype group of the G protein-coupled receptor (GPCR) superfamily, other members of which include the glucagon, calcitonin and parathyroid hormone (PTH) receptors (Bale and Vale, 2004; Grammatopoulos and Chrousos, 2002; Hauger *et al*, 2006; Perrin *et al*, 2006). The CRFR1 and CRFR2 receptors share a 70% sequence homology at the amino acid level (Bale and Vale, 2004; Fekete and Zorrilla, 2007; Grammatopoulos and Chrousos, 2002; Catalano *et al*, 2003). The genes which encode the *CRFR1* and *CRFR2* receptors are however located on different chromosomes (17 and 7 respectively) with each having several splice variants which are differentially expressed in the CNS and peripheral tissues (Grammatopoulos and Chrousos, 2002; Bale and Vale, 2004; Kuizon *et al*, 2009).

The existence of CRFR1 and CRFR2 splice variants can be attributed to the fact that class II GPCR superfamily genes exhibit extron-intron organisation whereas other GPCR classes are devoid of introns, especially in their protein coding regions. This unique characteristic of the class II GPCR genes allows extensive alternative splicing resulting in a variety of receptor subtypes with alternative domains from one gene, which can exhibit differential ligand binding, specificity and G-protein coupling (Catalano *et al*, 2003; Gentles and Karlin, 1999; Hillhouse and Grammatopoulos, 2006).

In this respect, the CRFR1 and CRFR2 receptors have been shown to vary in their pharmacological ligand binding profile (Takahashi, 2001; Bale and Vale, 2004; Fekete and Zorrilla, 2007; Grammatopoulos and Chrousos, 2002). For instance, the CRFR1 receptor binds CRF, UCNI, Urotensin I and Sauvagine whilst *CRFR2* predominantly binds UCNI, UCNII, UCNIII, Sauvagine and Urotensin I(Grammatopoulos and Chrousos, 2002). As UCNI binds to CRFR2 with a higher affinity than other CRF related peptides, and UCNII and UCNIII only bind to CRFR2, it has therefore been proposed that the Urocortins are the likely endogenous agonists for CRFR2 receptors (Koob and Heinrichs, 1999; Fekete and Zorrilla, 2007; Catalano *et al*, 2003). The differential tissue distribution and pharmacology of the CRFR1 and CRFR2 receptors implies that they perform diverse physiological roles (Fekete and Zorrilla, 2007; Catalano *et al*, 2003).

CRFR receptors are predominantly, but not exclusively, coupled to a G_S protein signalling pathway activating adenylate cyclase and increasing cAMP levels, culminating in activation of Protein Kinase A (PKA) dependent mechanisms such as, the activation of L-type calcium channels and P42/44 Mitogen Activated Protein Kinase (MAPK) pathways (Grammatopoulos and Chrousos, 2002; Perrin *et al*, 2006; Fekete and Zorrilla, 2007). These receptors have also been shown to couple with G_q proteins resulting in Phospholipase C (PLC) activation and subsequent hydrolysis of phosphatidylinositol 4,5, bisphosphate (PIP_2) to generate diacylglycerol (DAG) and inositol-1,4,5-triphosphate (IP_3). The produced inositol-1,4,5-triphosphate (IP_3) increases intracellular calcium levels via release of calcium from the endoplasmic reticulum, whilst DAG activates Protein Kinase C (PKC) dependent MAPK mediated responses(Grammatopoulos and Chrousos, 2002; Perrin *et al*, 2006; Chen *et al*, 2005; Fekete and Zorrilla, 2007).

A third CRF receptor subtype was identified by Arai *et al* (2001) in the brain of catfish species, termed catfish CRFR3 (cfCRFR3); but this receptor appears to be unique to the catfish and shares a high degree of homology with the catfish CRFR1 receptor – approximately 85% amino acid homology (Dautzenberg and Hauger, 2002; Fekete and Zorrilla, 2007; Arai *et al*, 2001). Figure 1.7 illustrates the principal CRFR signalling pathways.

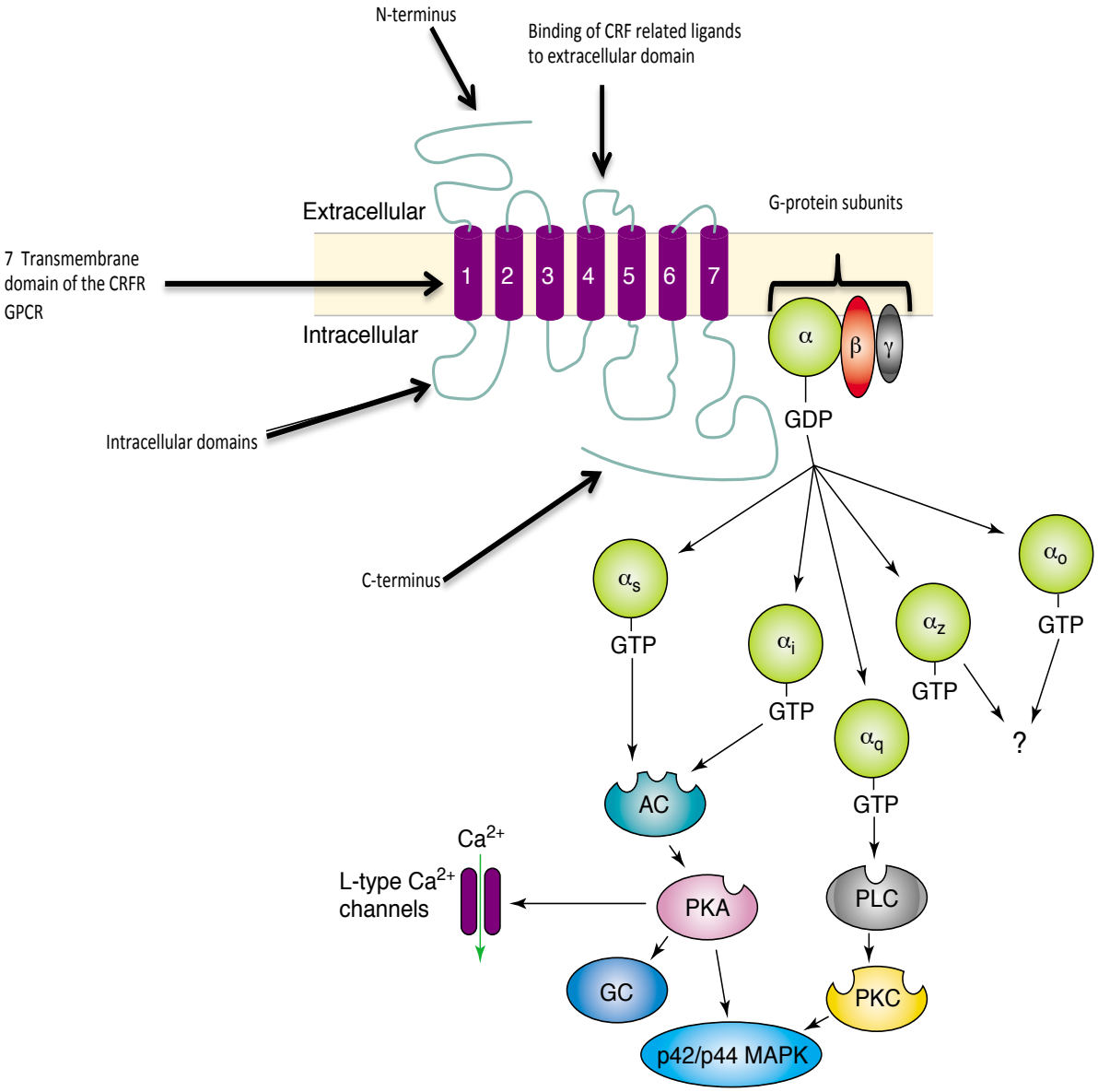

Figure 1.7: A schematic representation of the principal CRF receptor signalling pathways following interaction of CRF family peptides ligands (e.g. UCNI, CRF) to the CRF receptor. PKA=Protein Kinase A, PKC= Protein Kinase C, AC= adenylate cyclase, PLC= phospholipase C, GC= guanylate cyclase, GTP= guanosine triphosphate, GDP= guanosine diphosphate, MAPK= mitogen activated protein kinase, GPCR= G-protein coupled receptor, CRF= corticotropin releasing factor. Adapted from (Grammatopoulos and Chrousos, 2002).

1.5.1 Corticotropin Releasing Factor Receptor 1-(*CRFR1*)

In 1993, the first Corticotropin Releasing Factor Receptor denoted, *CRFR1,* was discovered by Chen *et al* (Chen et al, 1993). The human *CRFR1* gene has been localised to the long arm of chromosome 17 (17q12-q22) and consists of 14 exons and 13 introns (figure1.8), which span approximately 20kb (Zmijewski and Slominski, 2010; Hauger *et al*, 2006; Hillhouse and Grammatopoulos, 2006).

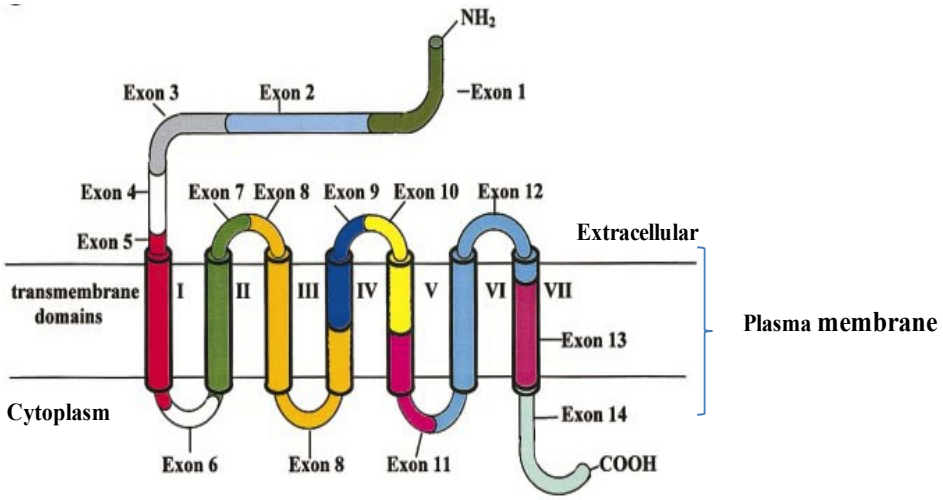

Figure 1.8: A diagrammatic representation of the *CRFR1* receptor exon organisation containing all 14 exons.
The 7 transmembrane domains of the *CRFR1* receptor are indicated (I, II, III, IV,V, VI, VII). NH_2= N terminus and COOH= C-terminus of the receptor. Adapted from: (Slominski *et al*, 2001).

To date, eight human, three rat, four mouse and nine hamster *CRFR1* mRNA transcripts have been identified, resulting from alternatively splicing of the *CRFR1* gene (Fekete and Zorrilla, 2007). Of the eight *CRFR1* human isoforms (*CRFR1*α, *CRFR1*β, *CRFR1c*, *CRFR1d*, *CRFR1e*, *CRFR1f*, *CRFR1g* and *CRFR1h*) shown in figure 1.9, only one, *CRFR1*α, is physiologically functional inducing signal transduction in its' resident human tissues (Fekete and Zorrilla, 2007; Hauger *et al*, 2006; Grammatopoulos and Chrousos, 2002). Consequently, the *CRFR1*β, and *CRFR1c-h* splice variants, all of which appear to lack ligand binding and/or signalling properties, are currently regarded as non-functional and thus not classified by the International Union of Pharmacology Committee on Receptor Nomenclature and Drug Classification (NC-IUPHAR) as receptor splice variants (Hauger *et al*, 2006; Hillhouse and Grammatopoulos, 2006; Hauger *et al*, 2003).

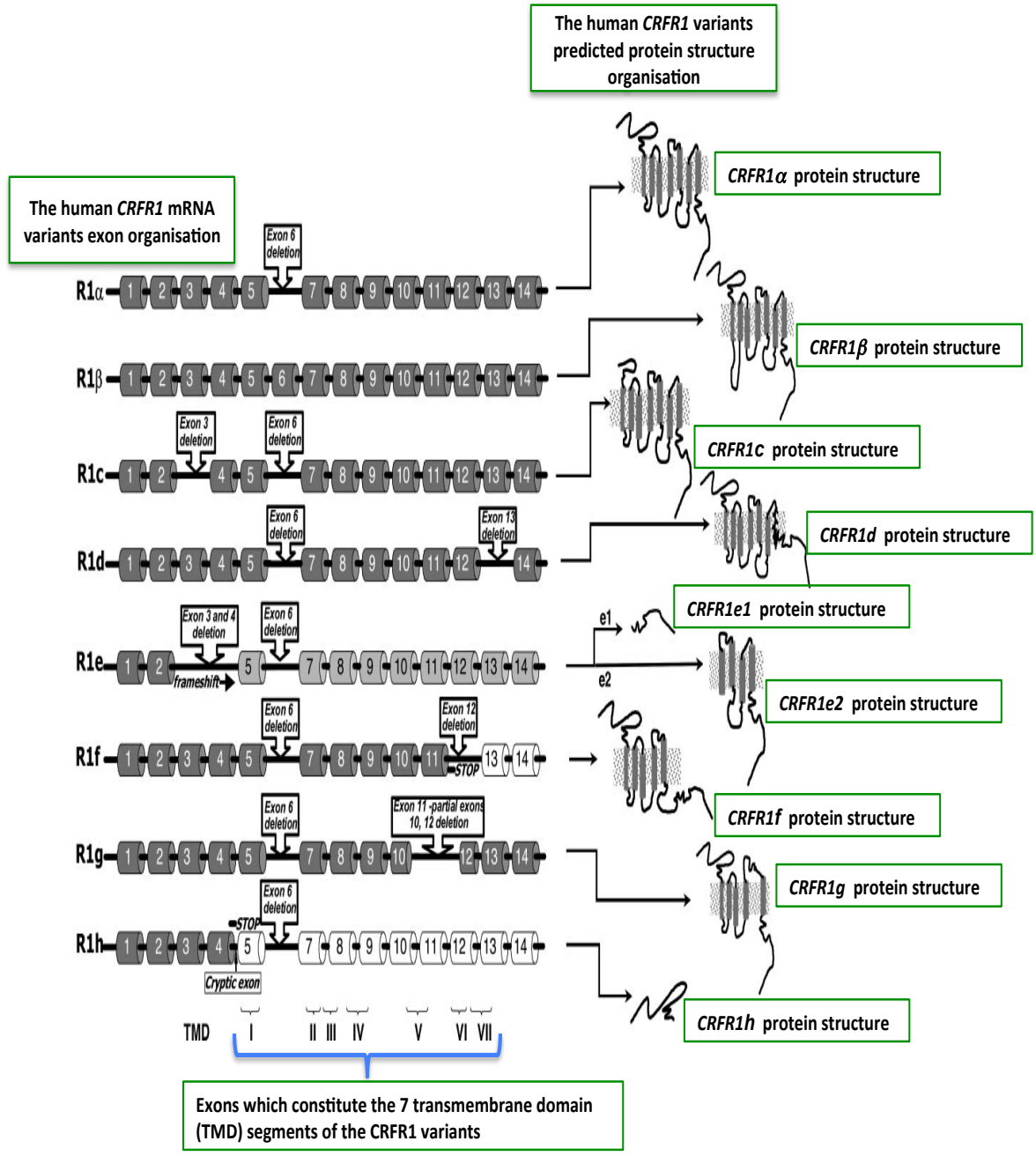

Figure 1.9: The eight human *CRFR1* receptor variants.
The diagram shows the schematic representation of the exon organisation and the structural differences of the potential protein structures of the human *CRFR1* receptor variants following alternative splicing of the *CRFR1* gene. Adapted from:(Hillhouse and Grammatopoulos, 2006).

Despite the fact that the variants other than CRFR1α are likely to be non-functional variants (as illustrated in figure 1.9), the predicted protein sequences for these results in receptor subtypes with varying agonist binding characteristics and signalling capabilities (Hillhouse and Grammatopoulos, 2006; Grammatopoulos and Chrousos, 2002). However, there is arising evidence to suggest that some of these variants may be generated in response to a variety of factors such as UV irradiation and cAMP (Pisarchik and Slominski, 2001; Zmijewski and Slominski, 2010).

The CRFR1 receptor is extensively expressed in the Central Nervous system (CNS) including the hippocampus, anterior pituitary and cerebral cortex and olfactory bulbs (Grammatopoulos and Chrousos, 2002) and has also been identified at a variety of sites in the periphery including the ovaries, testes, lungs, skin, placenta, spleen, arterial smooth muscle and foetal membranes and immune cells (Slominski *et al*, 2001; Dautzenberg and Hauger, 2002; Chen *et al*, 2005).

Whilst the mRNA expression of the isoforms has been widely demonstrated in the human periphery e.g. *CRFR1*α, *CRFR1*β, *CRFR1c* and*CRFR1d* in the pregnant myometrium (Slominski *et al*, 2001; Grammatopoulos *et al*, 1999) and *CRFR1g* in the skin, adrenal glands and pituitary (Pisarchik and Slominski, 2001), a lack of isoform specific antibodies for the non-functional variants means that their protein expression has yet to be confirmed.

The sole functional *CRFR1* variant, *CRFR1*α, contains 13 exons (following deletion of exon 6) producing a 415 amino acid protein. Exon 6, encodes for a 29 amino acid insert, which would normally be located in the first intracellular domain of the *CRFR1* transcript (see figure 1.8,) but with the exception of *CRFR1*β, this exon is absent in all of the *CRFR1* isoforms. Consequently, as the CRFR1α receptor remains functional it appears that exon 6 is not essential for physiological function (Slominski *et al*, 2001; Hillhouse and Grammatopoulos, 2006; Grammatopoulos and Chrousos, 2002) interacting predominantly with the G_s protein pathway that stimulates adenylate cyclase activation (Zmijewski and Slominski, 2010).

Conversely, the *CRFR1β* receptor, contains all 14 exons (see figure 1.9), and generates a 444 amino acid protein isoform and as a result it is also regarded as pro-*CRFR1*. The insertion of exon 6 renders this receptor non-functional resulting in an inability to bind ligands and impaired cAMP production (Hillhouse and Grammatopoulos, 2006; Zmijewski and Slominski, 2010).

The *CRFR1c* variant is produced from splicing out of exons 3 and 6 (see figure 1.9). Therefore this receptor is composed of 12 exons with 375 amino acids. Though the *CRFR1c* contains all the exons that encode for the 7 transmembrane domains of the *CRF* receptor, the stability of the extracellular domain is compromised by deletion of exon 3; consequently, this receptor subtype is incapable of ligand binding. In addition, experiments have also demonstrated that *CRFR1c* fails to stimulate signal transduction mechanisms (Grammatopoulos *et al*, 1999; Zmijewski and Slominski, 2010).

In addition to the deletion of exon 6, the further five *CRFR1* isoforms (*CRFR1d-h*) have been predicted to contain alterations within their seventh transmembrane domain resulting in modification to the structure of the predicted protein products (see figure 1.9). The *CRFR1d* receptor lacks exon 13, which encodes for the majority of the last transmembrane domain (see figure 1.8) resulting in this domain becoming shorter with a consequent distortion of the intracellular C-terminus and a failure to perform G-protein coupling and signal transduction (Grammatopoulos *et al*, 1999; Hillhouse and Grammatopoulos, 2006; Zmijewski and Slominski, 2010).

CRFR1e is predicted to exist in two isoforms (see figure 1.9). The first, designated CRFR1e1, is a truncated receptor devoid of transmembrane domains and is composed of 40 amino acids encoded by exons 1 and 2 and a further 154 amino acids derived from a coding sequence that has no homology to the other CRFR1 isoforms or known proteins. The second, designated CRFR1e2, is composed of 240 amino acids with a sequence which begins in the third transmembrane domain and therefore has no ligand binding domain (Zmijewski and Slominski, 2010; Grammatopoulos and Chrousos, 2002; Pisarchik and Slominski, 2001).

The *CRFR1f* and *CRFR1h* isoforms have no intracellular C-terminus domain due to a deletion of exons 12-14 and exons 5-14 respectively (see figure 1.9), which make their signal transduction capabilities questionable, although it is likely that both will retain the ability to bind ligands.

Finally, although the *CRFR1g* transcript conserves the original *CRFR1* reading frame and produces a C-terminus with the correct amino acid sequence, the deletion of exon 11 and partial deletion of exons 10 and 12 (see figure 1.9), would result in abnormal/ incomplete transmembrane domains and impaired signalling. It is likely however, that this variant would still retain ligand-binding properties (Zmijewski and Slominski, 2010; Grammatopoulos and Chrousos, 2002; Pisarchik and Slominski, 2001; Hillhouse and Grammatopoulos, 2006).

Though CRFR1 is expressed both in the brain and periphery it appears to be predominantly involved in regulating the physiological functions of the nervous system (Dautzenberg and Hauger, 2002) whilst the CRFR2 receptor may be more important in mediating actions in the periphery. Indeed, the CRFR2 receptor was first discovered following reports, which demonstrated that the effects of *CRF* may not be mediated via CRFR1 in the periphery (Dautzenberg and Hauger, 2002; Parkes and May, 2000).

1.5.2 Corticotropin Releasing Factor Receptor 2-(CRFR2)

The human *CRFR2*, which spans about 50kb, was mapped to the short arm of chromosome 7(p21-p15) (Hillhouse and Grammatopoulos, 2006; Grammatopoulos *et al*, 1999). The *CRFR2* mRNA transcript is slightly larger than *CRFR1* consisting of 15 exons (figure 1.10) and as a result of alternative splicing at the N terminus generates three human *CRFR2* variants: CRFR2α, CRFR2β and CRFR2γ all of which are functional; whilst two isoforms have been identified in rat; CRFR2α, CRFR2β (Hauger et al, 2006; Chen et al, 2005).

The *CRFR2*α variant contains exons 4-15 encoding for a 411 amino acid protein, whilst the *CRFR2*β containing exons 1,2 and 5-15 resulting a 438 amino acid protein. The *CRFR2*γ variant, the smallest of the three, contains exons 3 and 5-15 is a 397 amino acid protein (Slominski *et al*, 2001; Grammatopoulos and Chrousos, 2002). The *CRFR2*α variant is widely expressed in the human CNS (e.g. septum, thalamus, hippocampus and hypothalamus) and is also the main variant expressed in human peripheral tissues (e.g. lungs, skeletal muscle, and colonic mucosa of the gastrointestinal tract (GI) (Chen *et al*, 2005; Kuizon *et al*, 2009; Muramatsu *et al*, 2000).

CRFR2β is also found in the human CNS, particularly the septum, hippocampus and amygdala regions of the brain and it too is found in the periphery including the left atrium of the heart, and skeletal muscle, with lower levels in the GI tract (Slominski *et al*, 2001; Kostich *et al*, 1998; Kuizon *et al*, 2009; Muramatsu *et al*, 2000). The *CRFR2*β is the predominant isoform, which is expressed in the rat periphery, whilst the *CRFR2*α is the splice variant predominantly expressed in the rat brain (Chen *et al*, 2005). To date however, *CRFR2*γ expression has only been clearly identified in the human brain (predominantly in the Hippocampus and septum regions), although very low amounts of mRNA have been detected in the lungs (Slominski *et al*, 2001; Kostich *et al*, 1998)

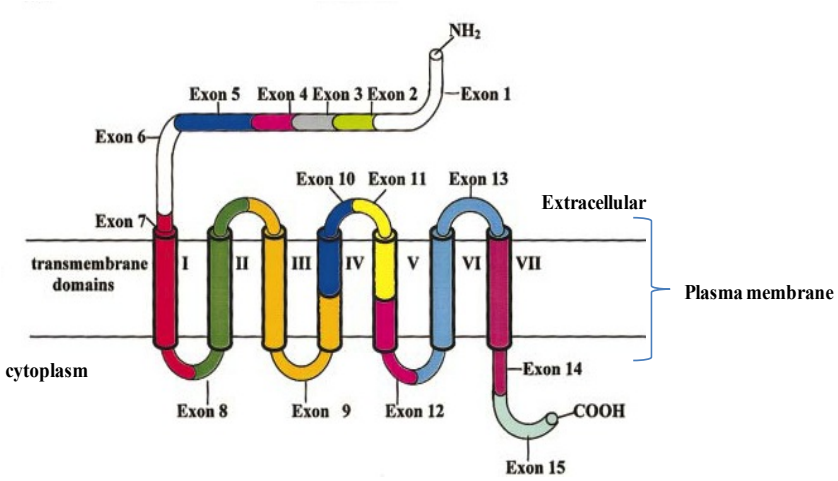

Figure 1.10: A diagrammatic representation of the *CRFR2* receptor exon organisation containing all 15 exons.
The 7 transmembrane domains of the *CRFR2* receptor are indicated (I, II, III, IV, V, VI, VII). NH_2= N terminus and COOH= C-terminus of the receptor. Adapted from: (Slominski *et al*, 2001).

1.6 Other UCNI mediated cytoprotection mechanisms

Evidence from the cardiovascular system would suggest that UCNI may affect cellular protection by acting, at least partly, through ion channels. Specifically, it has been suggested that UCNI may mediate its effects through two distinct types of ion channels, L-type calcium channels and inwardly rectifying potassium channels, both of which are involved in regulating intracellular cation concentrations and therefore resting membrane potential (Lawrence *et al*, 2002; Tao and Li, 2005a; Mobasheri *et al*, 2007).

In the case of the L-type calcium channel, it has been suggested that *UCNI* binding to this cell membrane channel may protect cells by reducing/preventing intracellular calcium overload (Tao and Li, 2005a), whilst UCNI upregulation of the Kir6.1 subunit of inwardly rectifying potassium channels has been shown to be involved in the prevention of cardiac myocyte death in response to ischaemia/re-perfusion injury (Lawrence *et al*, 2002).

Lawrence *et al*, (2002) demonstrated that *UCNI* induces expression of the Kir6.1 subunit in cardiac myocytes, potentially resulting in activation of the mitochondrial ATP sensitive potassium (mitoK_{ATP}) channels, the inhibition of which completely abrogated the cardioprotective effects of UCNI. Further work in 2004, indicated that activation of mitoK_{ATP} channels prevents/reduces mitochondrial damage potentially helping to protect the cardiac myocytes from apoptosis (Lawrence *et al*, 2004; Lawrence *et al*, 2002) via a CRFR dependent pathway.

The effects of UCNI on these ion channels, particularly the K_{ATP} channels, may therefore represent a possible chondroprotective mechanism, especially given the observations of Intekhab-Alam (2006) and Petsa (2007) who noted that the UCNI peptide appears to be more effective against SNAP induced cell death, a potential mitochondrially active pro-apoptotic stimuli.

1.6.1 The ATP sensitive potassium channels (K_{ATP} channels)

The ATP sensitive potassium (K_{ATP}) channel, a member of the Inwardly Rectifying Potassium channel family (K_{IR}), is a non-voltage dependent, potassium (K^+) selective channel which is regulated by intracellular ATP and ADP concentrations; the activation of which occurs when intracellular levels of ATP decrease (Shi *et al*, 2005; Mobasheri *et al*, 2007; Burke *et al*, 2008).

The K_{ATP} channels are present in a variety of tissues these include: pancreatic islet cells, skeletal muscle, heart, brain and vascular smooth muscle (Seino and Miki, 2003). Two types of K_{ATP} channels have been identified so far: those situated at the plasma membrane/sarcolemma (sarcK_{ATP} or cellK_{ATP}) and those on the inner mitochondrial membrane (mitoK_{ATP}). Though the structure of the mitoK_{ATP} remains uncertain, evidence from the sarcK_{ATP} channel suggests that K_{ATP} channels are hetero-octameric complex constituting of two protein subunits: a ~40kDa pore forming subunit, Kir6.x and a ~160kDa regulatory subunit, the sulfonylurea receptor (SURx). The principal Kir6.x isoforms are: *Kir6.1* and *Kir6.2*, and the SURx subunits existing in two main forms: SUR1, SUR2 (Burke *et al*, 2008; Shi *et al*, 2005; Moreau *et al*, 2005).

The K_{IR}6.x subunits: Kir6.1 and Kir6.2, are members of the Inwardly Rectifying K^+ (K_{IR}) channel family. They are classified as inwardly rectifier K^+ channels as the Kir6.x pore forming subunits are selective for K^+ which favour the flow of K^+ ions into the cell rather than out, favouring the maintenance of the resting membrane potential of the cell (Mobasheri *et al*, 2007; Bryan *et al*, 2007). The human *Kir6.1* gene is designated KCNJ8, for potassium inwardly-rectifying channel, subfamily J, member 8. It is approximately 9.7kb in length consisting of three exons and mapped to chromosome 12p11.23. The resulting *Kir6.1* subunit gene product composed of 424 amino acids, shares a 98% sequence homology at the amino acid level to the rat Kir6.1 (Inagaki *et al*, 1995; Aguilar-Bryan *et al*, 1998; Seino, 1999). The human *Kir6.2* gene, KCNJ11, approximately 8.6kb is localised to chromosome 11p14.3 and produces a 390 amino acid protein. The amino acid sequence homology between Kir6.1 and Kir6.2 is approximately 71%. Each Kir6.x subunit is composed of a K^+ selective pore loop flanked by two transmembrane

domains referred to as M1 and M2, the N and C-termini of which are located within the cell as cytoplasmic domains as illustrated in figure 1.11 (Aguilar-Bryan *et al*, 1998; Seino, 1999).

The SURx subunit is a member of the adenosine triphosphate (ATP) Binding Cassette (ABC) transporter family of proteins who utilise the energy released from ATP hydrolysis to adenosine diphosphate (ADP) to facilitate the transport of substances (e.g. ions and lipids) across membranes or regulate intracellular processes. Consistent with such role, the SURx subunit functions as regulatory subunits modulating the activity of the K_{ATP} channels in response to intracellular ATP concentrations (Burke *et al*, 2008; Seino and Miki, 2003).

The two predominant SURx isoforms: *SUR1* and *SUR2* are encoded for by separate genes, ABCC8 and ABCC9 respectively; interestingly both genes are located in close proximity to the Kir6.x genes. The gene, which encodes for the *SUR1*, ABCC8 cloned in 1995, contains 39 exons and is localised to chromosome 11(11p15.1) where the *Kir6.2* gene is mapped approximately 4.5kb downstream (Bryan *et al*, 2007; Seino, 1999; Aguilar-Bryan *et al*, 1998). Furthermore, the *SUR2* gene, ABCC9, composed of 38 exons is on chromosome 12(12p11.12) and is separated from the Kir6.1 gene by approximately 26.2kb. Consequently, it has been suggested that these genes were previously encoded for by a single gene (Seino, 1999; Aguilar-Bryan *et al*, 1998). The *SUR2* subunits exist in two major isoforms: *SUR2A* and *SUR2B*; though alternative splicing of each has been identified and characterised (Shi *et al*, 2005).

Structurally, the SURx subunits are composed of three transmembrane domains (TMD) namely: TMDO (the N-terminus transmembrane domain), TMD1 and TMD2 (the C-terminus transmembrane domain) with each domain consisting of five, six and six transmembrane spanning segments, respectively. The TMD0 domain is linked to TMD1 by a cytoplasmic loop referred to as L0 and interaction of L0 with the N-terminus of Kir6.x is shown to modulate opening of the K_{ATP} channel. The TMD1 and TMD2 domains also contain intracellular cytoplasmic loops named: Nucleotide binding domain 1 and 2 (NBD1 and NBD2) see figure 1.11; these NBD's contain binding sites for ATP. Upon hydrolysis of ATP to ADP, NBD2 binds ADP resulting in opening of the K_{ATP} channel.

Thus these domains are involved in regulating K_{ATP} channel opening (Burke *et al*, 2008). In addition to regulation by ATP concentrations, K_{ATP} channels can also be regulated by G-protein coupled receptors (Seino, 1999, Seino and Mikki, 2003). Typically, K_{ATP} channel consists of four $K_{IR}6.x$ (*Kir6.1* or *Kir6.2*) and four SURx subunits each (*SUR1* or *SUR2*) as shown in Figure1.11C (Shi *et al*, 2005; Moreau *et al*, 2005).

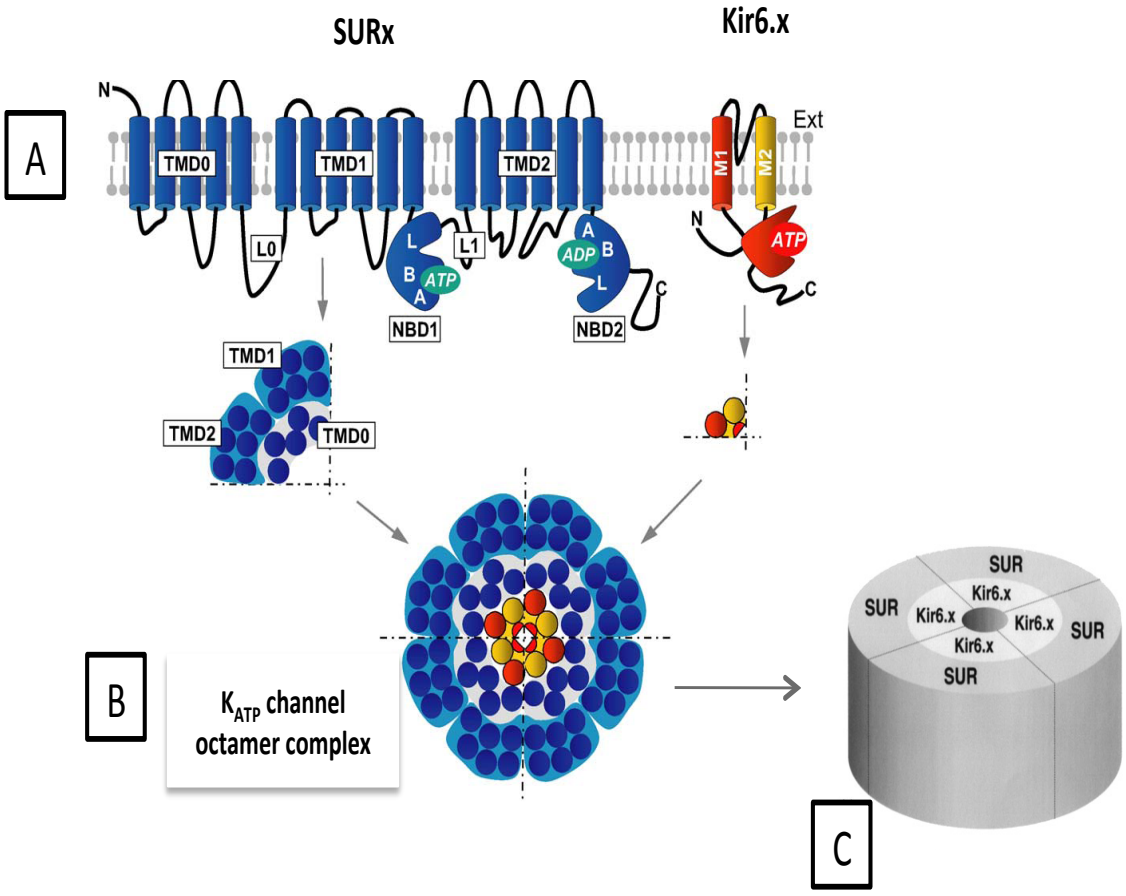

Figure 1.11: A schematic representation of the molecular structure of a K_{ATP} channel.
A: typically a K_{ATP} channel consists of SUR and Kir6.x subunits as shown in the membrane structure. The SUR has three transmembrane domains denoted: TMD0, TMD1, TMD2 each consisting of five, six and six membrane spanning regions respectively, whilst the Kir6.x subunits consist of two transmembrane domains M1 and M2. The SUR subunit cytoplasmic loops L0 and L1 are also indicated along with the cytoplasmic nucleotide binding domains NBD1 and NBD2 with the Walker A, B and Linker L consensus sequences incorporated. The ATP inhibitory binding site on the cytoplasmic domain of the Kir6.x subunit is also shown. **B**: the SUR and Kir6.x subunits exists in a 4:4 stoichiometry as shown here in the hetero-octamer complex to form a KATP channel which can function, **C**: assembly of the KATP channel hetero-octamer complex as represented in **B**. Adapted from: (Moreau *et al*, 2005; Seino and Miki, 2003).

Studies performed so far in other cell types indicate that the protective effects of UCNI may be mediated through any, or indeed all, of the mechanisms discussed. However, it is not yet known what upstream or downstream events of these pathways exist and whether the alternative mechanisms observed in cardiac myocytes play a significant role in UCNI mediated chondroprotection. Thus, the research proposed here is aimed at determining which, if any, of these mechanisms exists in chondrocytes and thus if they offer a potential route for therapeutic intervention in OA. With this in mind, the following aims detailed in section 1.7 have been developed.

1.7 Aims

The aims of this present study are as follows:

- To evaluate the paracrine/autocrine chondroprotective role of UCNI against NO induced apoptosis with the emphasis on mechanisms of action and effector systems.
- To investigate the mRNA expression of *CRF* receptors (*CRFR*) by C-20/A4 chondrocytes as potential cell surface targets for UCNI mediated chondroprotection
- To determine C-20/A4 chondrocyte mRNA expression of K_{ATP} channel subunits (*Kir6.x* and *SURx*) and their potential to constitute functional K_{ATP} channels that may act as downstream effectors involved in CRFR mediated chondroprotection.
- To explore UCNI regulation of detected CRF receptor variant(s) and K_{ATP} channels subunits, by quantitative PCR studies, to determine the relative mRNA expression of *CRF* receptors and K_{ATP} channel subunits in NO and UCNI treated C-20/A4 chondrocytes
- To examine the significance of K_{ATP} channels in the chondroprotective effects of UCNI by pharmacological manipulation with K_{ATP} channel modulators following SNAP/NO induced apoptosis

Chapter 2:

Materials and Methods

2 Materials and Methods

2.1 Materials:

2.1.1 Cells and Culture reagents:

2.1.1.1 The C-20/A4 Chondrocyte cell line

Prior to the development of stable human chondrocyte cell lines, the study of chondrocyte physiology and the mechanisms underlying degenerative joint pathologies was restricted principally, due to the lack of a reproducible source of human articular chondrocytes. Obtaining an adequate number of primary chondrocytes is difficult but moreover, human articular cartilage samples vary in condition and age resulting in data with high variability between different preparations. Furthermore, following expansion in primary cultures, adult human articular chondrocytes quickly become quiescent losing their cartilage specific phenotype altering their morphology and gene expression patterns (Goldring *et al*, 1994; Finger *et al*, 2003). As a consequence, immortalised chondrocyte cell lines have been established in an attempt to circumvent these issues.

Chondrocytes isolated from primary cultures of juvenile (human or animal) or embryonic origins (Goldring *et al*, 1986; Gerstenfeld *et al*, 1990; Adams *et al*, 1991) are considered to be more advantageous for immortalisation, as the chondrocyte phenotype is maintained for a longer period (Goldring *et al*, 1994). Previous efforts were made to develop immortalised cell lines using chondrocytes from rabbit (Thenet *et al*, 1992), rat (Horton *et al*, 1988) and human chondrosarcomas (Takigawa *et al*, 1989; Block *et al*, 1991) but these did not express the unique cartilage-specific components and thus were not perceived as ideal representatives for investigating differentiated chondrocyte physiology (Goldring *et al*, 1994).

The C-20/A4 is an immortalised human chondrocyte cell line, which was established in 1993 with chondrocytes from a specimen of rib cartilage discarded from surgical repair of pectus exacavatum. These normal chondrocytes isolated from the costal cartilage ofa5 year old male, were immortalised by transfection with vectors containing origin-defective Simian virus 40 large T antigen (SV40Tag)

on day 10 of primary culture. Following continuous passage from a single focus, the resulting immortalised cell line was designated: C-20/A4.

Following its' establishment, investigations on the C-20/A4 cells demonstrated that these cells displayed the polygonal cobblestone morphology (figure 2.1) and the differentiated phenotype typical of human chondrocytes such as the expression of various cartilage specific molecules: collagen type II, IX and XI. They were also capable of maintaining this morphology over continuous propagation for >80 passages when cultured in monolayer in 10% serum containing medium. Such a continuous proliferative capacity would imply a continuous supply of cells for experiments without a high risk of dedifferentiated cells (Goldring *et al*, 1994). As a result, the C-20/A4 chondrocytes constitute a representative model system to investigate chondrocyte function and their environment. However, this and other generated immortalised cell lines cannot replace primary chondrocytes entirely, as cell lines do have the capacity for dedifferentiation and so it is always recommended that experimental findings from immortalised culture systems be validated with primary chondrocyte cultures (Finger *et al*, 2003).

The C-20/A4 cell line was used for all investigations documented in this thesis and was a kind gift from Professor Mary B, Goldring, Hospital for Special Surgery, New York, USA.

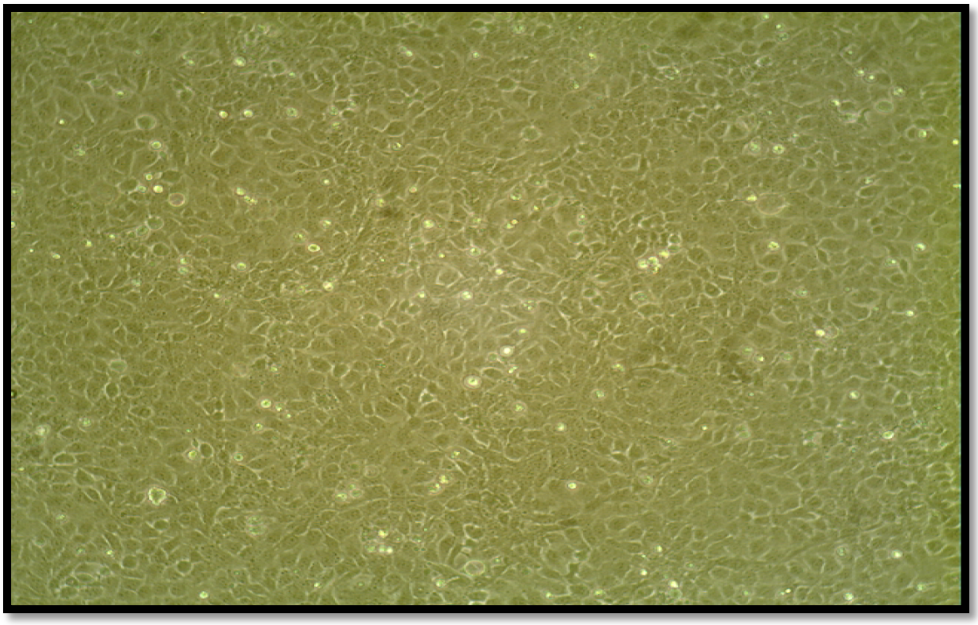

Figure 2.1: Light microscopy image (x 100 magnifications) of the C-20/A4 human chondrocyte cell line in culture

The C-20/A4 cell line displays the cobblestone morphology typical of human chondrocytes in primary culture. The chondrocytes were cultured in DMEM supplemented with 10% FCS.

2.1.1.2 Cell Culture materials for C-20/A4 chondrocytes:

The following cell culture reagents were supplied by Lonza, Wokingham, UK: Dulbecco's Modified Eagle's Medium (DMEM) with sodium pyruvate, 4.5 g/L glucose and without L-glutamine, penicillin-streptomycin mixture (10,000 units/ml potassium penicillin G/10,000 units/ml streptomycin sulphate), 1x Dulbecco's phosphate buffered saline (DPBS) without calcium (Ca^{2+}) and magnesium (Mg^{2+}), 10x trypsin-ethylenediaminetetraacetic acid (EDTA) [5 g/L trypsin, 2 g/L EDTA] solution and L-glutamine (200 mM) solution. Heat inactivated foetal calf serum (FCS) (South American origin) was purchased from Biosera Ltd, Ringmer, UK and dimethyl sulfoxide (DMSO) was from Sigma Aldrich, Poole, UK. Cell culture flasks 25 and 75 cm^2, 96 well tissue culture plates, Millipore Millex GP PES 0.2 μm sterile syringe filters, 50 ml and 15 ml centrifuge tubes, 10 ml and 25 ml disposable pipettes were all supplied by Fisher Scientific, Loughborough, UK; while the 6 well tissue culture plates and 2 ml CRYO.S cell freezing vials were purchased from Greiner Bio-one, Stonehouse, UK.

2.1.2 *In vitro* stimulation of C-20/A4 cells and Cell death Studies

S-nitroso-N-acetyl-L-penicillamine (SNAP) was from Ascent Scientific, Bristol, UK. Human UCNI, α helical Corticotropin Releasing Hormone (CRH) $_{(9\text{-}41)}$ [$\alpha hCRH_{(9\text{-}41)}$], Diazoxide and TOX-7 *In Vitro* Toxicology Lactate Dehydrogenase (LDH) assay kit, were from Sigma-Aldrich, Poole, UK. Southern Biotech Apoptosis™ Annexin V-Fluorescein isothiocyanate (FITC) conjugate (200 μg/ml stock solution, supplied in 1X binding buffer), Apoptosis™10X Annexin V binding buffer, Propidium iodide (100 μg/ml stock solution, supplied in PBS/sodium azide-NaN_3) were all purchased from Cambridge Bioscience Ltd, Cambridge, UK.

2.1.3 Reagents for molecular biology studies

2.1.3.1 RNA extraction, agarose gel electrophoresis (AGE) and sequence analysis

RNeasy® Mini kit, RNeasy® Plus Mini Kit, and Qiaquick® Gel Extraction kit were obtained from Qiagen Ltd, Crawley, UK. Ethidium bromide (10 mg/ml) and 50X tris base acetic acid EDTA (TAE) buffer (composed of Tris Base/Trizma Base, glacial acetic acid and disodium EDTA) were purchased from Sigma-Aldrich, Poole, UK. Molecular biology grade agarose, Hyperladder™ IV (100-1000 bp) DNA ladder and 5x sample loading buffer were from Bioline Ltd, London, UK.

2.1.3.2 Reverse Transcriptase-Polymerase chain Reaction (RT-PCR) and quantitative PCR (qPCR)

Omniscript® Reverse Transcriptase (RT) kit, Qiagen® RNase inhibitor 7,500 units (30 units/μl), *Taq* Polymerase Chain Reaction (PCR) master mix and Qiagen® one-step RT-PCR kit, were all supplied by Qiagen, Crawley, UK. Oligo-$(dT)_{15}$ primers (0.5 μg/μl) were from Promega Ltd, Southampton, UK. All reverse transcriptase-quantitative PCR (RT-qPCR) experiments were conducted using the Rotor Gene ™ SYBR® Green one-step RT-qPCR kit purchased from Qiagen Ltd, Crawley, UK.

The following forward and reverse primers used for PCR reactions were obtained from Sigma-Genosys, Poole, UK: *GAPDH*, *SUR1* and *SUR2*, whilst the *Kir6.1*, *Kir6.2*, *CRFR2*α, *CRFR2*β and *CRFR2*γ primers were purchased from MWG Biotech London, UK and the *UCNI*, *CRFR1*, *CRFR2* (generic), *SUR2A*, *SUR2A-*Δ*-14* and *SUR2B* were from Invitrogen, Fisher Scientific, Loughborough, UK.

The primer sets employed in RT-PCR experiments are detailed in table 2.1 and for qPCR in table 2.2. Where appropriate the primers were designed to span exonic splicing junctions to ensure that amplicon generation are from the mRNA avoiding amplification of genomic DNA (gDNA).

The following primer sets were designed using Primer 3 software version 0.4.0 (URL http://fokker.wi.mit.edu/primer3/) and primer specificity for their human targets were verified by input of the sequences into the Basic Local Alignment Search Tool (BLAST) (URL http://blast.ncbi.nlm.nih.gov/Blast.cgi): *Kir6.1*, *Kir6.2*, *SUR1*, *SUR2*, and *CRFR2* (generic) (see table 2.1). Primers which were designed using the PrimerBlast software (URLhttp://www.ncbi.nlm.nih.gov/tools/primer-blast/index.cgi) are as follows: *GAPDH*, *CRFR1*, *SUR2A*, *SUR2A-Δ-14*and *SUR2B* (see table 2.1.). The *CRFR2*α, *CRFR2*β and *CRFR2*γ primer sets were previously designed by Petsa (Petsa, 2007); whilst the *UCNI* primers were from published data by Takahashi (Takahashi *et al*, 1998) (see table 2.1). However sequences were verified for human specificity and expected amplicon sizes using the PrimerBlast Software.

2.2 Methods

2.2.1 C-20/A4 chondrocyte culture:

2.2.1.1 Recovery of C-20/A4 cells from frozen stocks

C-20/A4 cell stocks in 2 ml CRYO.S vials were stored in liquid nitrogen at -196 °C in chondrocyte freezing medium composed of: 50% FCS, 20% DMSO and 30% Dulbecco's Modified Eagle's Medium (DMEM). For the initiation of culture, a vial of C-20/A4 cells was recovered from liquid nitrogen, thawed, suspended in 10 ml of culture medium (see section 2.2.1.2) and centrifuged at 250 g for 10 min. The culture medium was aspirated and the pellet was re-suspended again in culture medium and centrifugation repeated to ensure complete removal of DMSO. The resulting pellet was then reconstituted in 7 ml of culture medium and incubated at 37 °C, 5% CO_2 in a 25 cm^2 flasks. The medium was replaced after approximately 24 hrs to remove dead cells and the culture then grown to confluence.

2.2.1.2 Continuous culture conditions for C-20/A4 cells

The C-20/A4 chondrocytes were cultured in DMEM supplemented with 10% FCS, 1% L-glutamine and 1% penicillin/streptomycin. Cell viability and confluence was observed by light microscopy and when fully confluent (normally achieved within 3 - 4 days), the cell culture medium was aspirated and cells rinsed with 10 ml of Ca^{2+} and Mg^{2+} free dulbecco's phosphate buffered saline (DPBS) followed by treatment with 5 ml of 1x trypsin-EDTA solution for 2 min to detach cells from tissue culture flasks. Inactivation of trypsin-EDTA was achieved by adding an equal volume of fully supplemented culture DMEM (mentioned above) and the resulting cell suspension was centrifuged at 250 g, for 10 min, at room temperature. Following aspiration of the supernatant, the obtained pellet was re-suspended in fresh culture medium and subcultured at a 1:2 split ratio.

Culturing was routinely performed in 75 cm^2 tissue culture flasks in a total volume of 15 ml per vessel and subculture was conducted twice weekly. The C-20/A4 monolayer cultures were maintained at 37°C in the presence of 5% CO_2 in a Galaxy S Carbon dioxide humidified incubator (Wolf Laboratories, York, UK). All tissue culture was carried out in a BIOAIR Aura 2000 class II cabinet (Wolf Laboratories, York, UK) and cells were checked daily for morphology, bacterial or fungal infection by observation of media colour and microscopic examination. Cells were used between passages 5-30 for experiments after which cultures were terminated and fresh cultures initiated as before (see section 2.2.1.1). C-20/A4 cells used in either cell death experiments or total RNA preparations were harvested in the same manner.

2.2.1.3 Preparation of cells for storage

To ensure a continuous supply of cells for future use, C-20/A4 cells were routinely stored in liquid nitrogen as this ensures good viability of cells following long-term storage. C-20/A4 chondrocytes were harvested as detailed in section 2.2.1.2 and following centrifugation, the pellet was re-suspended in 6 ml of freezing medium (composition: 50% FCS, 20% DMSO and 30% DMEM) and 2 ml aliquots placed in CYRO.S freezing vials. The vials were then frozen at -80 °C in a "Mr Frosty" freezing chamber (Merck, Leicester, UK) containing 200 ml of isopropanol (to ensure a controlled rate of freezing) for a minimum of 24 hrs and subsequently transferred into liquid nitrogen storage.

2.2.2 *In vitro* stimulation of C-20/A4 chondrocytes

In vitro stimulation of cells for cell death assays (apoptosis and necrosis studies) and quantitative PCR, was performed on chondrocytes seeded into 6 well tissue culture plates at a density of 4.5 $x10^5$ cells/well to reach approximately 70-80% confluency (~$5x10^5$ cells/well). The cells were then serum starved overnight prior to treatment, by replacing normal growth medium with medium containing 1% FCS.

Cells were then treated for 6hrs in culture medium supplemented with 1% FCS and the appropriate treatment: SNAP, UCNI, Diazoxide, α-helical $CRH_{(9-41)}$ alongside an untreated control. The following treatment conditions for experimental assay were established: control (untreated), UCNI (10^{-8} M), SNAP (10^{-3} M), α-helical $CRH_{(9-41)}$ (10^{-8} M), Diazoxide (10^{-4} M), SNAP (10^{-3} M)+UCNI (10^{-8} M), SNAP (10^{-3} M)+UCNI (10^{-8} M)+α-helical $CRH_{(9-41)}$ (10^{-8} M) and SNAP (10^{-3} M)+Diazoxide (10^{-4} M). The control cells (untreated) were supplemented with fresh 1% FCS culture medium for the duration of the treatment.

Stock solutions for each reagent were prepared as follows: SNAP was reconstituted at a stock concentration of 10^{-1} M in ethanol, UCNI at a stock concentration of 10^{-4} M in DMEM, Diazoxide was dissolved at stock concentration of 10^{-1} M in 0.1 M Sodium Hydroxide (NaOH) and α-helical $CRH_{(9-41)}$ at stock concentration of 2.5 x 10^{-5} M in 1%(v/v) acetic acid (in distilled water). The solutions were stored at -80 °C.

Following treatment, C-20/A4 cells were harvested and prepared either for Flow cytometry analysis or total RNA extraction as detailed in sections 2.2.3.1, 2.2.3.2 respectively. An aliquot of treatment medium was removed and stored at -80 °C for LDH Release Assay (section 2.2.4).

2.2.3 Cell death induction experiments

The assessment of apoptosis in C-20/A4 chondrocytes following treatment with various stimuli was determined by Annexin-V-FITC/Propidium iodide (PI) labelling in conjunction with flow cytometry. The LDH release assay was performed on spent media to assess necrosis.

The Annexin-V-FITC/PI labelling is based on the observation that during the early stages of apoptosis the phosphatidylserine (PS) phospholipids normally located on the inner leaflet of the plasma membrane become translocated to the outer surface of the membrane following loss of plasma membrane symmetry. This externalisation of PS to the extracellular environment can be detected by the binding of Annexin V a calcium dependent phospholipid binding protein with a high

affinity for PS. Visualisation of this binding of Annexin V to the PS residues can be achieved by conjugating Annexin V to a fluorochrome such as Fluorescein isothiocyanate (FITC) see figure 2.2. In addition, following loss of membrane integrity that may occur in the latter stages of programmed cell death apoptotic cells may permeable to PI. Consequently, based on the principle of Annexin-V-FITC/PI labelling: viable cells (Annexin-V-FITC negative/PI negative), early apoptotic (Annexin-V-FITC positive/PI negative) and late apoptotic cells (Annexin-V-FITC positive/PI positive) can be detected and visualised by flow cytometry analysis.

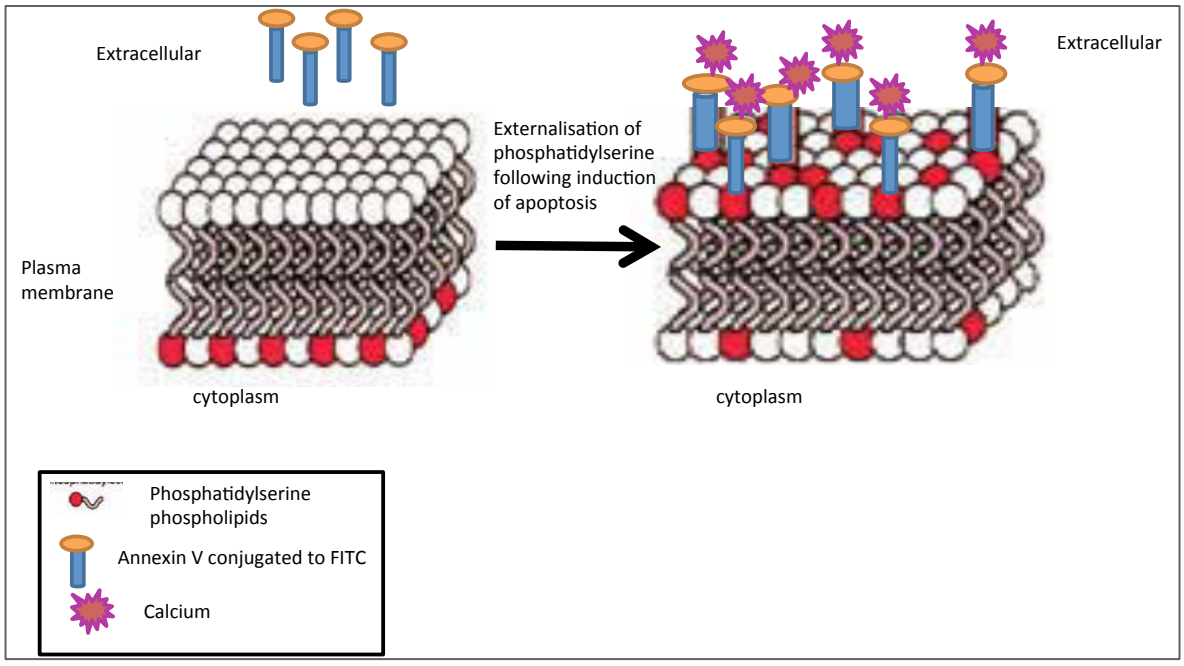

Figure 2.2: A schematic representation of Annexin-V-FITC conjugate calcium dependent binding to PS following its externalisation to the extracellular surface of plasma membrane. Adapted from: (www.abgab.com).

The LDH release assay was developed by Wroblewski and Ladue in 1995 (Wroblewski and Ladue, 1955) and since then, the assay has been routinely used as a method of assessing cell viability. LDH is a cytosolic enzyme which is released from cells following loss of plasma membrane integrity and this release of LDH into the cell culture medium results in the reduction of NAD^+ to NADH which

subsequently catalyses the conversion of a tetrazolium dye to a coloured compound, the absorbance of which may be measured spectrophotometrically at 490 nm.

Cell death experiments for apoptosis and necrosis determination were conducted on the following treatment conditions: control (untreated), UCNI (10^{-8} M), SNAP (10^{-3} M), α-helical $CRH_{(9-41)}$ (10^{-8} M), Diazoxide (10^{-4} M), SNAP (10^{-3} M)+UCNI (10^{-8} M), vehicle control (1% ethanol), SNAP (10^{-3} M)+UCNI (10^{-8} M)+α-helical $CRH_{(9-41)}$(10^{-8} M) and SNAP (10^{-3} M)+Diazoxide (10^{-4} M). The preparation of samples for flow cytometry and LDH assay analysis is detailed below.

2.2.3.1 Detection of apoptosis in C-20/A4 chondrocytes byAnnexin-V-FITC/PI labelling using Flow cytometry

Initial optimisation of flow cytometry protocol was performed by a 4-tube protocol: tube 1: unstained cells (cells in 500 μl of Aposcreen™ 1X Annexin V binding buffer without staining); tube 2: stained cells with Annexin-V-FITC only; tube 3: cells stained with PI only and tube 4: Annexin-V-FITC and PI labelled cells. Optimisation was required to establish the correct voltage for focusing the light emission from the flourochromes onto the photon detectors and to establish the fluorescence compensation on the flow cytometer used in post data analysis.

Following protocol optimisation, apoptotic cell death in C-20/A4 chondrocytes was determined using the Southern Biotech Aposcreen™ Annexin-V-FITC apoptosis detection reagents. Following appropriate treatment for 6 hr in 6 well tissue culture plates chondrocytes were harvested as follows: the supernatant (containing spent media and detached cells) was removed and the adherent cells were then rinsed with 1 ml DPBS all of which was collected. Adherent cells were released by trypsinisation (see section 2.2.1.2) and both supernatants and the adherent cells were combined and centrifuged at 250 g for 10 min and there after the supernatant was carefully and completely aspirated.

The resulting pellet was re-suspended in 1 ml cold dulbecco's phosphate buffered saline (DPBS) to remove any remnants of culture medium used to deactivate the trypsin and centrifuged at 4 °C, 250 g for 5 min. Following centrifugation the DPBS was aspirated, cells were disaggregated by gently flicking the pellet and re-suspended in 100 μl ofAposcreen™1X Annexin-V binding buffer. The tubes were placed on ice and 5 μl of Aposcreen™ Annexin-V-FITC conjugate (0.5 μg/ml) added to each, mixed and incubated in the dark for 15 min. A further 390 μl of Aposcreen™1X Annexin V binding buffer was then added to each tube followed by 5 μl of Propidium iodide (1 μg/ml) and gently agitated. Samples (500 μl total volume) were analysed immediately by flow cytometry on a Cyan™ ADP flow cytometer (Dako Cytomation, Ely, UK).

Subsequent unstained samples were prepared following protocol optimisation for each experiment, and consisted of cells in 500 μl of Aposcreen™ 1X Annexin V binding buffer without Annexin-V-FITC and PI staining. This cell population was required for the post-analysis of data to properly determine the quadrant regions used for estimating the viable, early and late apoptotic cell populations generated from the FITC and PI fluorescence channels. A total of ~$5.5x10^5$ cells were prepared for each sample of which 10,000 cells/events were counted and analysed per experimental condition. Cells were gated on forward scatter (FSC) and side scatter (SSC) dot plot histogram to exclude cellular debris. Percentage apoptosis was determined from the 10,000 cells/events gated into four subpopulations/quadrants (viable cells, early apoptotic, late apoptotic and necrotic) and the number of events/cells in each quadrant represents the number of apoptotic or viable cells.

Analysis of flow cytometry data was performed using Summit v4.3 software (DakoCytomation, Ely, UK).

2.2.3.2 LDH release assay for the assessment of necrosis in C-20/A4 chondrocytes

The levels of necrosis in chondrocytes following stimulation were determined using the TOX-7 *In Vitro* Toxicology Lactate Dehydrogenase (LDH) assay kit according to manufacturers' protocol.

Briefly, an aliquot of spent medium was removed following treatment and centrifuged at 250 g for 4 min to pellet any suspended cells. The LDH assay mixture was then prepared by mixing equal volumes of LDH Assay substrate solution, LDH Assay Dye solution and 1x LDH Assay Cofactor Preparation.

A volume of 50 μl of spent medium was added to the wells of 96 well plates and 100 μl of the LDH assay mixture added to each sample. The plate was incubated at room temp in the dark for 30 min and reaction subsequently terminated by adding 15 μl of 1 M Hydrochloric acid (HCl) to each well. Cell culture medium containing 1% heat inactivated FCS was added to several wells on the 96 well plate to obtain a background absorbance reading.

Absorbance of the samples was read spectrophotometrically at 490 nm using a THERMOmax plate reader ROM version 1.72 (Molecular Devices, Hampshire, UK) and a background absorbance was read at 690 nm. LDH release (OD units) was calculated by subtracting the background absorbance at 690 nm from the initial 490 nm measurement.

2.2.4 Total RNA isolation from C-20/A4 chondrocytes

For Reverse Transcriptase-PCR (RT-PCR), total cellular RNA was extracted and purified from the C-20/A4 chondrocytes using the Qiagen RNeasy® Mini extraction kit according to the manufacturers' protocol. Extraction and purification of total cellular RNA for RT-qPCR experiments was conducted using the Qiagen RNeasy® Mini Plus kit, which includes a gDNA elimination step, according to manufacturers' protocol. In brief, cells were rinsed with DPBS and disassociated via trypsinisation as detailed in section 2.2.1.2 and following centrifugation the medium aspirated, the pellet disrupted by flicking the tube and the appropriate volume of lysis buffer

added from the Qiagen RNeasy® Mini or Mini Plus kit. Subsequent addition of appropriate extraction reagents and centrifugation steps resulted in the elution of the total RNA from the spin column membrane into 30-50 μl of PCR grade water which was then stored at -80 °C.

RNA purity and concentration (ng/μl) was determined by measuring the Optical Density (OD) of OD 260/280 using the Thermo Scientific NanoDrop™ 1000 v3.7.1 (Fisher Scientific, Loughborough, UK) an OD 260/280 average absorption ratio typically between 1.8 and 2, generally suggests that the extracted RNA is largely undegraded, pure and of good quality free of protein interference (Fleige and Pfaffl, 2006).

RNA integrity was verified electrophoretically (on a 1% (w/v) agarose gel electrophoresis (AGE) in TAE) by ethidium bromide (200 ng/ml) staining and the 18S and 28S ribosomal RNA bands visualised by a UV transilluminator (UViTec, Cambridge, UK).

2.2.5 Reverse Transcriptase-Polymerase Chain reaction (RT-PCR)

RT-PCR was performed both as two-step RT-PCR and one step RT-PCR. Initially, two-step PCR (where cDNA generation from mRNA was performed in a separate tube from the PCR reaction) was used to determine the optimum annealing temperature for designed primer sets. This optimisation was conducted by gradient PCR where using an Eppendorf Mastercycler PCR machine generated PCR products from each tube given a different annealing temperature (55 °C±10).

However, with the development of one-step RT-PCR kits by Qiagen Ltd (Crawley, UK), which enables reverse transcription, and PCR amplification to occur at a highly sensitive and specific rate with less need for reaction optimisation the method of PCR was changed from two-step RT-PCR to one-step RT-PCR. The Qiagen one-step RT-PCR kit ensures efficient RT-PCR in a variety of ways, these include: firstly, the reverse transcriptase enzymes (Qiagen Ominiscript and Sensiscript) which has a high specificity for any RNA templates facilitating the transcription to cDNA even in the presence of secondary structures which would

otherwise cause lack efficient of cDNA synthesis. Secondly, a Hotstart *Taq* DNA polymerase enquires which requires initial activation at 95 °C ensuring specific PCR amplification. Thirdly, a RT-PCR buffer with a balanced combination of cations ensuring minimal PCR optimisation and Q solution which facilitates the amplification of RNA and cDNA templates which are otherwise difficult to amplify.

2.2.5.1 Two-step RT-PCR

cDNA synthesis from C-20/A4 mRNA was performed using the Qiagen® Ominiscript® Reverse Transcriptase (RT) kit according to manufacturers' protocol. In brief, 2 μg of total RNA was reverse transcribed into cDNA in a total reaction volume of 20 μl containing 2 μl of 10 μM oligo $(dT)_{15}$ primer (0.5 μg/μl), 2 μl 10x Qiagen® RT buffer, 2 μl dNTP mix, 1 μl Qiagen RNase inhibitor (10 units/μl), 1 μl Omniscript RT enzyme and RNase free water (variable volume). The oligo (dT) primers and RNA were initially incubated at 70 °C for 10 min to denature secondary RNA structures and allow annealing of primer to RNA template. cDNA generation was performed for 1 hr at 37 °C with subsequent storage at -20 °C until required.

Gradient PCR was conducted for *GAPDH*, *Kir6.1*, *Kir6.2* and *UCNI* using the Qiagen® *Taq* Polymerase Chain Reaction (PCR) Master Mix according to manufacturers' protocol. Briefly, cDNA was amplified by PCR in a total reaction volume of 25μl containing 5 μl of cDNA (20 ng/μl), 12.5 μl 2X Qiagen *Taq* PCR master mix, 5.5 μl water and 1 μl each of forward and reverse gene specific primers (10 μM each). A negative control was also prepared for each PCR reaction containing all the above reagents but replacing cDNA with water to detect any contamination of PCR reagents.

PCR was performed using an initial denaturation of 94 °C for 3 min with amplification settings of 94 °C for 1 min, 55 °C ±10 (i.e. 45-65 °C) for 1 min (primer annealing), 72 °C for 1 min (for elongation) and a terminal elongation step of 72 °C for 10 min. Products from PCR amplification were electrophoresed through a 2% (w/v) agarose gel (in 1x TAE buffer) containing ethidium bromide and visualised

under a UV transilluminator (UViTec, Cambridge, UK). The number of PCR cycles for each gene is detailed in table 2.1.

2.2.5.2 One-step-RT-PCR

The Qiagen® one-step RT-PCR kit was used for the PCR amplification of total RNA isolated from C-20/A4 chondrocytes and was performed according to manufacturers' protocol in a total volume of 50 μl containing: 10 μl 5x Qiagen® one-step RT-PCR buffer, 2 μl dNTP mix (with 10 mM of each dNTP), 10 μl 5x Q-Solution, 3 μl each of forward and reverse primer (10 μM each), 2 μl Qiagen® one-step RT-PCR enzyme mix and RNase free water (volume variable). An RNase inhibitor was not required in the reaction mixture as the one-step RT-PCR buffer contains RNase inhibitory components. A negative control was also prepared for every RT-PCR experiment, the negative control contained all the above reagents but replacing RNA template with water to detect any contamination of PCR reagents. *GAPDH* (glyceraldehyde 3 phosphate dehydrogenase) was used as the reference gene.

The PCR program for one-step RT-PCR consisted of 3 sections:(1) reverse transcription: 50 °C for 30 min (for cDNA synthesis from mRNA using gene specific primers), (2) 95 °C for 15 min (inactivation of RT enzymes, initial denaturation of cDNA template and activation of Hotstart *Taq* DNA Polymerase PCR enzyme), and (3) three-step PCR cycling: 94 °C for 1 min, primer annealing 58 °C for 1 min, 72 °C for 1 min and a terminal elongation step of 72 °C for 10 min. Products from PCR amplification were electrophoresed through a 2% (w/v) agarose gel (in 1x TAE buffer) containing ethidium bromide and visualised under a UV transilluminator (UViTec, Cambridge, UK). The number of PCR cycles for each gene is detailed in table 2.1.

One-step RT-PCR was performed for the following mRNA targets: *CRFR1*, *CRFR2*, *CRFR2α, CRFR2β, CRFR2γ*, *SUR1*, *SUR2*, *SUR2A*, *SUR2A-Δ-14* and *SUR2B*. Details of the forward and reverse primers used for RT-PCR and their cycling conditions are detailed in table 2.1.

The *CRFR1* forward and reverse primers were designed to distinguish between the two isoforms of this gene. A 280 bp product denotes *CRFR1*α mRNA expression whilst a 367 bp product signifies *CRFR1*β. All *CRFR2* isoforms (α, β, & γ) primers share the same common reverse primer (see table 2.1).

2.2.5.3 Preparation of PCR products for sequence analysis

The PCR products generated from one-step and two-step PCR amplification were excised from a 2% agarose gel and isolated using the Qiaquick® Gel Extraction kit according to manufacturers' protocol. The resulting PCR products were verified by sequence analysis conducted by GATC Biotech, London, UK in which PCR fragments were sequenced from both ends (forward and reverse) and homology to human their human targets verified by the input of sequences into BLAST (URL:http://blast.ncbi.nlm.nih.gov/Blast.cgi).

Gene	Accession Number	Forward primer	Reverse primer	Expected product size, (bp)	Annealing temperature, °C	PCR Cycles
GAPDH **	NM 002046	5' GCCAAAAGGGTCATCATCTC 3'	5' GGTGCTAAGCAGTTGGTGGT 3'	131	60	**30**
Urocortin I ***	NM 003353	5' CAGGCGAGCGGCCGCG 3'	5'CTTGCCCACCGAGTCGAAT 3'	146	57	**33**
Kir6.1*	NM 004982	5' GCTTTGTGTCCATTGTGACTG 3'	5' GCTGTCATGATTCCGATGTG 3'	312	60	**35**
Kir6.2*	NM 000525	5' ATGATCATCAGCGCCACCAT 3'	5' CACCACGCCTTCCAGGAT 3'	249	60	**35**
SUR1*	NM 000352	5' CGATTTAACCTGGACCCTGA 3'	5' GGCTGTCATCACCACCTTTT 3'	273	58	**45**
SUR2*	NM 005691	5' TTCTGGATTGGTAGGCTTGG 3'	5' TTGATCTCCCCTTCTTGTGG 3'	207	58	**45**
SUR2A **	NM 005691	5' CCGTGTCTCTTCTATTATGGATGCAGG 3'	5' GCCATTCTTGTGGGCGAGCAA 3'	103	58	**45**
SUR2A-Δ-14 **	NM 020298	5' TCTCTTGAGTGATGAGATTGGTGACGA 3'	5' TCCATTTGTGACAACTCCAGTGTGCTT 3'	100	58	**45**
SUR2B **	NM 020297	5' TGACGGCAGACCTGGTTATTGTGA 3'	5' TGTCTGCGCGAACAAAAGAAGC 3'	114	58	**45**
CRFR1 **	NM004382	5' ACAAACAATGGCTACCGGGA 3'	5' GGACCACGAACCAGGTGGCG 3'	280 or 367	58	**45**
CRFR2*	NM 001883	5' AGCCCATTTTGGATGACAAG 3'	5' AGGTGGTGATGAGGTTCCAG 3'	180	58	**45**
CRFR2α §	NM 001883	5 'TCCACAGCCTGCTGGAGGCC 3'	5' CTCCAAGCATTCTCGATAGGC 3'	239	58	**45**
CRFR2β §	NM 001202475	5' CCTCCTCTACGTCCCACACC 3'	5' CTCCAAGCATTCTCGATAGGC 3'	310	58	**45**
CRFR2γ §	NM 001202481	5' TGGGAAGAGAGCCTTGGCC 3'	5' CTCCAAGCATTCTCGATAGGC 3'	212	58	**45**

Table 2.1: Sequences and conditions of primers sets employed in one-step and two-step RT-PCR experiments.
Key: *= primers designed using Primer3 primer design software, **= primers designed using PrimerBlast software, §= primers previously designed by Petsa (2007), ***= primers published by Takahasi *et al*, 1998)

2.2.6 Quantitative PCR (qPCR) studies

qPCR was conducted to determine any changes in expression of *CRFR1*, *CRFR2*, and *Kir6.1*m RNA following treatment of C-20/A4 chondrocytes with various stimuli and specifically to determine whether UCNI mediates cytoprotective effects in chondrocytes by altering expression of these genes. For the qPCR experiments conducted herein, relative expression analysis was performed using the Comparative C_q (or $2^{-\Delta\Delta C}{}_q$) method which requires that PCR efficiencies of both target and reference genes are similar or within 10% of each other as this ensures reproducible results and the most accurate estimation of gene expression levels (Schmittgen and Livak, 2008).

Therefore, to commence qPCR studies, standard curves were generated for the target and reference genes and the log of amount of RNA template (on the x-axis) plotted against the C_q values of the target and reference genes (on the y-axis). The PCR efficiency is the calculated where: $E= 10^{(1/m)}-1$; where E=PCR efficiency, m=slope of the line. If the slope of the resulting line is less than 0.1 or the PCR efficiencies are within 10% of each other; this demonstrates that the PCR efficiencies of the target and reference genes are comparable and so the Comparative C_q method can be used for the relative quantification of changes in gene expression (Schmittgen and Livak, 2008). Alternatively, if the PCR efficiencies are not comparable, the Relative Expression Software Tool (REST) can be used as a method of analysis. The REST mathematical model for relative quantification contains an efficiency-corrected calculation program which would provide a more accurate quantification of the relative expression of gene targets (Pfaffl, 2001). However, REST, has been suggested to be more beneficial in analysing qPCR data with large quantities of samples and gene targets (Wong and Medrano, 2005).

Standard curves for the target (*CRFR1*α, *CRFR2*, *Kir6.1*) and reference (*GAPDH*) genes was constructed using the Rotor Gene™ SYBR® Green one-step reverse transcriptase-quantitative PCR (RT-qPCR) kit (Qiagen Ltd, Crawley, UK) according to the manufacturers' protocol. This kit allows reverse transcription of

mRNA to cDNA and consequent amplification of this cDNA in a single tube using a combined primer annealing and extension time. The one-step RT-qPCR reaction buffer contains the Q-bond additive, which strongly increases the affinity of the Taq DNA Polymerase to short single stranded DNA, and so primer and polymerase will bind together to the cDNA template immediately forming the ternary complex (primer/*Taq* DNA polymerase to template complex) in one step allowing primer extension to take place with high specificity.

For the standard curves a final concentration of 100, 80, 60, 40 and 20 ng/reaction of total RNA was used. RT-qPCR was conducted in a total volume of 25 μl containing: 12.5 μl of 2x Rotor Gene SYBR green RT-PCR master mix, 1.25 μl of forward and reverse gene specific primer (10 μM each), 0.25 μl Rotor Gene RT mix, RNase free water (variable) and total RNA corresponding to the required final concentration of RNA mentioned above. For the standard curve generation, each RNA concentration was performed in triplicates. The PCR efficiency readings from the standard curves generated for *GAPDH*, *Kir6.1*, *CRFR1* and *CRFR2* were as follows: 99%, 95%, 99% and 97% respectively.

RT-qPCR was performed using the following cycling conditions:(1) reverse transcription: 55 °C for 10 min (for cDNA synthesis from mRNA using gene specific primers), (2) 95 °C for 5 min (inactivation of RT enzymes, initial denaturation of cDNA template and activation of Hotstart *Taq* Plus DNA Polymerase), and (3) two-step PCR cycling: 95 °C for 5 sec, combined primer annealing and extension 60 °C for 10 sec (*GAPDH*) or 20 sec (*Kir6.1*, *CRFR1*α and *CRFR2*β). All Real Time PCR cycling was performed using the Rotor-Gene Q 2plex HRM System PCR machine (Qiagen Ltd, Crawley, UK). A melt curve analysis of PCR amplicons was performed to determine specificity of primers. Details of the forward and reverse primers used or RT-qPCR, their conditions and number of PCR cycles are detailed in table 2.2.

2.2.6.1 qPCR for the relative quantification of Gene expression

qPCR was conducted to determine changes in relative expression of *Kir6.1*, *CRFR1* and CRFR2 mRNA in chondrocytes following treatment with UCNI, SNAP and SNAP+UCNI. One-step RT-qPCR was conducted on 100 ng of total RNA using the Rotor Gene SYBR Green one-step RT-qPCR kit according to manufacturers' protocol using the reagent volumes and RT-qPCR cycling mentioned above (section 2.2.6). A negative control was also included in each experiment, which consisted of all the reagents except RNA and reverse transcriptase enzyme. No DNA control was used in these experiments. Each treatment condition was performed in triplicates of three experiments for each gene (*CRFR1*α, *CRFR2*β and *Kir6.1*).

2.2.7 Statistical analysis

Results for cell death studies are presented as mean ± standard error of the mean (SEM). The statistical analysis for differences between treatment groups was determined byone-way analysis of variance (ANOVA) with a post Hoc Bonfferoni's correction test. Values where $p < 0.05$ were considered statistically significant. Data analysis was performed using Microsoft Excel2007 (Microsoft, USA) and graphs were plotted using Graphad Prism® v5 (Graphpad software, USA) and statistical analysis was performed using SPSS (version 18) software (IBM cooperation, USA).

The Comparative C_q (or $2^{-\Delta\Delta C}{}_q$) method was used for analysing qPCR data for relative expression quantification. Calculations for $2^{-\Delta\Delta C}{}_q$ was performed using Microsoft Excel (Microsoft, USA) and the students unpaired T-test of the delta C_q (ΔC_q) values determined the statistical significance of relative expression changes. Values where $p < 0.05$ were considered statistically significant (Yuan *et al*, 2006).

Gene	Accession Number	Forward primer	Forward primer Tm, °C	Reverse primer	Reverse primer Tm, °C	Annealing and extension, °C	No. of PCR Cycles	Expected product size, (bp)
GAPDH	NM 002046	5' GCCAAAAGGGTCATCATCTC 3'	63	5' GGTGCTAAGCAGTTGGTGGT 3'	64	60	30	**131**
CRFR1α	NM 004382	5' ACAAACAATGGCTACCGGGA 3'	60	5' GGACCACGAACCAGGTGGCG 3'	68	60	45	**280**
CRFR2	NM 001883	5' AGCCCATTTTGGATGACAAG 3'	58	5' AGGTGGTGATGAGGTTCCAG 3'	62	60	45	**180**
Kir6.1	NM 004982	5' GCTTTGTGTCCATTGTGACTG 3'	63	5' GCTGTCATGATTCCGATGTG 3'	64	60	40	**312**

Table 2.2: Sequences and conditions of primers sets used in one-step RT-qPCR experiments.
Tm= melting temperature, temp= temperature, bp= base pairs

Chapter 3:
Results

3 Results

Introduction

Several studies have reported NO to be an inducer of apoptosis in a variety of cell types (Blanco *et al*, 1995; Figueroa *et al*, 2006; Ushmorov *et al*, 1999; Maneiro *et al*, 2005) and there is evidence to demonstrate that NO produced spontaneously or via NO donors induces apoptosis in chondrocytes (Blanco *et al*, 1995; Goldring, 2000; Lotz *et al*, 1999) which has been noted as a predominant event in the pathogenesis of OA (Blanco *et al*, 1998; Kim and Blanco, 2007).

Research by Intekhab-Alam in 2006, in which C-20/A4 chondrocytes were stimulated with the pro-apoptotic stimuli: SNAP, TNFα and IL-1β has also documented that the predominant cell death resulting from these stimuli was apoptosis and not necrosis. Furthermore, it was shown that the 40 amino acid peptide, UCNI, protected the stimulated chondrocytes from apoptotic cell death, with the chondroprotective action of UCNI being more evident against SNAP/NO induced apoptosis than that induced by TNFα and IL-1β (Intekhab-Alam, 2006).

Though UCNI mediated cytoprotection against apoptotic cell death in C-20/A4 chondrocytes has been demonstrated, what still remains unclear is the underlying mechanisms by which the chondroprotective effects occur. Possible intracellular signalling pathways have been identified by Western Blotting and pharmacological inhibition studies namely: Phosphatidyl inositol (PI) 3 Kinase, P38 Mitogen Activated Protein Kinase (MAPK) and P42/44 MAPK (Intekhab-Alam, 2006), although the cell surface targets (e.g. ion channels (L-type Calcium channels) or receptors (*CRFR1* and *CRFR2*)) and full cell signalling pathways are yet to be elucidated. Thus, the focus of this thesis is a continuation of the above work by Intekhab-Alam (2006), to establish the potential targets for UCNI mediated chondroprotection in the C-20/A4 chondrocyte cell line. The mRNA expression of *CRF* receptors (*CRFR1* and/or *CRFR2*) and K_{ATP} channel subunits were investigated as potential cell surface targets and downstream mediators for UCNI chondroprotection. Furthermore, modulation of these *CRF* receptors and the *Kir6.1* K_{ATP} channel subunit by UCNI using qPCR was determined to establish their role in the anti-apoptotic effects of UCNI. In addition, activation of the mitoK_{ATP} channel in response SNAP, a mitochondrial pro-apoptotic stimulus, was examined. The findings of these experiments are detailed in this chapter.

3.1 The effects of exogenous UCNI in C-20/A4 chondrocytes

To determine the effect of various stimuli on chondrocyte survival, the cells were cultured for *in vitro* stimulation studies as detailed in section 2.2.2. Following treatment, flow cytometry analysis was performed according to the protocol in section 2.2.3.1 for the detection of apoptosis. LDH release for the assessment of necrosis was conducted according the protocol of section 2.2.3.2.

3.1.1 Flow cytometric analysis of the effects of UCNI, SNAP and α-hCRH$_{(9-41)}$ singly and in combination on C-20/A4 chondrocyte survival

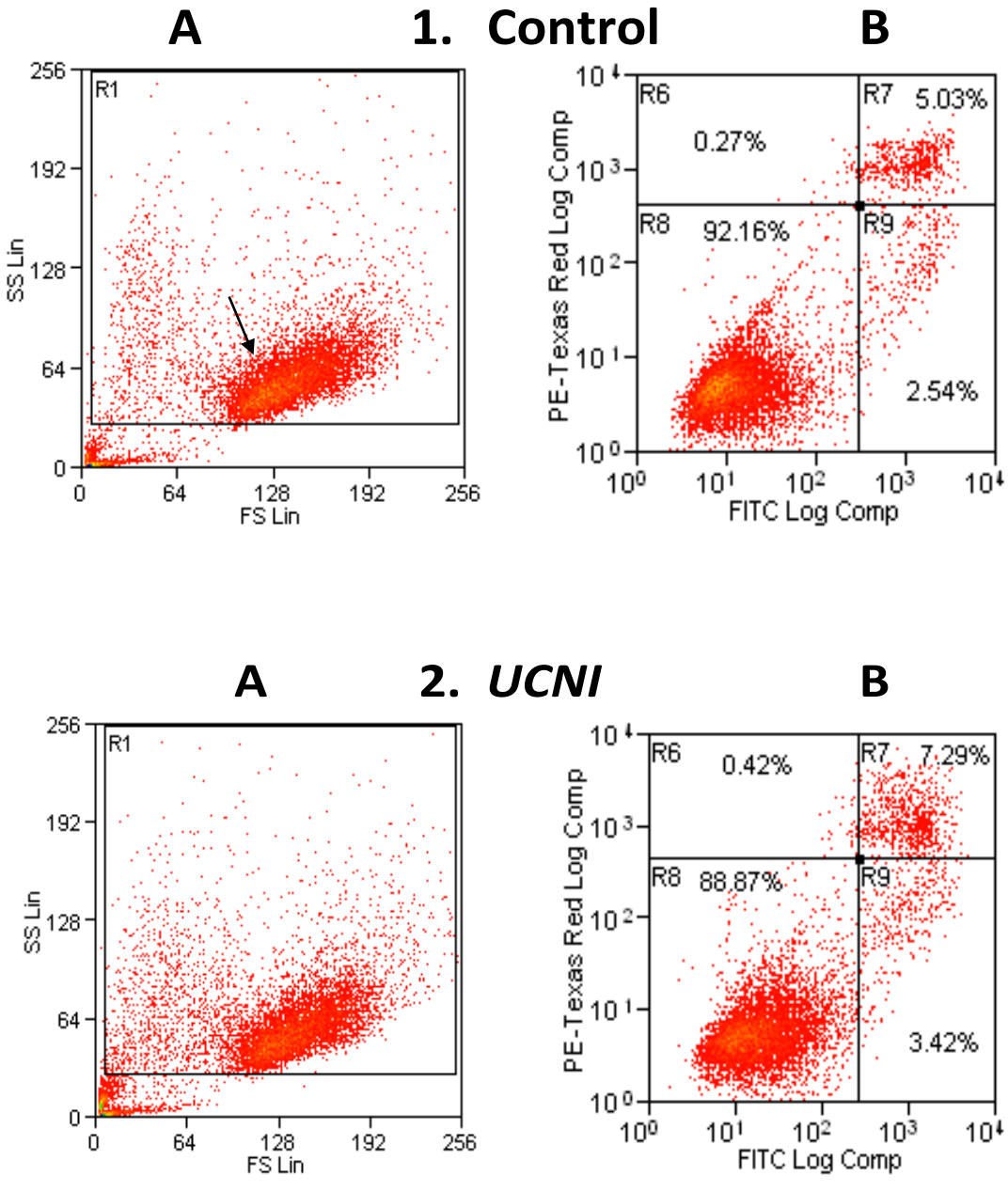

3. SNAP

A

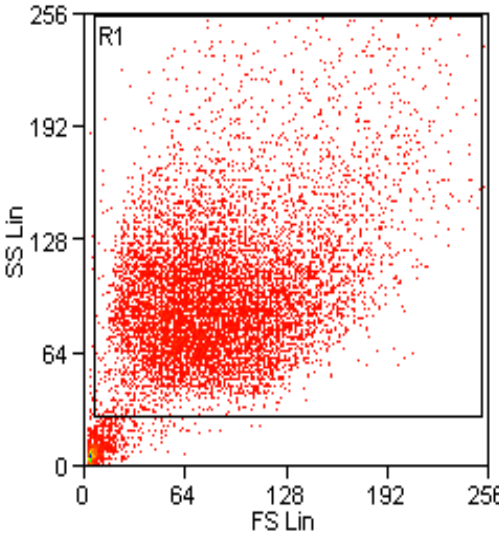

B

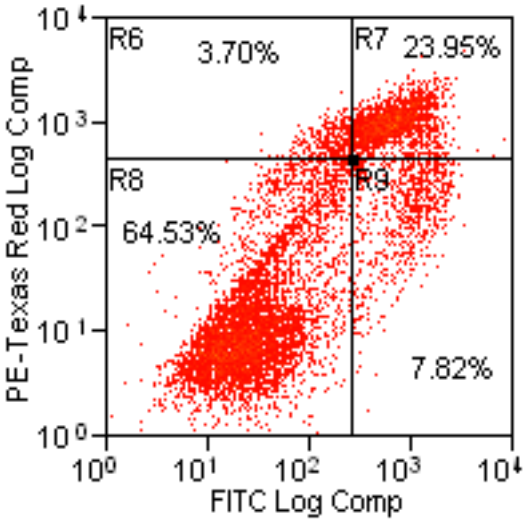

4. SNAP+*UCNI*

A

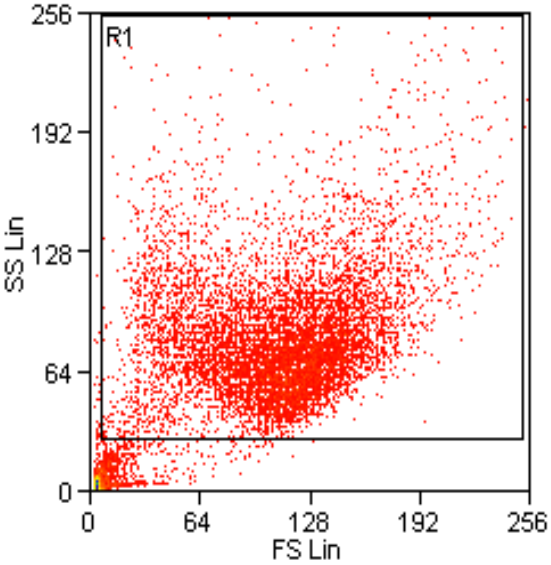

B

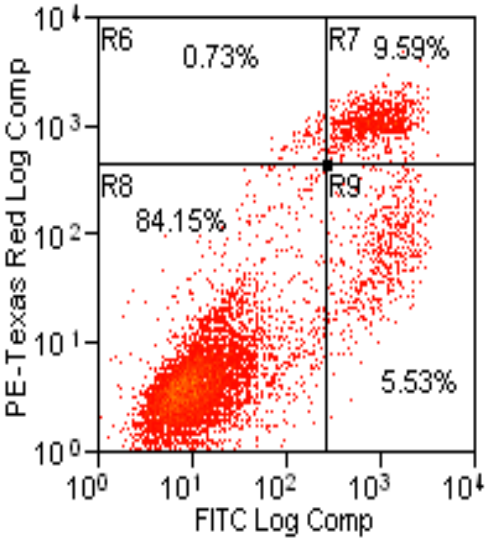

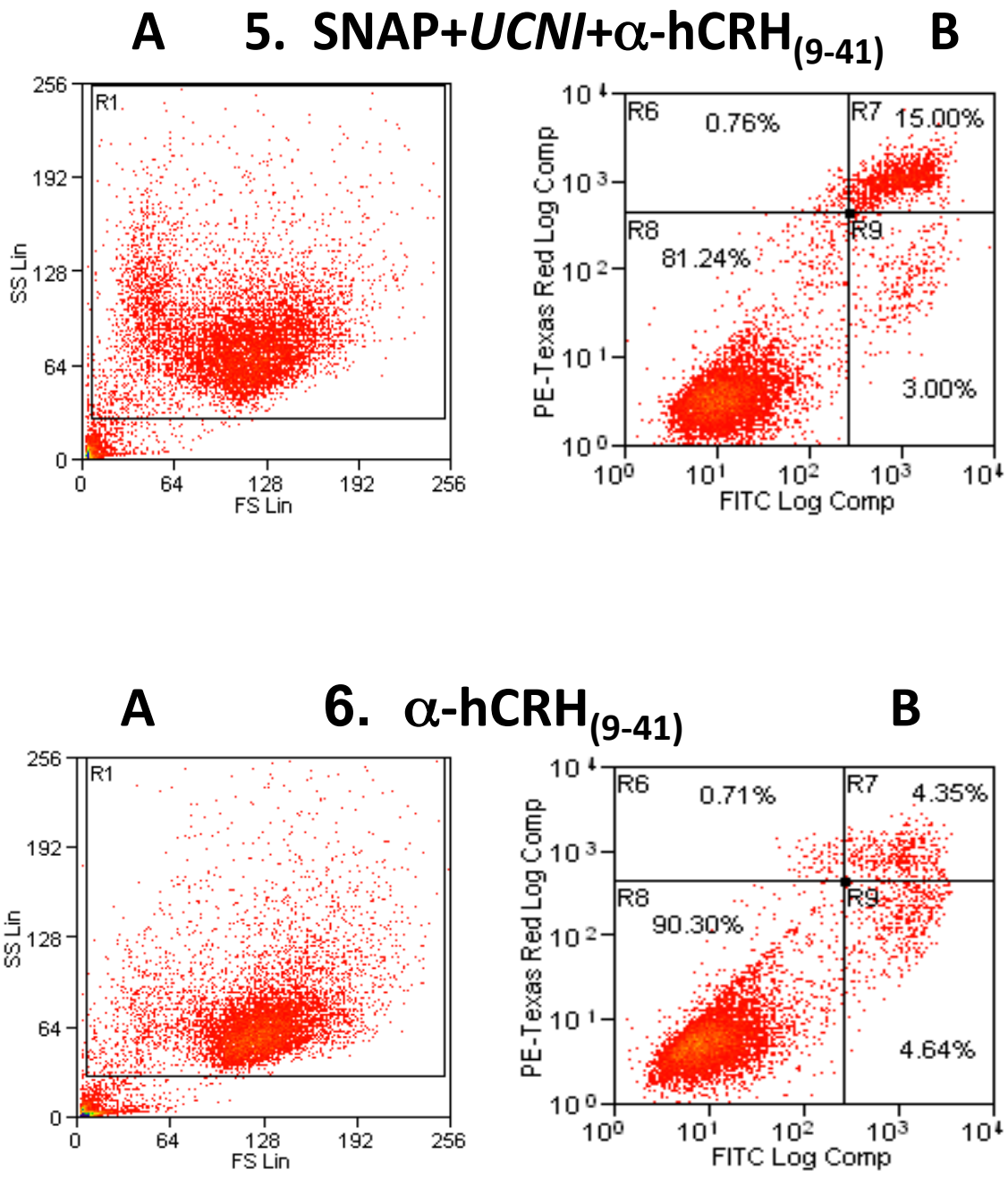

Figure 3.1: A diagrammatic representation of a typical flow cytometric analysis of C-20/A4 chondrocytes showing the effects of various treatments: (1) control (untreated), (2) UCNI, (3) SNAP, (4) SNAP+UCNI, (5) SNAP+UCNI+α-hCRH$_{(9-41)}$ and (6) α-hCRH$_{(9-41)}$) on chondrocyte morphology and viability. Results presented here are from a representative experiment of at least three repeats performed. **A:** Histogram for forward scatter (FSC) & side scatter (SSC); **B**: Histogram for Annexin-V-FITC vs PI fluorescence staining. In the control histogram (histogram A), the arrow indicates the "viable region". A total of 10,000 cells/events were counted per sample. The number of cells in each quadrant (in histograms B) is equivalent of the percentage of viable or apoptotic cells of the 10,000 counted.

Figure 3.1 shows representative flow cytometric histograms (column A) and their corresponding Annexin-V-FITC and PI double labelled histograms (column B) for each set of experimental conditions. The forward scatter (FSC) vs side scatter (SSC) histogram analysis (plotted on a linear scale) gives information regarding the size of the cells/events (FSC) and their granularity, refractiveness and internal complexity (SSC), hence allowing the distinction of cells from debris and other artefacts which may then be eliminated from the analysis.

The double labelled histograms in column B however, are plotted on a logarithmic scale and demonstrate the Annexin-V-FITC and PI staining patterns obtained from the fluorescent channels (FL1: FITC fluorescence and FL3: PI/PE-Texas Red fluorescence). During analysis, this data is divided into four quadrants enabling the differentiation of distinct cell populations. Cells located in the lower left quadrant (designated R8) are both Annexin-V-FITC and PI negative representing the viable cells not undergoing measurable apoptosis whilst cells located in the lower right quadrant (R9) are positive for Annexin-V-FITC and negative for PI representing early apoptotic cells. The upper right quadrant (R7) contains a population of cells, which are positive for both Annexin-V-FITC and PI, representing cells in the later stages of apoptosis whilst the upper left hand quadrant (R6) represents cells positive for PI only, indicative of a necrotic cell population.

The histogram for the control sample of chondrocytes (histogram 1A) shows a large square “gate” which represents the population for analysis after the exclusion of debris and artefacts, which appear below and to the left of the gate. Within that gate is a large population of cells, which have a low SSC, and high FSC (indicated by a black arrow), which represents live cells and is described as the “viable region”. Situated to the left of this viable region, but inside the main gate, is a smaller collection of cells, which have a low FSC and high SSC characteristic of apoptotic cells. Similarly, the Annexin-V-FITC and PI binding shown in the fluorescence (histogram 1B) for the control sample, shows that most of the cells are alive (R8, 92.16%) with low levels of apoptosis occurring (R9, 2.54% and R7, 5.03% representing early and late apoptosis).

The same is true for the cells treated with UCNI (histogram 2B), where most cells are viable (R8, 88.87%) and not undergoing measurable apoptosis. However, it can be observed that following stimulation of cells with SNAP, the cell population in the FSC/SSC histogram (histogram 3A) is shifted to the left when compared to the control (histogram 1A); a consequence of an increase in the size of the population of cells undergoing apoptosis displaying a low FSC and high SSC, coupled with a loss of a distinctive viable region as seen in histogram 1A. A higher percentage of Annexin-V-FITC/PI positive (late apoptotic), cells may also be observed in the upper right quadrant (R7, 23.95%) of the fluorescence histogram, (histogram 3B) after SNAP treatment.

Subsequent treatment of cells with SNAP+UCNI (histograms 4A and 4B), it can be seen that a considerably higher percentage of cells remaining in the viable region (histogram 4A: high FSC/low SSC) with a smaller population of cells located to the left of the viable region that are apoptotic with high SSC and low FSC. Thus, in comparison to the chondrocytes treated with SNAP only (see histogram 3B), it is evident that SNAP+UCNI co-treatment causes a reduction in the percentage of Annexin-V-FITC positive/PI negative (R9, 5.53%, early apoptotic) and Annexin-V-FITC/PI positive (R7, 9.59%, late apoptotic) chondrocytes (see histogram 4B).

Concurrent treatment of cells with SNAP+UCNI+α–helical $CRH_{(9\text{-}41)}$ (histograms 5A and 5B), shows that most cells also remain in the viable region and the flow cytometric plots are similar to those seen for SNAP+UCNI (see histograms 4A and 4B). Analysis of data indicates that the percentage of Annexin-V-FITC positive/PI negative (early apoptotic) and Annexin-V-FITC/PI positive (late apoptotic) cells in the fluorescence histogram for SNAP+UCNI+α–helical $CRH_{(9\text{-}41)}$ treatment (histogram 5B), had remained largely unchanged (R9, 3%; R7, 15%), suggesting that additional treatment with α–helical $CRH_{(9\text{-}41)}$ had no observable effect on cell viability when compared to the SNAP+UCNI treatment (histogram 4B: R9, 5.53%; R7, 9.59%). In addition, treatment of cells with α–helical $CRH_{(9\text{-}41)}$ alone give a similar cell viability pattern (see histogram 6B: R8, 90.30%; R9, 4.64% and R7, 4.35%) to that observed in the control (see histogram 1B: R8, 92.16%; R9, 2.54% and R7, 5.03%) and UCNI (see histogram 2B: R8, 88.87%; R9, 3.42% and R7, 7.29%) fluorescence histogram cell populations suggesting that treatment α–helical $CRH_{(9\text{-}41)}$ does not significantly affect cell morphology or viability.

3.1.2 The effects of various stimuli on the levels of apoptosis and necrosis in C-20/A4 cultured chondrocytes

Following optimisation of the flow cytometry protocol as documented in section 2.2.3.1. Studies were performed to investigate the chondroprotective properties of UCNI in cells exposed to the Nitric Oxide (NO) donor, SNAP.

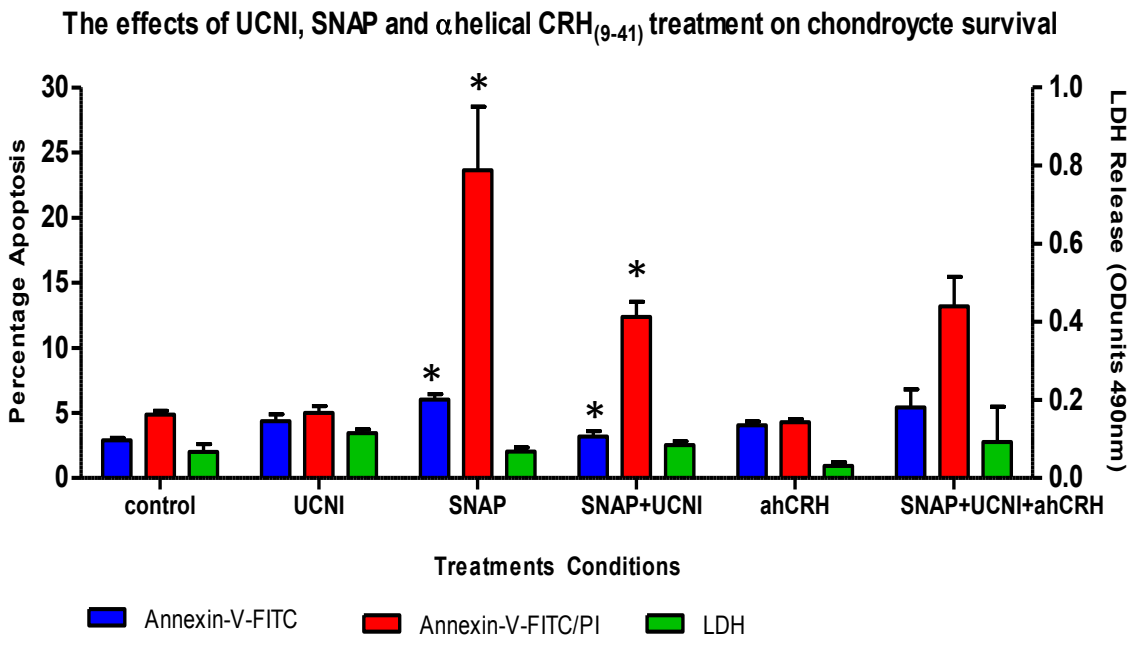

Figure 3.2: The cytoprotective effects of exogenous UCNI (10^{-8}M) when administered concurrently with the pro-apoptotic stimulus of SNAP (10^{-3}M) in the presence or absence of α-helical $CRH_{(9-41)}$ (ahCRH) (10^{-8}M). Annexin-V-FITC only represents percentage of early apoptosis and Annexin-V-FITC/PI indicates late apoptotic percentage of apoptosis. Necrosis was measured by LDH released from C-20/A4 cells from stimulated and unstimulated cells. Data presented as mean values (±SEM), n=3 of a minimum of three different experiments performed in triplicates. *P<0.05

Figure 3.2 shows the assessment of apoptosis in C-20/A4 cells by flow cytometry in which cells were labelled with Annexin-V-FITC and PI prior to analysis. The data indicate that stimulation of cells with the pro-apoptotic stimulus SNAP, causes a significant increase in apoptotic cell death ($p<0.05$) compared to the control which was significantly reduced ($p<0.05$) following the addition of exogenous UCNI.

Co-treatment of chondrocytes with SNAP+UCNI+α-helical $CRH_{(9-41)}$ partially revoked the protective effects of UCNI causing minimal increase in apoptosis; however, this was not statistically significant ($p>0.05$). UCNI alone appears to induce some chondrocyte apoptosis but again this increase was not of statistical significance when compared to the control.

Necrotic cell death, as measured by LDH release, was not observed to be significantly different from the control in any of the experiments performed ($p>0.05$), indicating that apoptosis is the dominant form of cell death occurring in these studies.

3.1.3 SNAP: an inducer of apoptosis in C-20/A4 chondrocytes

The nitric oxide donor, SNAP, was reconstituted in ethanol prior to use for cell death experiments (see section 3.1.2). Given that ethanol can have toxic effects on a number of cell types (Fernandez-Sola *et al*, 2007), it was therefore necessary to determine if the vehicle used (ethanol) was contributing to the apoptosis observed in the chondrocytes stimulated with SNAP. For this purpose, chondrocytes were stimulated with 1% ethanol (final concentration) or 10^{-3}M SNAP in 1% ethanol to establish their effect on chondrocyte viability.

Apoptosis was determined by Annexin-V-FITC/PI labelling by flow cytomtery and necrosis by assessing LDH release in treatment medium. Results of these experiments are shown in figure 3.3.

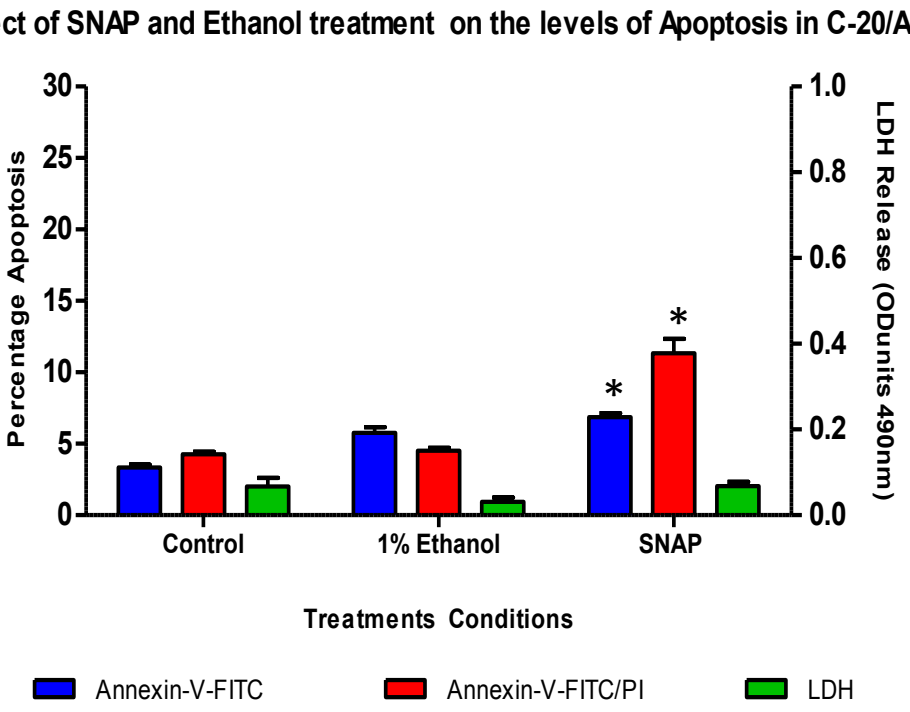

Figure: 3.3: The effects of Ethanol (1%) and SNAP (10^{-3}M) treatment on the levels of apoptosis in C-20/A4 cells. Data presented as mean values (±SEM), n=3 of three different experiments. Annexin-V-FITC only represents percentage of early apoptosis and Annexin-V-FITC/PI indicates late apoptotic percentage of apoptosis. Necrosis was measures by LDH released from C-20/A4 cells from stimulation and unstimulated cells. *P<0.05

The data presented in figure 3.3, shows a significant increase in apoptosis ($p<0.05$) when the chondrocytes were stimulated with 10^{-3}M SNAP in 1% ethanol. The graph also demonstrates that treatment of chondrocytes with 1% ethanol alone (the vehicle for SNAP) does not significantly increase apoptosis ($p>0.05$). Therefore, the apoptotic cell death observed following SNAP treatment of chondrocytes is attributable to the SNAP and not the vehicle used to dissolve it.

3.2 The endogenous mRNA expression of *UCNI* and *GAPDH* genes by C-20/A4 chondrocytes

Studies in other cell types have indicated that *UCNI* exerts cytoprotective effects against apoptosis (Tao *et al*, 2004; Brar *et al*, 1999; Lawrence *et al*, 2002). These findings are comparable to our data in chondrocytes, which demonstrate that UCNI exerts a chondroprotective effect in C-20/A4 cells. Further to such findings, the possible mechanisms by which these anti-apoptotic effects in C-20/A4 chondrocytes are mediated, remains to be identified and so will be the objective of the work detailed in this thesis. To commence the investigation of potential mechanisms for UCNI protection, RT-PCR was performed to confirm the endogenous expression of *UCNI* mRNA in the C-20/A4 chondrocyte cell line. RT-PCR studies were also performed for the expression of a reference gene (*GAPDH*). A negative control was included in all RT-PCR experiments and showed no amplification of products (data not shown). Sequence analysis on the generated PCR products was performed by GATC Biotech, London, UK and sequence homology to the human gene targets at the nucleotide level was conducted by input of sequences into BLAST human sequence resources.

3.2.1 The mRNA expression of *UCNI* by C-20/A4 chondrocytes

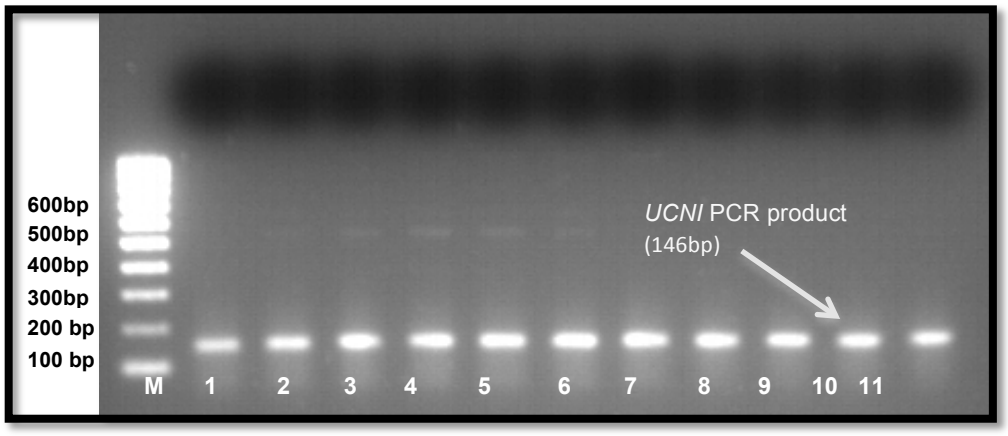

Figure 3.4: Expression of *UCNI* by C-20/A4 chondrocytes on a 2% (w/v) agarose gel stained with ethidium bromide.
Gradient PCR for the mRNA expression of *UCNI* was conducted using a range of annealing temperatures 55 ± 10˚C. M= hyperladder IV marker (1Kb ladder), lanes 1-11 *UCNI* gradient PCR product. Annealing temperatures for each lane are as follows: lane 1= 45 °C, lane 2= 46 °C, lane 3= 47 °C, lane 4= 49 °C, lane 5= 52 °C, lane 6= 54 °C, lane 7=57 °C, lane 8= 60 °C, lane 9= 62 °C, lane 10= 64 °C and lane 11= 65 °C.

Figure 3.4, demonstrates the gradient PCR conducted for the mRNA expression of *UCNI* in untreatedC-20/A4 cells, to establish an optimum annealing temperature for the *UCNI* forward and reverse primers.

The expected 146bp product observed in figure 3.4, demonstrates that the C-20/A4 chondrocytes do indeed express the mRNA for the *UCNI* peptide endogenously. Furthermore, the PCR products in the gel image also suggest that in order for an efficient amplification of the *UCNI* mRNA, annealing temperatures of 57°C (lane 7), 60°C (lane 8) or 62°C (lane 9) could be used. However, if several PCR runs of different targets were to be performed simultaneously, an annealing temperature of 57°C is more appropriate for the *UCNI* primer pair allowing many PCR assays to be conducted using the same PCR cycling conditions. The mRNA expression of *UCNI* was also previously detected using RT-PCR by Intekhab-Alam (2006), in which the identification of the generated PCR amplicon was also confirmed by sequence analysis as the mRNA for the human *UCNI* (Intekhab-Alam, 2006).

3.2.2 The mRNA expression of *GAPDH* by C-20/A4 chondrocytes

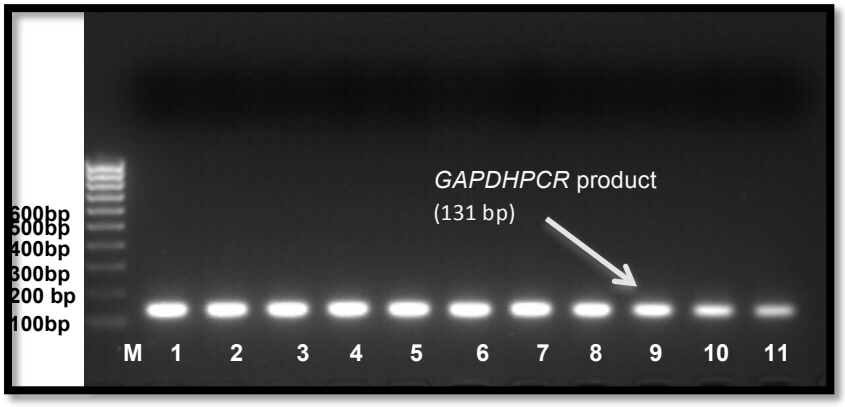

Figure 3.5: Expression of *GAPDH* by C-20/A4 chondrocytes on a 2% (w/v) agarose gel stained with ethidium bromide.
Gradient PCR was conducted with annealing temperatures 55 ± 10 ˚C. M= hyperladder IV marker (1Kb ladder), lanes 1-11 *GAPDH* gradient PCR products. Lane 1= 45 °C, lane 2= 46 °C, lane 3= 47 °C, lane 4= 49 °C, lane 5= 52 °C, lane 6= 54 °C, lane 7=57 °C, lane 8= 60 °C, lane 9= 62 °C, lane 10= 64 °C and lane 11= 65 °C

GAPDH was selected as the reference gene for RT-PCR and RT-qPCR studies. Following Gradient PCR using the designed primers detailed in table 2.1 (see chapter 2), an expected PCR product size of 131 bp was visualised on a 2% gel stained with ethidium bromide. Subsequent sequence analysis of the generated PCR product further confirmed the resulting product as the human *GAPDH* mRNA. Details of the results for the sequence analysis of the GAPDH PCR product are in section 3.2.3.

It is evident from the gel image above that a specific product for *GAPDH* can be obtained with these primers using a range of optimum annealing temperatures: from 45 °C to 62 °C (lanes 1 to 9). However, given that the melting temperatures of the *GAPDH* forward and reverse primers is ≤ 63 °C (see table 2.2), annealing temperatures above 64 °C would not appear to be favourable for amplification of this mRNA as a smaller amount of product is generated compared to the amplicons generated at lower temperatures. A temperature of 60 °C was used to allow for greater operational flexibility.

3.2.3 Sequence analysis data for the human *GAPDH* mRNA

Human *GAPDH* mRNA sequence: NM 002046

- ***GAPDH* mRNA forward sequence:**

TGAGAAGTATGACAACAGCCTCAAGATCATCAGCAATGCCTCCTGCACCACC
AACT

Length of sequence=56 nucleotides
Identities =56/56 (100%)
Sequence location on human *GAPDH* mRNA: nucleotides 513-568

- ***GAPDH* mRNA reverse sequence:**

TTCTCATGGTTCACACCCATGACGAACATGGGGGCATCAGCAGAGGGGGCA
GAGATGATGA

Length of sequence =61 nucleotides
Identities =61/61 (100%)
Sequence location on human *GAPDH* mRNA: 518-458 nucleotides

3.3 The mRNA expression of potential *UCNI* receptors on C-20/A4 chondrocytes

UCNI and other members of the Corticotropin Releasing Factor family of peptides may be expected to predominantly mediate their physiological functions by initial ligation to the G-protein coupled receptors known as Corticotropin Releasing Factor Receptors (CRFRs) (Grammatopoulos and Chrousos, 2002; Brar *et al*, 2000).

The identification of potential endogenous expression of *UCNI* receptors (*CRFR1* and *CRFR2* variants) and K_{ATP} channel subunits (Kir6.x and SURx) at the mRNA level (which could function as putative targets for UCNI mediated chondroprotection) were identified by employing reverse transcriptase-PCR (RT-PCR) studies.

Following C-20/A4 culture as detailed in section 2.2.1.2, total RNA was extracted and quantified from the cells according to protocol 2.2.4. The RT-PCR experiments for the mRNA expression of *GAPDH*, *UCNI* and *Kir6.1* and *6.2* subunits were performed by two-step RT-PCR using protocol 2.2.5.1. In addition, the expression of *CRF* receptor and *SUR*s subunit genes were detected by performing one-step RT-PCR as detailed in protocol 2.2.5.2.Sequence analysis on the generated PCR products were performed by GATC Biotech, London, UK and sequence homology to the human gene targets at the nucleotide level was conducted by input of sequences into BLAST human sequence resources.

3.3.1 The endogenous mRNA expression of *Corticotropin Releasing Factor Receptors* (*CRFRs*) by the C-20/A4 chondrocytes

Initial RT-PCR experiments were performed with two primers pairs designed to amplify any functional *CRFR* mRNA, regardless of the isoforms. The *CRFR1* primers were designed to generate PCR fragment sizes of 280bp (*CRFR1*α) or 367bp (*CRFR1*β), whilst the *CRFR2* primers were designed to amplify a generic band of 180bp to indicate mRNA expression of any*CRFR2* variants (*CRFR2*α, *CRFR2*β or *CRFR2*γ).

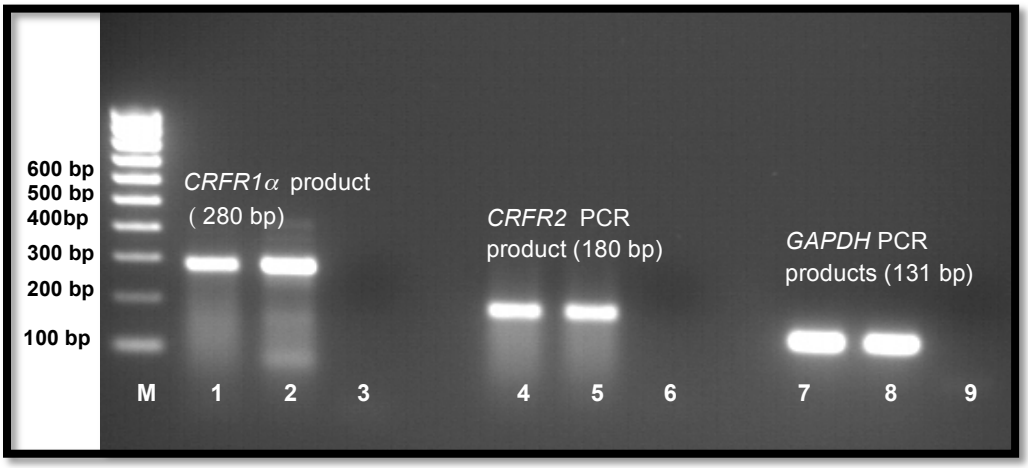

Figure 3.6: The mRNA expression of *CRFR1α* and *CRFR2* by C-20/A4 chondrocytes on a 2% (w/v) agarose gel stained with ethidium bromide.
M= hyperladder IV marker (1Kb ladder). Lanes 1-2= *CRFR1α* PCR products, lane 3= *CRFR1α* negative control; lanes 4-5= *CRFR2* PCR products, lane 6= *CRFR2* negative control; lanes 7-8= *GAPDH* PCR products, lane 9= *GAPDH* negative control.

The RT-PCR products displayed in figure 3.6 indicate that the C-20/A4 chondrocytes express mRNA for both *CRFR1* and *CRFR2* receptors. The observed product size of 280bp for the *CRFR1* primers (lanes 1-2) indicates chondrocyte expression of mRNA for the functional *CRFR1α* receptor. The gel image also indicates the expression of a *CRFR2* receptor by the C-20/A4 chondrocytes (lanes 4 and 5, 180 bp). Identification of the observed *CRFR1* and *CRFR2* PCR amplicons in figure 3.6 were subjected to sequencing and both PCR products confirmed by subsequent sequence analysis as the mRNA for the human *CRFR1α* and a *CRFR2* gene. The sequence analysis data for the *CRFR1α* and *CRFR2* mRNA is detailed is section 3.3.1.1 and 3.3.1.2 respectively.

Further RT-PCR experiments were then conducted to establish the specific mRNA isoform (*CRFR2α*, *CRFR2β* or *CRFR2γ*) of the CRFR2 receptor present, the results of which are documented in section 3.3.2. The PCR products in lanes 7 and 8 of the gel image are for the reference gene, *GAPDH*, the sequence data for which was shown previously (see pg 75).

3.3.1.1 Sequence analysis for the mRNA expression of *CRFR1α* human variant in C-20/A4 chondrocytes

Human *CRFR1α* mRNA: NM004382

- ***CRFR1α* mRNA forward sequence**

CGTGATTACTCCGAGTGCCAGGAGATCCTCAATGAGGAGAAAAAAAGCAAGG
TGCACTACCATGTCGCAGTCATCATCAACTACCTGGGCCACTGTATCTCCCTG
GTGGCCCTCCTGGTGGCCTTTGTCCTCTTTCTGCGGCTCAGGAGCATCCGGT
GCCTGCGAAACATCATCCACTGGAACCTCATCTCCGCCTTCATCCTGCGCAA
CGCCACCTGGTTCGTGGT

Length of sequence= 228 nucleotides
Identities= 227/228 (99%)
Sequence location on human *CRFR1α* mRNA: nucleotides 553-780

- **CRFR1α mRNA reverse sequence**

TTTCGCAGGCACCGGATGCTCCTGAGCCGCAGAAAGAGGACAAAGGCCACC
AGGAGGGCCACCAGGGAGATACAGTGGCCCAGGTAGTTGATGATGACTGCG
ACATGGTAGTGCACCTTGCTTTTTTTCTCCTCATTGAGGATCTCCTGGCACTC
GGAGTAATTCACGCGGGCGGCCCAGCTGCCATTGGCCAGGCACTCCCGGTA
GCCATTGTTT

Length of sequence= 216 nucleotides
Identities= 216/216 (100%)
Sequence location on human *CRFR1α* mRNA: nucleotides 720-505

- **CRFR1α mRNA sequence consensus:**

ATTACTCCGAGTGCCAGGAGATCCTCAATGAGGAGAAAAAAAGCAAGGTGCA
CTACCATGTCGCAGTCATCATCAACTACCTGGGCCACTGTATCTCCCTGGTG
GCCCTCCTGGTGGCCTTTGTCCTCTTTCTGCGGCTCAGGAGCATCCGGTGCC
TGCGAAA

Length of consensus sequence= 163 nucleotides
Identities= 163/163 (100%)
Sequence location on human *CRFR1α* mRNA: nucleotides 558-720

3.3.1.2 Sequence analysis for the mRNA expression of human *CRFR2* in C-20/A4 chondrocytes

Human *CRFR2* mRNA sequence: NM 001883

- ***CRFR2* mRNA forward sequence:**

GGGCCACTGCGTATCTGTGGCAGCCCTGGTGGCCGCCTTCCTGCTTTTCCTG
GCCCTGCGGAGCATTCGCTGTCTGCGGAATGTGATTCACTGGAACCTCAT

Length of sequence= 102 nucleotides
Identities= 102/102 (100%)
Sequence location on human *CRFR2* mRNA: nucleotides 611-712

- ***CRFR2* mRNA reverse sequence:**

GCAGGAAGGCGGCCACCAGGGCTGCCACAGATACGCAGTGGCCCAGGTAG
TTGACGACAAGGGCGATGCGGTAGTGCAGGTCATACTTCCTCTGCTTGTCAT
CCAAAAT

Length of sequence= 109 nucleotides
Identities= 109/109 (100%)
Sequence location on human *CRFR2* mRNA: nucleotides 654-546

- ***CRFR2* mRNA sequence consensus:**

GGGCCACTGCGTATCTGTGGCAGCCCTGGTGGCCGCCTTCCTGC

Length of consensus sequence= 44 nucleotides
Identities= 44/44 (100%)
Sequence location on human *CRFR2* mRNA: nucleotides 611-654

3.3.2 The mRNA expression of the *CRFR2* receptor variant: CRFR2β by C-20/A4 chondrocytes

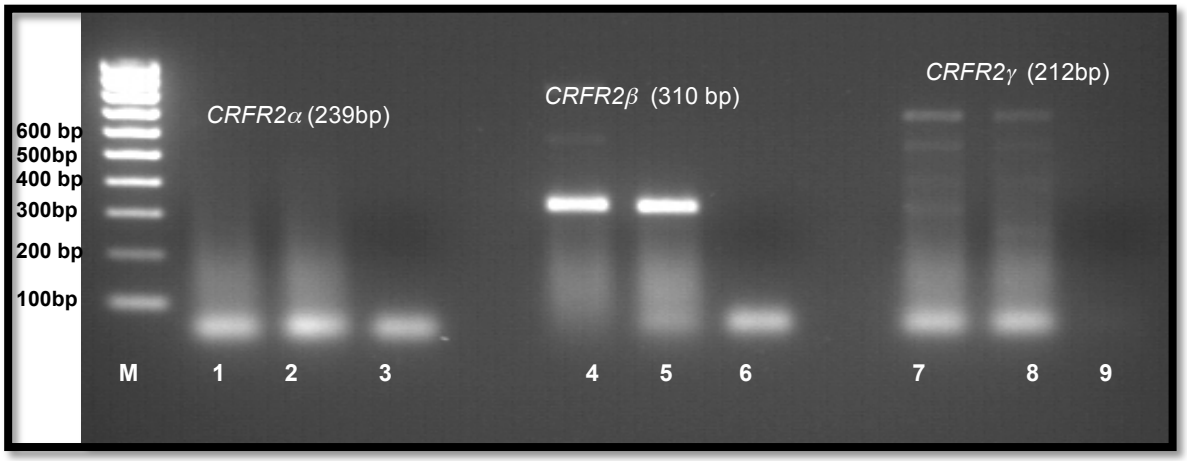

Figure 3.7: A 2% (w/v) agarose gel stained with ethidium bromide showing the mRNA expression of *CRFR2β* isoform by C-20/A4 chondrocytes.
M = hyperladder IV marker (1Kb ladder), Lanes 1-2= *CRFR2α* PCR product, lane 3= *CRFR2α* negative control; lanes 4-5= *CRFR2β* PCR product, lane 6= *CRFR2β* negative control, lanes 7-8= *CRFR2γ* PCR product, lane 9= *CRFR2γ* negative control.

RT-PCR experiments were conducted to establish the *CRFR2* variant following the initial RT-PCR data in figure 3.6, which indicated the expression of*CRFR2* receptor mRNA in the C-20/A4 chondrocytes. As a result, forward primers were designed towards the N terminus of the *CRFR2* mRNA transcript to generate specific products for the three splice variants of the *CRFR2* receptor (*CRFR2α*, *CRFR2β* or *CRFR2γ*) based on the alternative splicing which occurs at the N terminus of the receptor(Grammatopoulos and Chrousos, 2002). Thus, 239bp, 310bp and 212bp products would indicate *CRFR2α*, *CRFR2β* or *CRFR2γ*expression, respectively.

Results from the RT-PCR experiments, which were electrophoresed on a 2% agarose gel (figure 3.7) indicated the presence of a 310bp product, which, suggests that the*CRFR2β* variant of the *CRFR2* receptor is expressed by C-20/A4 chondrocytes. No specific PCR products of 239 bp and 212bp were visible which would have indicated the mRNA expression of *CRFR2α* and *CRFR2γ* variants, respectively. Subsequent sequence analysis of the 310 bp observed PCR

amplicon (see section 3.3.2.1), confirmed the PCR product as the human *CRFR2β* mRNA.

3.3.2.1 Sequence analysis for the mRNA expression of *CRFR2β* in C-20/A4 chondrocytes

Human CRFR2β isoform mRNA sequence: NM 001202475

- **CRFR2β mRNA forward sequence:**

GCCGCTCCATACGCAGCCGGGCAGAGCCAGATGCCCAAAGACCAGCCCCTG
TGGGCACTTCTGGAGCAGTACTGCCACACCATCATGACCCTCACCAACCTCT
CAGGTCCCTACTCCTACTGCAACACGACCTTGGACCAGATCGGAACGTGCTG
GCCCCGCAGCGCTGCCGGAGCCCTCGTGGAGAGGCCGTGCCCCGAGTACT
TCAACGGCGTCAAGTACAACACGACCCGGAATGCCTATCGAGAATGCTTG

Length of sequence= 256 nucleotides
Identities= 255/256 (100%)
Sequence location on human *CRFR2β* mRNA: nucleotides 148-403

- **CRFR2β mRNA reverse sequence:**

GGGCTCCGGCAGCGCTGCGGGGCCAGCACGTTCCGATCTGGTCCAAGGTC
GTGTTGCAGTAGGAGTAGGGACCTGAGAGGTTGGTGAGGGTCATGATGGTG
TGGCAGTACTGCTCCAGAAGTGCCCACAGGGGCTGGTCTTTGGGCATCTGG
CTCTGCCCGGCTGCGTATTGGAGCGGCGGTGGGAGGAGGCAGAGCAGGCA
GAGGAGGAGGTGTGGGACGTAGAGG

Length of sequence= 227 nucleotides
Identities= 227/227 (100%)
Sequence location on human *CRFR2β* mRNA: nucleotides 326-100

- **CRFR2β mRNA sequence consensus:**

ATACGCAGCCGGGCAGAGCCAGATGCCCAAAGACCAGCCCCTGTGGGCACT
TCTGGAGCAGTACTGCCACACCATCATGACCCTCACCAACCTCTCAGGTCCC
TACTCCTACTGCAACACGACCTTGGACCAGATCGGAACGTGCTGGCCCCGCA
GCGCTGCCGGAGCCC

Length of consensus sequence= 170 nucleotides
Identities= 170/170 (100%)
Sequence location on human *CRFR2β* mRNA: nucleotides 157-326

3.4 Investigation of the mRNA expression of K_{ATP} channel subunits: *Kir6.x* and *SURx* by C-20/A4 chondrocytes

Studies by Lawrence *et al* in 2004, have suggested a role for K_{ATP} channels, in particular the mitochondrial K_{ATP} channel (mitoK_{ATP}) with pore forming subunit, Kir6.1, in UCNI mediated prevention of cell death. Their findings documented that *UCNI* reduced cell death by activation of the mitoK_{ATP} channel and subsequent prevention of damage to the cells mitochondria (Lawrence *et al*, 2004).

To determine if these K_{ATP} channels may be involved the chondroprotective effects of *UCNI* in the C-20/A4 chondrocytes, the existence of the mRNA and protein expression of the subunits (*Kir6.x* and *SURx*), which constitute functional K_{ATP} channels, firstly needs to be confirmed in the chondrocytes. Consequently, RT-PCR studies were performed to optimise the detection of the mRNA expression of the mitochondrial K_{ATP} channel subunits in C-20/A4 cells.

All RT-PCR products generated from these studies were confirmed by sequence analysis. Sequence analysis was performed by GATC Biotech, London, UK and sequence homology to the human gene targets at the nucleotide level was conducted by input of sequences into BLAST human sequence resources. A negative control was included in all RT-PCR experiments and showed no amplification of products (data not shown).

3.4.1 The endogenous mRNA expression of the *Kir6.1* K_{ATP} channel subunit by C-20/A 4 chondrocytes

Result for the investigation of the mRNA expression of the K_{ATP} channel pore forming subunit, *Kir6.1* is shown illustrated in figure 3.8 (below).

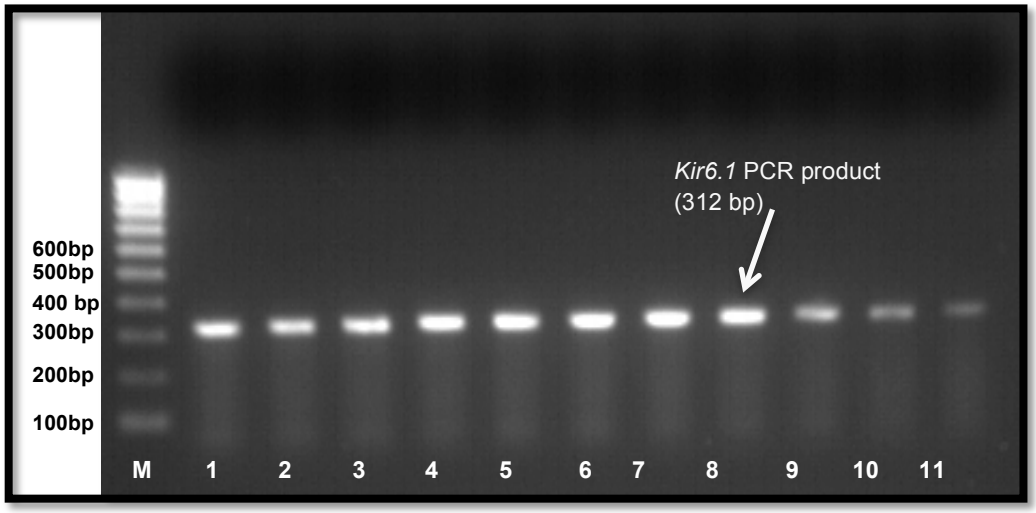

Figure 3.8: The mRNA expression of *Kir6.1* by C-20/A4 cells on a 2% (w/v) agarose gel stained with ethidium bromide.
Gradient PCR for *Kir6.1* mRNA expression was conducted with annealing temperatures 55±10 ˚C. M= hyperladder IV marker (1Kb ladder). Annealing temperature for each lane are as follows: lane 1= 45 °C, lane 2= 46 °C, lane 3= 47 °C, lane 4= 49 °C, lane 5= 52 °C, lane 6= 54 °C, lane 7=57 °C, lane 8= 60 °C, lane 9= 62 °C, lane 10= 64 °C and lane 11= 65 °C.

Figure 3.8 shows the results of the gradient PCR for the K_{ATP} channel pore forming subunit, *Kir6.1*.The result indicates the expression of mRNA for this mitochondrial subunit-*Kir6.1*, by C-20/A4 chondrocytes. The gel image also illustrates that a range of annealing temperature exists for amplification, however for operational flexibility, the annealing temperature of 60 °C (lane 8) was considered favourable for the optimum amplification of *Kir6.1* mRNA. The 312bp generated PCR product in figure 3.8, was confirmed as the human *Kir6.1* subunit by sequence analysis (see section 3.4.1.1).

3.4.1.1 Sequence analysis for the mRNA expression of *Kir6.1* in C-20/A4 chondrocytes

Human *Kir6.1* mRNA sequence: NM 004982

- ***Kir6.1* mRNA forward sequence**:

TTTGGCACACTGTTAAAGTAGCTGCTCCACGGTGCAGTGCCCGAgaGCTGGA
TGAGAAACCTTCCATCCTTATTCAGACCCTCCAAAAGAGTGAACTGTCTCATC
AAAATTCTCTGAGGAAGCGCAACTCCATGAGAAGAAACAATTCCATGAGGAG
GAACAATTCTATCCGAAGGAACAATTCTTCCCTCATGGTACCAAAGGTGCAAT
TTATGACTCCAGAAGGAAATCAAAACACATCGG

Length of sequence= 244 nucleotides
Identities= 243/244 (99%)
Sequence location on human mRNA: nucleotides 1362-1605

- ***Kir6.1* mRNA reverse sequence**:

TTGTTCCTTCGGATAGAATTGTTCCTCCTCATGGAATTGTTTCTTCTCATGGAG
TTGCGCTTCCTCAGAGAATTTTGATGAGACAGTTCACTCTTTTGGAGGGTCTG
AATAAGGATGGAAGGTTTCTCATCCAGCTCTCGGGCACTGCACCGTGGAGCA
GCTACTTTAACAGTGTTGCCAAATTTGGAGTAATCCACAGAATACACTCCTTC
TTCCTCAGTCACAATGGACACAAA

Length of sequence= 236 nucleotides
Identities= 236/236 (100%)
Sequence location on human mRNA: nucleotides 1543-1308

- ***Kir6.1* mRNA sequence consensus:**

ACACTGTTAAAGTAGCTGCTCCACGGTGCAGTGCCCGAgaGCTGGATGAGAA
ACCTTCCATCCTTATTCAGACCCTCCAAAAGAGTGAACTGTCTCATCAAAATT
CTCTGAGGAAGCGCAACTCCATGAGAAGAAACAATTCCATGAGGAGGAACAA
TTCTATCCGAAGGAACAA

Length of consensus sequence=175 nucleotides
Identities= 175/175(100%)
Sequence location on human mRNA: nucleotides 1369-1543

3.4.2 The mRNA expression of the*Kir6.2* K_{ATP} channel subunit by the C-20/A4 chondrocytes

RT-PCR was also conducted to determine C-20/A4 expression of the second K_{ATP} channel pore forming subunit, *Kir6.2*.

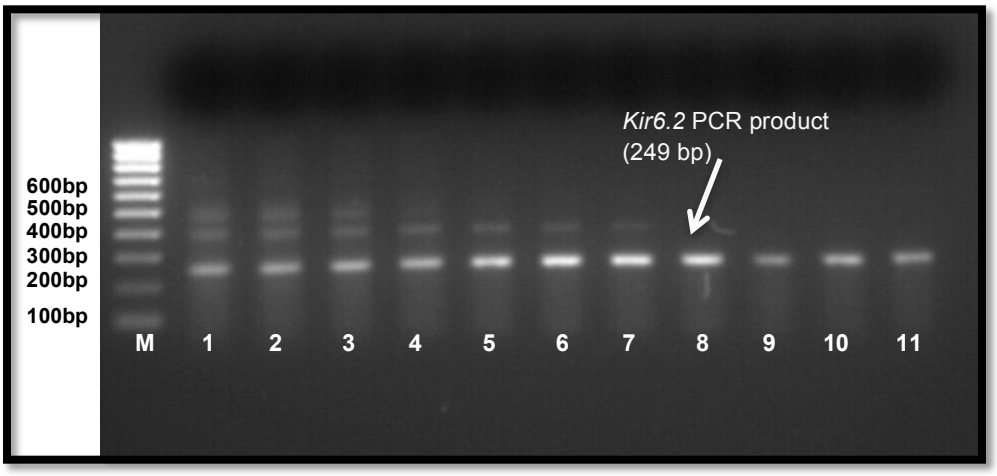

Figure 3.9: The mRNA expression of *Kir6.2* by C-20/A4 chondrocytes on a 2% (w/v) agarose gel stained with ethidium bromide.
The gradient PCR for the mRNA expression of *Kir6.2* was conducted using a range of annealing temperatures 55±10˚C. M = hyperladder IV marker (1Kb ladder). Lanes 1-11= *Kir6.2* PCR product. Annealing temperature for each lane are as follows: lane 1= 45 °C, lane 2= 46 °C, lane 3= 47 °C, lane 4= 49 °C, lane 5= 52 °C, lane 6= 54 °C, lane 7=57 °C, lane 8= 60 °C, lane 9= 62 °C, lane 10= 64 °C and lane 11= 65 °C.

Results from the gradient PCR (figure 3.9) and sequencing analysis (section 3.4.2.1), confirmed the expression of mRNA at 249 bp for the *Kir6.2* K_{ATP} channel subunit by C-20/A4 chondrocytes. Moreover, it is evident from the PCR amplicons generated from the different annealing temperatures in figure 3.9, that for future PCR studies an annealing temperature of 60 °C (lane 8) would yield optimum amplification of the *Kir6.2* subunit.

3.4.2.1 Sequence analysis for the mRNA expression of *Kir6.2* in C-20/A4 chondrocytes

Human *Kir6.2* mRNA sequence: NM 000525

- ***Kir6.2* mRNA forward sequence:**

GAGGGCGAGGTGGTGCCCCTCCACCAGGTGGACATCCCCATGGAGAACGG
CGTGGGTGGCAACAGCATCTTCCTGGTGGCCCCGCTGATCATCTACCATGTC
ATTGATGCCAACAGCCCACTCTACGACCTGGCACCCAGCGACCTGCACCACC
ACCAGGACCTCGAGATCATCGTCATCCTGGAAGGCGTGG

Length of sequence= 193 nucleotides
Identities= 193/193 (100%)
Sequence location on human mRNA: nucleotides 1247-1439

- ***Kir6.2* mRNA reverse sequence:**

GGGCTGTTGGCATCAATGACATGGTAGATGATCAGCGGGGCCACCAGGAAG
ATGCTGTTGCCACCCACGCCGTTCTCCATGGGGATGTCCACCTGGTGGAGG
GGCACCACCTCGCCCTCGGGGCTGGTGGTCTTGCGTACCACCTGCATGTGG
ATGGTGGCGCTG

Length of sequence= 165 nucleotides
Identities= 165/165 (100%)
Sequence location on human mRNA: nucleotides 1365-1201

- ***Kir6.2* mRNA sequence consensus:**

GAGGGCGAGGTGGTGCCCCTCCACCAGGTGGACATCCCCATGGAGAACGG
CGTGGGTGGCAACAGCATCTTCCTGGTGGCCCCGCTGATCATCTACCATGTC
ATTGATGCCAACAGCCC

Length of consensus sequence= 119 nucleotides
Identities= 119/119 (100%)
Sequence location on human mRNA: nucleotides 1247-1365

3.4.3 The mRNA expression of K_{ATP} channels *Sulfonyl Urea Receptor* (*SUR*) regulatory subunits by C-20/A4 Chondrocytes

Typically, Kir6.x subunits associate with SURx subunits and so existence of the latter are essential for the formation of functional K_{ATP} channels. The SURs are the regulatory components and so will modulate the activation and closure of the pore (Kir6.x) subunit of the channel. To confirm the possibility that C-20/A4 chondrocytes may express functional K_{ATP} channels, RT-PCR was conducted for the expression of mRNA for the K_{ATP} channels regulatory subunits (*SUR*) of which there are two main groups – *SUR1* and *SUR2*.

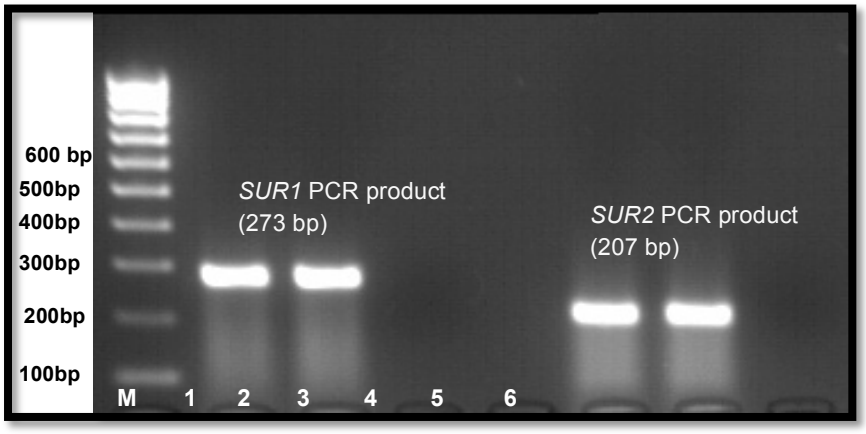

Figure 3.10: The mRNA expression of *SUR1* and*SUR2* regulatory subunits by the C-20/A4 cells demonstrated on a 2% (w/v) agarose gel stained with ethidium bromide.
M= hyperladder IV marker (1Kb ladder), lanes1-2= *SUR1* PCR products, lane 3= *SUR1* negative control, lanes 4-5= *SUR2* PCR products, lane 6= *SUR2* negative control.

The PCR products in figure 3.10 demonstrate that the C-20/A4 chondrocytes express products corresponding to SUR1 (lanes 1 and 2, 273bp) and also SUR2 (lanes 4 and 5, 207bp) mRNA. Sequence analysis (see section 3.4.3.1) of these PCR products confirmed the amplicons generated as *SUR1* and *SUR2* subunits. *SUR2* subunits however, exist in two predominant isoforms: *SUR2A* and *SUR2B*.

Further RT-PCR studies were performed to establish which functional *SUR2* receptor subunit was present in these chondrocytes.

3.4.3.1 Sequence analysis for the mRNA expression of K_{ATP} channel *SUR1* and *SUR2* subunitsin C-20/A4 chondrocytes

3.4.3.1.1 Sequence analysis for the mRNA expression of the K_{ATP} channel subunit: *SUR1*

Human *SUR1* sequence: NM 000352

- ***SUR1* mRNA forward sequence:**

GCTGGTGGTGAAGGCACTGCCAGGAGGCCTCGATGCCATCATCACAGAAGG
CGGGGAGAATTTCAGCCAGGGACAGAGGCAGCTGTTCTGCCTGGCCCGGGC
CTTCGTGAGGAAGACCAGCATCTTCATCATGGACGAGGCCACGGCTTCCATT
GACATGGCCACGGAAAACATCCTCCAAAAGGTGGTG

Length of sequence= 190 nucleotides
Identities= 190/190 (100%)
Sequence location on human mRNA: nucleotides 4506-4695

- ***SUR1* mRNA reverse sequence:**

GTGGCCTCGTCCATGATGAAGATGCTGGTCTTCCTCACGAAGGCCCGGGCC
AGGCAGAACAGCTGCCTCTGTCCCTGGCTGAAATTCTCCCCGCCTTCTGTGA
TGATGGCATCGAGGCCTCCTGGCAGTGCCTTCACCACCAGCTTCAGCTGGG
CGATTTCCAGGGCCTCCCACAGTGTGCTATCTGAGCACTTCCTCTCAGGGTC
CAGGTTAAA

Length of sequence= 215 nucleotides
Identities= 215/215 (100%)
Sequence location on human mRNA: nucleotides 4649-4435

- ***SUR1* mRNA consensus sequence:**

GCTGGTGGTGAAGGCACTGCCAGGAGGCCTCGATGCCATCATCACAGAAGG
CGGGGAGAATTTCAGCCAGGGACAGAGGCAGCTGTTCTGCCTGGCCCGGGC
CTTCGTGAGGAAGACCAGCATCTTCATCATGGACGAGGCCAC

Length of consensus sequence=144 nucleotides
Identities= 144/144 (100%)
Sequence location on human mRNA: nucleotides 4506-4649

3.4.3.1.2 Sequence analysis for the mRNA expression of the K_{ATP} channel subunit: *SUR2*

Human *SUR2* mRNA sequence: NM 005691

- ***SUR2* mRNA forward sequence:**

GATTGGGTTGTGAGGACTTGGCTGACCTGGAGGTCCAGATGGGTGCAGTGA
AGAAGGTGAACAGTTTCCTGACTATGGAGTCAGAGAACTATGAAGGCACAAT
GGATCCTTCTCAAGTTCCAGAACATTGGCCACAAGAAGGGGAGATC

Length of sequence= 149 nucleotides
Identities= 148/149 (99%)
Sequence location on human mRNA: nucleotides 3808-3956

- ***SUR2* mRNA reverse sequence**

TTCTCTGACTCCATAGTCAGGAAACTGTTCACCTTCTTCACTGCACCCATCTG
GACCTCCAGGTCAGCCAAGTTCCTCACAACCCAATTCAAATAATTGGTTATCG
TAAGTGCATACAGAAGACCCAAGCCTACCAATCC

Length of sequence= 140 nucleotides
Identities= 140/140 (100%)
Sequence location on human mRNA: nucleotides 3895-3756

- ***SUR2* mRNA consensus sequence:**

TTGGCTGACCTGGAGGTCCAGATGGGTGCAGTGAAGAAGGTGAACAGTTTCC
TGACTATGGAGTCAGAGAA

Length of consensus sequence= 71 nucleotides
Identities= 71/71 (100%)
Sequence location on human mRNA: nucleotides 3825-3895

3.4.4 The mRNA expression of K_{ATP} channel *SUR2* isoform subunits by the C-20/A4 Chondrocytes

Investigation into the specific *SURx (SUR1 or SUR2)* isoform expressed at the mRNA level by the C-20/A4 chondrocytes demonstrated that they express both *SUR1* and *SUR2*subunits (figure 3.10). Consequently, the mRNA of the specific*SUR2* isoform(s) expressed by the C-20/A4 chondrocytes was investigated (figure 3.11).

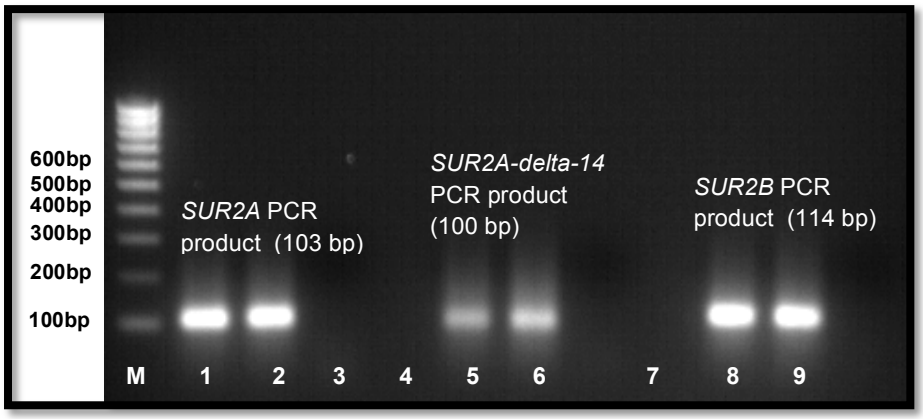

Figure 3.11: The mRNA expression of the *SUR2* isoforms present in C-20/A4 chondrocytes electrophoresed a 2% (w/v) agarose gel stained with ethidium bromide.
M= hyperladder IV marker (1Kb ladder), lanes 1-2= *SUR2A* PCR products, lane 3= *SUR2A* negative control, lanes 4-5= *SUR2A-delta-14* PCR products, lane 6= *SUR2A-delta-14* negative control, lanes 7-8= *SUR2B* PCR products, lane 9= *SUR2B* negative control.

The gel image in figure 3.11 illustrates the findings from further RT-PCR experiments that were conducted to establish which *SUR2* subunit is expressed by the C-20/A4 cells. The PCR products of figure 3.11 indicate that the chondrocytes express a *SUR2A* (lanes 1 and 2) and *SUR2B* (lanes 7 and 8) regulatory subunits. *SUR2A* can exist both as a functional and non-functional splice variant(Shi *et al*, 2005). The amplification of a product in lanes 4 and 5 indicate that the *SUR2A* isoform expressed by the C-20/A4 chondrocytes is the isoform denoted *SUR2A-delta-14 [SUR2A-Δ-14]*, a non-functional variant(Chutkow *et al*, 1999). Thus the functional *SUR2* subunit that is expressed by the chondrocytes is *SUR2B*. Sequence analysis data of the generated *SUR2* isoforms (*SUR2A*, *SUR2A-Δ*-14 and *SUR2B*) PCR products in figure 3.11, are demonstrated in section 3.4.4.1.

3.4.4.1 Sequence analysis for the mRNA expression of the K_{ATP} channel *SUR2* isoforms subunits: *SUR2A, SUR2A-Δ-14 and SUR2B* in C-20/A4 chondrocytes

3.4.4.1.1 Sequence analysis for *SUR2A* isoform mRNA expression

Human *SUR2A* isoform sequence: NM 005691

- ***SUR2A* isoform mRNA forward sequence:**

TTAGTGGAGTGTGATACTGTCCCAATTTGCTCGCCCACAAGAATGGC

Length of sequence= 48 nucleotides
Identities= 47/48 (98%)
Sequence location on human mRNA: nucleotides 4590-4637

- ***SUR2A* isoform mRNA reverse sequence**

AAAGACTAAAACAAGGCCTGCATCCATAATAGAAGAGACA

Length of sequence= 40 nucleotides
Identities = 40/40 (100%)
Sequence location on human mRNA: nucleotides 4577-4538

3.4.4.1.2 Sequence analysis for *SUR2A-Δ-14* mRNA expression

Human *SUR2A delta 14* isoform sequence: NM 020298

- ***SUR2A delta 14* isoform mRNA forward sequence:**

TTTTGATCCTGTAAGAAGCACACTGGAGTTGTCACAAATGG

Length of sequence= 41 nucleotides
Identities = 24/24 (100%)
Sequence location on human mRNA: nucleotides 1908-1931

- ***SUR2A delta 14* isoform mRNA reverse sequence:**

GTCACCAATCTCATCACTCAAGAG

Length of sequence= 24nucleotides
Identities= 24/24 (100%)
Sequence location on human mRNA: nucleotides 1868-1845

3.4.4.1.3 Sequence analysis for *SUR2B* isoform mRNA expression

Human *SUR2B* isoform sequence: NM 020297

- ***SUR2B* isoform mRNA forward sequence:**

GCTCAGGAAAATGGAGTATTTGCTTCTT

Length of sequence= 28 nucleotides
Identities= 28/28 (100%)
Sequence location on human mRNA: nucleotides 4623-4650

- ***SUR2B* isoform mRNA reverse sequence:**

TTTCTGGAGTGTCATATTCTAAAATATTTCCTCGCTTCATCACAATAACCAGGT
CTGCCGT

Length of sequence= 61 nucleotides
Identities= 61/61 (100%)
Sequence location on human mRNA: nucleotides 4614-4554

3.5 qPCR studies for analysis of the relative expression of *CRFR1*, *CRFR2* and *Kir6.1* by the $2^{-\Delta\Delta C_q}$ method

This section aims to investigate the relative expression of *CRFR1*, *CRFR2* and *Kir6.1* by qPCR to determine their relative abundance following treatment and determine whether their expression is modulated by UCNI. The cell death studies in section 3.1.2 showed that *UCNI* is a cytoprotective agent in chondrocytes against SNAP induced apoptosis. Furthermore, RT-PCR experiments further demonstrated that previously described receptors and intracellular targets, for UCNI mediated protection exist in the C-20/A4 chondrocytes.

For the qPCR studies, chondrocytes were treated with UCNI, SNAP and SNAP+UCNI; total RNA extracted from these treated samples and an untreated control were subjected to qPCR experiments to determine the effects of treatment on the relative expression of *CRFR1*, *CRFR2* and *Kir6.1* mRNA. Chondrocytes were subjected to SNAP and UCNI treatment as detailed in 2.2.2 protocol and total cellular RNA extracted and quantified according to 2.2.4. qPCR experiments were conducted using one-step RT-qPCR as detailed in 2.2.6 and the relative quantification of these genes (*CRFR1*α, *CRFR2*β and *Kir6.1*) was performed using the Comparative C_q (or $2^{-\Delta\Delta C_q}$) method of analysis where expression changes are expressed as fold change relative to the calibrator (Livak and Schmittgen, 2001). Three different experiments (n=3) were performed for the reference gene (GAPDH) and each gene of interest (*CRFR1*α, *CRFR2*β, and *Kir6.1*). For each experiment (n=1), RT-qPCR on the control and treated samples were performed in triplicates and three different control and treated RNA preparations were used.

Relative Expression using the $2^{-\Delta\Delta C_q}$ method is calculated in three steps using the following equations:

(Step A):
Equation 1: ΔC_q =average $C_{q\ (Gene\ of\ interest)}$ – average $C_{q\ (reference\ gene)}$

(Step B):
Equation 4: $\Delta\Delta C_q = \Delta C_{q\ (sample\ of\ interest)} - \Delta C_{q\ (calibrator)}$

(Step C):
Equation 5: Fold change= $2^{-\Delta\Delta C_q}$

In general, if the calculated value for the $\Delta\Delta C_q$ is positive, this results in a $2^{-\Delta\Delta C_q}$ value that is negative indicating a reduction in expression levels. Conversely, a negative $\Delta\Delta C_q$ value generates a positive $2^{-\Delta\Delta C_q}$ value signifying an increase in expression of the target gene due to treatment (Schmittgen and Livak, 2008). The calculations for the relative expression by $2^{-\Delta\Delta C_q}$ was performed using Microsoft Excel, 2007 (Microsoft,USA).

The results for the relative quantification of *CRFR1α*, *CRFR2β* and *Kir6.1* following treatment are illustrated in the following sections (3.5.1-3.5.3). An unpaired T-test was performed on the ΔC_q values to determine the level of significance of the changes in the relative expression of the genes of interest following treatment and significance was at $p<0.05$ (Yuan *et al*, 2006).

3.5.1 Determination of the relative expression of *CRFR1α* in C-20/A4 cells following stimulation with UCNI and SNAP

qPCR experiments assessed the effect of treatment on the relative expression of the *CRFR1α* receptor, a potential UCNI receptor for mediating UCNI chondroprotection. Tables 3.1-3.3 shows the calculations employed for determining the fold changes in gene expression levels for each of three experiments performed and the average fold change from these three experiments is illustrated in table 3.4.

Treatments	(a) *CRFR1α* Cq	(b) Reference gene: *GAPDH* Cq	ΔCq	ΔΔCq = $\Delta Cq_{(a)}-\Delta Cq_{(b)}$	$2^{-\Delta\Delta C}q$
control	25.3	7.46			
	24.46	7.67			
	25.59	7.75			
Average Cq	**25.12**	**7.63**	**17.49**	**0**	**1**
SD	**±0.59**	**±0.15**	**±0.74**	**±0.74**	
UCNI	26.18	7.68			
	24.68	7.7			
	24.73	7.71			
Average Cq	**25.20**	**7.70**	**17.5**	**0.01**	**1.01**
SD	**±0.85**	**±0.02**	**±0.87**	**±0.87**	
SNAP	26.39	8.1			
	25.6	8.25			
	26.12	8.17			
Average Cq	**26.04**	**8.17**	**17.86**	**0.37**	**1.30**
SD	**±0.40**	**±0.04**	**±0.44**	**±0.44**	
SNAP+UCNI	26.12	8.36			
	26.04	8.35			
	26.48	8.35			
Average Cq	**26.21**	**8.35**	**17.86**	**0.37**	**1.29**
SD	**±0.23**	**±0.01**	**±0.24**	**±0.24**	

Table 3.1:The Cq values from experiment one and calculation of the expression levels of *CRFR1α* mRNA following stimulation of chondrocytes with: UCNI, SNAP and SNAP+UCNI for 6 hours using the Comparative C_q method for relative quantification. The $C_q$values are represented as mean±standard deviation (SD) and $2^{-\Delta\Delta C}{}_q$ presented as fold change. ΔC_q = delta C_q, $\Delta\Delta C_q$= Delta Delta C_q. N= 3 of three different experiments, in which each control, UCNI, SNAP and SNAP+UCNI treatment was performed in triplicates.

Treatments	(a)*CRFR1α* Cq	(b) Reference gene: *GAPDH* Cq	ΔCq	ΔΔCq = $\Delta Cq_{(a)}-\Delta Cq_{(b)}$	$2^{-\Delta\Delta}$Cq
control	24.91	9.27			
	26.94	9.32			
	25.42	9.3			
Average Cq	**25.76**	**9.30**	**16.46**	**0**	**1**
SD	**±1.06**	**±0.03**	**±1.08**	**±1.08**	
UCNI	25.36	9.13			
	25.76	9.09			
	25.32	9.27			
Average Cq	**25.48**	**9.16**	**16.32**	**-0.14**	**1.10**
SD	**±0.24**	**±0.09**	**±0.34**	**±0.34**	
SNAP	27.66	9.71			
	27.47	9.8			
	27.39	9.74			
Average Cq	**27.51**	**9.75**	**17.76**	**1.30**	**-2.46**
SD	**±0.14**	**±0.05**	**±0.18**	**±0.18**	
SNAP+UCNI	27.22	9.78			
	27.93	9.76			
	28.17	9.81			
Average Cq	**27.77**	**9.78**	**17.99**	**1.53**	**-2.89**
SD	**±0.49**	**±0.03**	**±0.52**	**±0.52**	

Table 3.2: The Cq values from experiment two and calculation of the expression levels of *CRFR1α* mRNA following stimulation of chondrocytes with: UCNI, SNAP and SNAP+UCNI for 6 hours using the Comparative C_q method for relative quantification. The C_q values are represented as mean±standard deviation (SD) and $2^{-\Delta\Delta C}{}_q$ presented as fold change. ΔC_q = delta C_q, $\Delta\Delta C_q$= Delta Delta C_q. N= 3 of three different experiments, in which each control, UCNI, SNAP and SNAP+UCNI treatment was performed in triplicates.

Treatments	(a) *CRFR1α*Cq	(b) Reference gene: *GAPDH* Cq	ΔCq	ΔΔCq = $\Delta Cq_{(a)}-\Delta Cq_{(b)}$	$2^{-\Delta\Delta C}q$
control	24.18	8.25			
	25.59	7.13			
	25.42	7.53			
Average Cq	**25.06**	**7.64**	**17.43**	**0**	**1**
SD	**±0.77**	**±0.57**	**±1.34**	**±1.34**	
UCNI	26.71	7.62			
	25.62	7.09			
	25.54	7.38			
Average Cq	**25.96**	**7.36**	**18.59**	**1.17**	**-2.24**
SD	**±0.65**	**±0.27**	**±0.92**	**±0.92**	
SNAP	25.47	7.99			
	25.94	8.25			
	25.66	8.3			
Average Cq	**25.69**	**8.18**	**17.51**	**0.08**	**-1.06**
SD	**±0.24**	**±0.17**	**±0.40**	**±0.4**	
SNAP+UCNI	24.96	8.63			
	25.35	8.77			
	25.22	8.13			
Average Cq	**25.18**	**8.51**	**16.67**	**-0.76**	**1.69**
SD	**±0.20**	**±0.34**	**±0.54**	**±0.54**	

Table 3.3: The Cq values from experiment three and calculation of the expression levels of *CRFR1α* mRNA following stimulation of chondrocytes with: UCNI, SNAP and SNAP+UCNI for 6 hours using the Comparative C_q method for relative quantification. The C_q values are represented as mean±standard deviation (SD) and $2^{-\Delta\Delta C}{}_q$ presented as fold change. ΔC_q = delta C_q, $\Delta\Delta C_q$= Delta Delta C_q. N= 3 of three different experiments, in which each control, UCNI, SNAP and SNAP+UCNI treatment was performed in triplicates.

Treatments	GOI (*CRFR1α*) average C_q	Reference gene *(GAPDH)* average C_q	ΔC_q	$\Delta\Delta C_q$	$2^{-\Delta\Delta C_q}$
Control	25.31 ± 0.26	8.19 ± 0.29	17.12 ± 0.56	0 ± 0.56	1 (0.7-1.5)
UCNI	25.54 ± 0.21	8.07 ± 0.28	17.47 ± 0.49	0.35 ± 0.49	-1.28 (0.9-1.8)
SNAP	26.41 ± 0.29	8.70 ± 0.26	17.71 ± 0.55	0.59 ± 0.55	-1.50 (1.0-2.2)
SNAP+UCNI	26.39 ± 0.39	8.88 ± 0.23	17.51 ± 0.62	0.39 ± 0.62	-1.31 (0.9-2.0)

Table 3.4: Calculation of the expression levels of *CRFR1α* mRNA following stimulation of chondrocytes with: UCNI, SNAP and SNAP+UCNI for 6 hours using the Comparative C_q method for relative quantification. The C_q values represented as mean±SEM of three different experiments performed and $2^{-\Delta\Delta C}$q presented as fold change with range: E.g. -1.28 fold decrease with range – (0.9-1.8). GOI= Gene of interest, ΔC_q = delta C_q, $\Delta\Delta C_q$= Delta Delta C_q. N= 3 of three different experiments, in which each control, UCNI, SNAP and SNAP+UCNI treatment was performed in triplicates.

Analysis of the qPCR experiments for the relative expression of the CRFR1α receptor following treatment was determined using the comparative C_q method and the calculations for such are displayed in tables 3.1-3.4. The data shown in tables 3.1-3.3 are the Cq values obtained for the target gene (*CRFR1α*) and the reference gene (*GAPDH*) from three independent experiments. The data in table 3.4 is an average of the three experiments performed.

The student unpaired T-test was used for statistical analysis of the qPCR data shown in table 3.4, for the relative expression of CRFR1α mRNA following treatment of chondrocytes with UCNI, SNAP and SNAP+UCNI. The statistical analysis of the ΔC_q values as described in section 3.5 suggested that chondrocytes subjected to treatment with UCNI, SNAP and SNAP+UCNI showed no significant ($p>0.05$) change in the mRNA expression of the CRFR1α following treatment.

3.5.2 Determination of the relative expression of *CRFR2β* in C-20/A4 cells following stimulation with UCNI and SNAP

Analysis of the qPCR experiments for the relative expression of the *CRFR2β* receptor (another potential UCNI receptor for mediating UCNI chondroprotection) following treatment was determined. Similarly, employing the equations described in section 3.5, the calculations for determining the fold changes in gene expression levels for CRFR2β are detailed in tables 3.5-3.8.

Treatments	(a) *CRFR2β* Cq	(b) *GAPDH* Cq	ΔCq	ΔΔCq = $\Delta Cq_{(a)}-\Delta Cq_{(b)}$	$2^{-\Delta\Delta C}q$
control	25.04	7.46			
	24.9	7.67			
	25.05	7.75			
Average Cq	**25.00**	**7.63**	**17.37**	**0**	**1**
SD	**±0.08**	**±0.15**	**±0.23**	**±0.23**	
UCNI	25.25	7.68			
	25.37	7.7			
	24.76	7.71			
Average Cq	**25.13**	**7.70**	**17.43**	**0.06**	**-1.04**
SD	**±0.32**	**±0.02**	**±0.34**	**±0.34**	
SNAP	25.7	8.1			
	26.35	8.25			
	25.99	8.17			
Average Cq	**26.01**	**8.17**	**17.84**	**0.47**	**-1.39**
SD	**±0.33**	**±0.08**	**±0.40**	**±0.4**	
SNAP+UCNI	26.47	8.36			
	25.28	8.35			
	26.84	8.35			
Average Cq	**26.20**	**8.35**	**17.84**	**0.47**	**-1.39**
SD	**±0.82**	**±0.01**	**±0.82**	**±0.82**	

Table 3.5: The Cq values from experiment one and calculation of the expression levels of *CRFR2β* mRNA following stimulation of chondrocytes with: UCNI, SNAP and SNAP+UCNI for 6 hours using the Comparative C_q method for relative quantification. The C_q values are represented as mean±standard deviation (SD) and $2^{-\Delta\Delta C}{}_q$ presented as fold change. ΔC_q = delta C_q, $\Delta\Delta C_q$= Delta Delta C_q. Each control, UCNI, SNAP and SNAP+UCNI treatment was performed in triplicates.

Treatments	(a) *CRFR2β*Cq	(b) Reference gene Cq	ΔCq	ΔΔCq = $\Delta Cq_{(a)}-\Delta Cq_{(b)}$	$2^{-\Delta\Delta C}q$
control	24.05	9.27			
	24.64	9.32			
	25.25	9.3			
Average Cq	**24.65**	**9.30**	**15.35**	**0**	**1**
SD	**±0.60**	**±0.03**	**±0.63**	**±0.63**	
UCNI	24.15	9.13			
	24.83	9.09			
	25.51	9.27			
Average Cq	**24.83**	**9.16**	**15.67**	**0.32**	**-1.25**
SD	**±0.68**	**±0.09**	**±0.77**	**±0.77**	
SNAP	25.22	9.71			
	25.5	9.8			
	25.93	9.74			
Average Cq	**25.55**	**9.75**	**15.8**	**0.45**	**-1.37**
SD	**±0.36**	**±0.05**	**±0.40**	**±0.4**	
SNAP+UCNI	25.62	9.78			
	25.08	9.76			
	26.8	9.81			
Average Cq	**25.83**	**9.78**	**16.05**	**0.7**	**-1.62**
SD	**±0.88**	**±0.03**	**±0.90**	**±0.9**	

Table 3.6: The Cq values from experiment two and calculation of the expression levels of *CRFR2β* mRNA following stimulation of chondrocytes with: UCNI, SNAP and SNAP+UCNI for 6 hours using the Comparative C_q method for relative quantification. The C_q values are represented as mean±standard deviation (SD) and $2^{-\Delta\Delta C}{}_q$ presented as fold change. ΔC_q = delta C_q, $\Delta\Delta C_q$= Delta Delta C_q. Each control, UCNI, SNAP and SNAP+UCNI treatment was performed in triplicates.

Treatments	(a) *CRFR2β* Cq	(b) Reference gene Cq	ΔCq	ΔΔCq = $\Delta Cq_{(a)}-\Delta Cq_{(b)}$	$2^{-\Delta\Delta C}q$
control	24.53	8.25			
	25.4	7.13			
	24.81	7.53			
Average Cq	**24.91**	**7.64**	**17.28**	**0**	**1**
SD	**±0.44**	**±0.57**	**±1.01**	**±1.01**	
UCNI	25.32	7.62			
	25.26	7.09			
	25.12	7.38			
Average Cq	**25.23**	**7.36**	**17.87**	**0.59**	**-1.51**
SD	**±0.10**	**±0.27**	**±0.37**	**±0.37**	
SNAP	26.17	7.99			
	25.49	8.25			
	27	8.3			
Average Cq	**26.22**	**8.18**	**18.04**	**0.76**	**-1.70**
SD	**±0.76**	**±0.17**	**±0.92**	**±0.92**	
SNAP+UCNI	26.62	8.63			
	25.85	8.77			
	27.17	8.13			
Average Cq	**26.55**	**8.51**	**18.04**	**0.76**	**-1.69**
SD	**±0.66**	**±0.34**	**±1.00**	**±1.00**	

Table 3.7: The Cq values from experiment three and calculation of the expression levels of *CRFR2β* mRNA following stimulation of chondrocytes with: UCNI, SNAP and SNAP+UCNI for 6 hours using the Comparative C_q method for relative quantification. The C_q values are represented as mean±standard deviation (SD) and $2^{-\Delta\Delta C}{}_q$ presented as fold change. ΔC_q = delta C_q, $\Delta\Delta C_q$= Delta Delta C_q. Each control, UCNI, SNAP and SNAP+UCNI treatment was performed in triplicates.

Treatments	GOI (*CRFR2β*) average C_T	Reference gene (*GAPDH*) average C_T	ΔC_q	$\Delta\Delta C_q$	$2^{-\Delta\Delta C_q}$
control	24.85 ± 0.14	8.19 ± 0.29	16.66 ± 0.43	0 ± 0.43	1 (0.7-1.3)
UCNI	25.06 ± 0.14	8.07 ± 0.28	16.99 ± 0.42	0.33 ± 0.42	-1.26 (0.9-1.7)
SNAP	25.93 ± 0.18	8.70 ± 0.26	17.23 ± 0.44	0.57± 0.44	-1.48 (1.1-2.0)
SNAP+UCNI	26.19 ± 0.25	8.88 ± 0.23	17.31 ±0.48	0.65 ±0.48	-1.57 (1.1-2.2)

Table 3.8: Calculation of the expression levels of *CRFR2β* mRNA following stimulation of chondrocytes with: UCNI, SNAP and SNAP+UCNI for 6 hours using the Comparative C_q method for relative quantification. The C_q values represented as mean± SEM and $2^{-\Delta\Delta C}{}_q$ presented as fold change with range. GOI= Gene of interest, ΔC_q = delta C_q, $\Delta\Delta C_q$= Delta Delta C_q. N=3 of the three different experiments performed of which raw data is shown in tables 3.5-3.7.

The relative quantification of *CRFR2β* mRNA for each experiment indicated in the calculation in table 3.5-3.7 demonstrates the fold change in *CRFR2β* due to treatment of cells with UCNI, SNAP and SNAP+UCNI relative to the calibrator. In addition, the average fold change for *CRFR2β* mRNA expression from the three independent experiments (shown in tables 3.5-3.7) are summarised in table 3.8.

It can be deduced from all of the above data that stimulation of cells with UCNI, SNAP, and SNAP+UCNI resulted in no statistical significant change ($p>0.05$) in *CRFR2β* mRNA expression when compared to the calibrator. Statistical significance of the relative expression of *CRFR2β* mRNA expression was determined by unpaired T-test.

3.5.3 Determination of the relative expression of *Kir6.1* in C-20/A4 cells following UCNI and SNAP treatment

The Kir6.1 was considered a potential target for UCNI inhibition of apoptosis in chondrocytes based on the work by Lawrence *et al*, which showed that UCNI mediated its cardioprotective effects partially via inducing expression of the KIr6.1 subunit localised to the mtioK_{ATP} channel in the cardiac myocytes (Lawrence *et al*, 2004). The calculations for determining the changes in mRNA expression levels for *Kir6.1* are detailed in table 3.9-3.12.

Treatments	(a) *Kir6.1* Cq	(b) Reference gene Cq	ΔCq	ΔΔCq = $\Delta Cq_{(a)}-\Delta Cq_{(b)}$	$2^{-\Delta\Delta C}q$
control	28.13	7.46			
	27.65	7.67			
	28.51	7.75			
Average Cq	**28.10**	**7.63**	**20.47**	**0**	**1**
SD	**±0.43**	**±0.15**	**±0.58**	**±0.58**	
UCNI	28.23	7.68			
	28.81	7.7			
	29	7.71			
Average Cq	**28.68**	**7.70**	**20.98**	**0.51**	**-1.43**
SD	**±0.40**	**±0.02**	**±0.42**	**±0.42**	
SNAP	26.89	8.1			
	27.32	8.25			
	26.3	8.17			
Average Cq	**26.84**	**8.17**	**18.66**	**-1.81**	**3.50**
SD	**±0.51**	**±0.08**	**±0.59**	**±0.59**	
SNAP+UCNI	26.08	8.36			
	26.12	8.35			
	26.35	8.35			
Average Cq	**26.18**	**8.35**	**17.83**	**-2.64**	**6.23**
SD	**±0.15**	**±0.01**	**±0.15**	**±0.15**	

Table 3.9: The Cq values from experiment one and calculation of the expression levels of *Kir6.1* mRNA following stimulation of chondrocytes with: UCNI, SNAP and SNAP+UCNI for 6 hours using the Comparative C_q method for relative quantification. The C_q values are represented as mean±standard deviation (SD) and $2^{-\Delta\Delta C}{}_q$ presented as fold change. ΔC_q = delta C_q, $\Delta\Delta C_q$= Delta Delta C_q. Each control, UCNI, SNAP and SNAP+UCNI treatment was performed in triplicates.

Treatments	(a) *Kir6.1* Cq	(b) Reference gene Cq	ΔCq	ΔΔCq = $\Delta Cq_{(a)}-\Delta Cq_{(b)}$	$2^{-\Delta\Delta C}q$
control	28.5	9.27			
	27.77	9.32			
	29.01	9.3			
Average Cq	**28.43**	**9.30**	**19.13**	**0**	**1**
SD	**±0.62**	**±0.03**	**±0.65**	**±0.65**	
UCNI	26.91	9.13			
	28.43	9.09			
	28.76	9.27			
Average Cq	**28.03**	**9.16**	**18.87**	**-0.26**	**1.20**
SD	**±0.99**	**±0.09**	**±1.08**	**±1.08**	
SNAP	28.71	9.71			
	28.02	9.8			
	28.84	9.74			
Average Cq	**28.52**	**9.75**	**18.77**	**-0.36**	**1.28**
SD	**±0.44**	**±0.05**	**±0.49**	**±0.49**	
SNAP+UCNI	28.07	9.78			
	29.82	9.76			
	24.06	9.81			
Average Cq	**27.32**	**9.78**	**17.53**	**-1.60**	**3.02**
SD	**±2.95**	**±0.03**	**±2.98**	**±2.98**	

Table 3.10: The Cq values from experiment two and calculation of the expression levels of *Kir6.1* mRNA following stimulation of chondrocytes with: UCNI, SNAP and SNAP+UCNI for 6 hours using the Comparative C_q method for relative quantification. The C_q values are represented as mean±standard deviation (SD) and $2^{-\Delta\Delta C}{}_q$ presented as fold change. ΔC_q = delta C_q, $\Delta\Delta C_q$= Delta Delta C_q. Each control, UCNI, SNAP and SNAP+UCNI treatment was performed in triplicates.

Treatments	(a) *Kir6.1* Cq	(b) Reference gene Cq	ΔCq	ΔΔCq = $\Delta Cq_{(a)}$-$\Delta Cq_{(b)}$	$2^{-\Delta\Delta C}q$
control	30.32	8.25			
	28.78	7.13			
	30.14	7.53			
Average Cq	**29.75**	**7.64**	**22.11**	**0**	**1**
SD	**±0.84**	**±0.57**	**±1.41**	**±1.41**	
		7.62			
UCNI	30.78	7.09			
	30.24	7.38			
	30.44				
Average Cq	**30.49**	**7.36**	**23.12**	**1.01**	**-2.02**
SD	**±0.27**	**±0.27**	**±0.54**	**±0.54**	
SNAP	30.53	7.99			
	31.23	8.25			
	31.76	8.3			
Average Cq	**31.17**	**8.18**	**22.99**	**0.88**	**-1.84**
SD	**±0.62**	**±0.17**	**±0.78**	**±0.78**	
SNAP+UCNI	30.34	8.63			
	30.84	8.77			
	32	8.13			
Average Cq	**31.06**	**8.51**	**22.55**	**0.44**	**-1.36**
SD	**±0.85**	**±0.34**	**±1.19**	**±1.19**	

Table 3.11: The Cq values from experiment three and calculation of the expression levels of *Kir6.1* mRNA following stimulation of chondrocytes with: UCNI, SNAP and SNAP+UCNI for 6 hours using the Comparative C_q method for relative quantification. The C_q values are represented as mean±standard deviation (SD) and $2^{-\Delta\Delta C}{}_q$ presented as fold change. ΔC_q = delta C_q, $\Delta\Delta C_q$= Delta Delta C_q. Each control, UCNI, SNAP and SNAP+UCNI treatment was performed in triplicates.

Treatments	GOI (*Kir6.1*) average C_T	Reference gene (*GAPDH*) average C_q	ΔC_q	$\Delta\Delta C_q$	$2^{-\Delta\Delta C_q}$
control	28.76 ±0.31	8.19 ± 0.29	20.57 ± 0.61	0 ± 0.61	1 (0.7-1.5)
UCNI	29.07 ± 0.41	8.07 ± 0.28	21.00 ± 0.69	0.43 ± 0.69	-1.35 (0.8-2.2)
SNAP	28.29 ±0.87	8.70 ± 0.26	19.59 ±1.13	-0.98 ±1.13	1.97 (1.1-4.3)
SNAP+UCNI	28.19 ± 0.90	8.88 ± 0.23	19.31 ± 1.13	-1.26± 1.13	2.39 (1.1-5.2)

Table 3.12: Calculation of the expression levels of *Kir6.1* mRNA following stimulation of chondrocytes with: UCNI, SNAP and SNAP+UCNI for 6 hours using the Comparative C_q method for relative quantification. The C_q values represented as mean± SEM and $2^{-\Delta\Delta C_q}$ presented as fold change with range. GOI= Gene of interest, ΔC_q = delta C_q, $\Delta\Delta C_q$= Delta Delta C_q. N= 3 of three different experiments, in which each control, UCNI, SNAP and SNAP+UCNI treatment was performed in triplicates.

The data in tables 3.9-3.11 which shows the Cq values and fold change calculation for three independent experiments indicates a varying in *Kir6.1* mRNA expression following stimulation of the C-20/A4 chondrocytes with UCNI, SNAP and SNAP+UCNI. An average fold change calculation for these three experiments in shown in table 3.12. The qPCR analysis in the latter table indicates that following treatment of chondrocytes with UCNI demonstrated a 1.35 fold decrease in *Kir6.1* mRNA expression. Treatment with SNAP resulted in *Kir6.1* being upregulated 1.97 fold; indicating that the *Kir6.1* gene is 1.97x more abundant in SNAP treated C-20/A4 cells than untreated cells. In addition, a fold increase of 2.39 fold was also observed following concurrent treatment of the cells with both SNAP+UCNI. Statistical analysis of the calculated ΔC_q values in table 3.12 implies that none of the observed changes in *Kir6.1* mRNA expression appears to be significant at the level $p<0.05$ according to unpaired T-test.

3.6 The effect of Diazoxide and SNAP treatment on C-20/A4 cells

In relation to the findings from earlier work by Lawrence *et al*, in 2004, and the relative quantification studies in table 3.12 of section 3.5.3 which demonstrated that stimulation of C-20/A4 cells with SNAP and SNAP+UCNI resulted in increased expression levels of *Kir6.1* (although this change was not statistically significant, p>0.05) , experiments were performed to assess involvement of this K_{ATP} channel in preventing apoptosis, emulating a proposed mechanism of action for UCNI.

In this section, cell death following treatment of chondrocytes with SNAP, and a pharmacological K_{ATP} channel opening agent, Diazoxide, was assessed by flow cytometry (apoptosis) and LDH release (necrosis). Chondrocytes were cultured for *in vitro* stimulation studies as detailed in section 2.2.2. Following treatment, flow cytometry analysis was performed according to the protocol in section 2.2.3.1 for the detection of apoptosis. LDH release for the assessment of necrosis was conducted according the protocol of section 2.2.3.2.

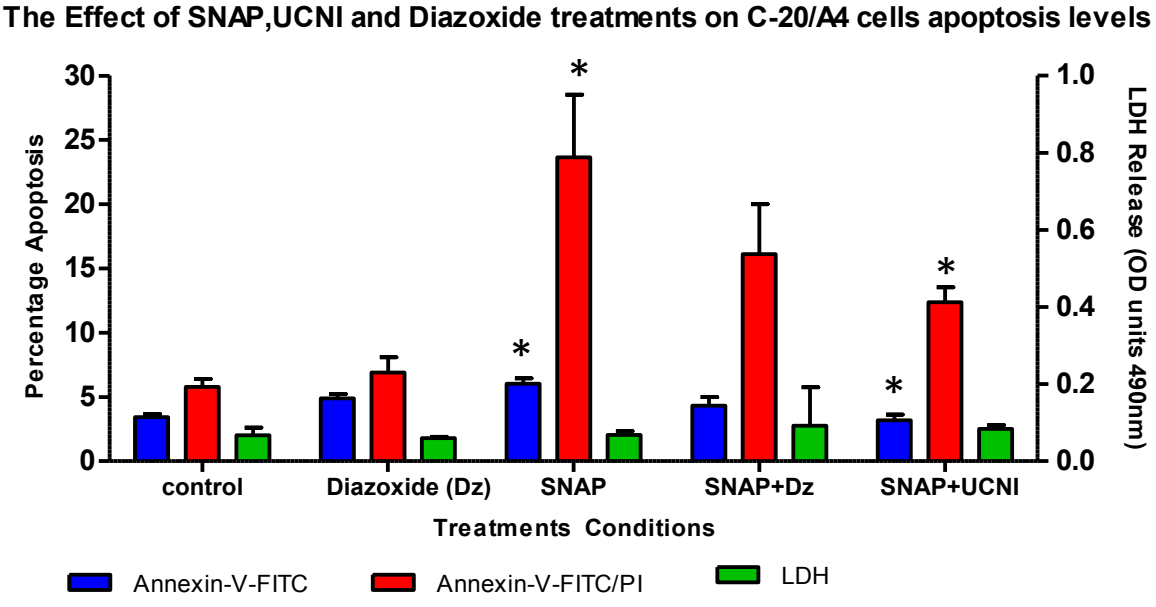

Figure 3.12: The effects of SNAP, UCNI and Diazoxide (Dz) treatment on cell death by apoptosis in C-20/A4 chondrocytes.
Data values are presented as means (± SEM), n=3, triplicates of a minimum of three different experiments except Diazoxide where n=2, triplicates of two different experiments. *P<0.05

The flow cytometry data of figure 3.18 demonstrates results for treatment of chondrocytes with Diazoxide and SNAP singly and in combination. As previously observed, SNAP alone caused a significant increase in apoptotic cell death ($p<0.05$).

These preliminary data also demonstrate that Diazoxide appears to ameliorate SNAP induced apoptotic cell death, similar to UCNI, when cells are stimulated concurrently with SNAP+Diazoxide. However, these preliminary experiments need to be repeated to establish whether the reduction in apoptotic cell death observed following treatment of C-20/A4 chondrocytes with SNAP+Diazoxide is statistically significant; but these initial findings are encouraging.

Chapter 4:

Discussion

4 Discussion

4.1 Introduction:

The principal aim of this thesis was to investigate the potential mechanism(s) of UCNI mediated protection in chondrocytes against SNAP/NO induced apoptosis. This aim was established following previous research by Intekhab-Alam, in 2006, which reported that (1) UCNI is a cytoprotective agent against apoptosis in C-20/A4 chondrocytes stimulated with the pro-apoptotic stimuli: TNFα, IL-1β and SNAP (a NO donor) and (2) UCNI exerted greater protection against apoptosis induced SNAP/NO than that induced by the death receptor ligands (TNFα and IL-1β) (Intekhab-Alam, 2006).

This 40 amino acid peptide, UCNI, has been shown to exert anti-apoptotic effects not only in C-20/A4 chondrocytes but also in other cell types including cardiac myocytes, where it has been reported to potentially mediate these properties via CRF receptors (CRFR2β) and K_{ATP} channels (particularly the mitoK_{ATP} channel) (Brar *et al*, 1999; Lawrence *et al*, 2002; Brar *et al*, 2000). Given the lack of data with regards to the targets for UCNI mediated protection in chondrocytes, it was therefore necessary to elucidate which, if any, of these potential signalling pathways exist in the C-20/A4 cells and whether they play a role in UCNI mediated chondroprotection. Towards this end, a number of experiments have been conducted to ascertain the potential contribution of CRFR's and ion channels to this observed chondroprotection following SNAP/NO stimulation.

4.2 The effects of exogenous UCNI in C-20/A4 chondrocytes:

The protective effects of exogenous UCNI against NO induced cell death, initially demonstrated by Intekhab-Alam 2006,were revisited. These initial studies used fluorescence microscopy based Annexin V-FITC/PI and TUNEL assays to quantify chondrocyte apoptosis which, whilst valid, can be very subjective and are highly dependent on the interpretation, and, indeed, experience of the operator. Herein, apoptotic chondrocyte death andthe cytoprotective effects of UCNI were assessed by a flow cytometry method following labelling of untreated and stimulated cells with Annexin- V-FITC and Propidium Iodide (PI) fluorochromes as shown figure 3.1.

Many studies investigating aspects of chondrocyte structure and physiology such as chondrocyte viability, proliferation and cell cycle phenotype have employed flow cytometry as method of analysis (Bell *et al*, 1988; Lopez-Armada *et al*, 2006; Takacs-Buia *et al*, 2008; Wang *et al*, 2001; Matsuki *et al*, 2008; Thuong-Guyot *et al*, 1994)as it is regarded as a multi-parametric and constant method for analysis of cells in culture which is less subjective. A variety of parameters (non-fluorescent and fluorescent) of single cells can be assayed rapidly and analysed by dedicated computer software generating histograms relating morphology and fluorescence of the cells as shown in figure 3.1 (Loo and Rillema, 1998; Wang *et al*, 2001). Flow cytometry analysis is typically performed on cell counts of 10,000 or more per sample in contrast to fluorescence microscopy based techniques where Annexin V/TUNEL positivity is determined by microscopy, typically based on counting 100 cells in 3 different, randomly selected, fields of view. Thus flow cytometry represents a much less subjective technique based on a much larger sample of the cell population. Other methods for apoptosis detection include: agarose gel electrophoresis and DNA fragmentation ELISA assays, caspase cleavage and activity assays and electron microscopy (Kim and Blanco, 2007; Kuhn *et al*, 2004; Schultz and Harrington, 2003).

In the assay developed here, assessment of cell death was performed by individual interrogation of 10,000 cells per sample with a 488 and 635nm laser. The flow cytometer then characterises and enumerates the counted C-20/A4 cells based on cell size, internal complexity and fluorescence intensity which, when analysed by dedicated software, allows the quantification of apoptosis dividing the cells into four distinct cell populations (i.e. viable, early apoptotic, late apoptosis and necrotic). The information regarding the cell size and internal structure of the C-20/A4 cells is generated from the non-fluorescent parameters: the Forward Scatter (FSC) and Side Scatter (SSC) respectively, whilst relative fluorescence intensity is produced from fluorescent labelled cells undergoing measurable cell death. Diagrammatic representations of FSC/SSC and fluorescence (FL1/FL2) histograms are shown in section 3.1.1, which documents representative data generated in this assay.

The flow cytometer generates FSC (i.e. cell size) and SSC (internal complexity/ granularity) data from the light scattering channels. The forward scatter is diffracted light which scattered in a forward direction and thus correlates with the relative cell size. Conversely, light which is detected at right angles to the laser beam is refracted and reflected light (SSC) and so correlates with granularity and internal structures which reflect the light. Accordingly, these two parameters provide vital information about the state of cells as analysis of scattered light can allow differentiation between cells undergoing measurable apoptosis from the viable cells. For instance, in the flow cytometric histogram of figure 3.1 column A, it is evident that the apoptotic cells have a decreased FSC and increased SSC (for e.g. histogram 3A: SNAP treatment). The observed decrease in FSC occurs as a result of cell shrinkage; a characteristic morphological feature of apoptotic cells (Takacs-Buia *et al*, 2008; Kim and Blanco, 2007), which correlates with a decrease in the intensity of the diffracted light and thus a low FSC. Furthermore, an increase in SSC results from an increase in refracted and reflected light, which is scattered at a right angle to the laser beam by the condensed chromatin and fragmented nuclei of apoptotic cells (Takacs-Buia *et al*, 2008).

In addition, FSC and SSC, cell death was also determined by Annexin-V-FITC/PI labelling, detected by the fluorescence channels within the flow cytometer. This was achieved as these fluorochromes (FITC and PI) absorb the light energy from the laser (at their excitation wavelenght) and emit this energy at a longer wavelength (the emission wavelength). On the fluorescence histogram (figure 3.1 column B), the data represented on the logarithmic scale demonstrates the emitted fluorescence intensity, which correlates with the binding sites of the fluorochromes on the cells (Takacs-Buia *et al*, 2008). Therefore, observing the fluorescence histograms of figure 3 .1, it is evident that the cells located further along the abscissa (towards 10^4) have more binding of Annexin-V-FITC, suggesting that a greater proportion of phosphotidylserine (PS) phospholipids are externalised on the plasma membrane of these C-20/A4 cells undergoing measurable apoptosis. PI fluorescence is conversely recorded on the ordinate giving a distinct location for an individual cell depending on the relative binding of the two fluorochromes.

Although flow cytometry is a more objective technique than fluorescence microscopy, the possibility of false positives results cannot be ruled out. User defined compensation is applied to minimise fluorochrome "bleed over" between channels so that the existence of false positives are reduced; hence the term "FITC log Comp" and PE-Texas Red Log Comp" when compensation is applied to data obtained from the fluorescence histograms.

In relation to the cell death studies documented in section 3.1.2, the detection of apoptosis as determined by flow cytometry illustrates in figure 3.2 that UCNI significantly reduces apoptotic cell death induced by the SNAP ($p<0.05$), a NO donor. In addition, section 3.2.1 demonstrates the exndogenous expression of UCNI mRNA. These findings agree with observations by Intekhab-Alam, 2006 which demonstrated that exogenous UCNI exerted protection against SNAP induced apoptosis. Furthermore Intekhab-Alam (2006) also demonstrated by qPCR that treatment of C-20/A4 cells with SNAP/NO resulted in a significant increase in UCNI mRNA expression compared to the control ($p>0.01$). Therefore this demonstrates that UCNI is a cytoprotective agent in C-20/A4 chondrocytes as it reduces SNAP/NO induced apoptosis in these cells. This observed protection against apoptotic cell death may occur as addition of exogenous UCNI would increase the amount of UCNI peptide, which was present in the medium to confer protection possibly through a CRFR dependent (or non-dependent) mechanism. Similarly, an increase in *UCNI* mRNA expression in cardiac myocytes has also been observed in following thermal injury and exogenous UCNI was protective against hypoxia (Okosi *et al*, 1998) and similar results were obtained for primary cultures of cardiac myocytes following cell death induced by ischemia (Brar *et al*, 1999) where a cardioprotective role of UCNI was implicated. Moreover, the result that apoptosis and not necrosis is the predominant form of cell death occurring in C-20/A4 cells is also in broad agreement with work by Intekhab-Alam, 2006 and Pesta, 2007.

Additionally, the data in figure 3.3 demonstrates that the observed apoptosis in the C-20/A4 chondrcoytes is a result of SNAP and not ethanol the vehicle for SNAP. Other *in vitro studies* have also documented chondrocyte death induction by NO donors (Blanco *et al*, 1995; Notoya *et al*, 2000; Maneiro *et al*, 2005; Kim *et al*, 2005). Furthermore, NO is considered a catabolic factor which induces apoptosis

and cartilage degeneration in OA (Abramson, 2008; Blanco *et al*, 1998; Martel-Pelletier *et al*, 2008; Goggs *et al*, 2003). Work by Hashimoto *et al*, in 1998, showed that chondrocyte apoptosis and NO production correlates with the severity of matrix degradation in OA cartilage (Hashimoto *et al*, 1998). Consequently, the implication of NO production with regards to OA pathogenesis is that NO generation may result in chondrocyte apoptosis which is related to cartilage degeneration (Lotz *et al*, 1999). In addition, previous studies by Kim *et al* in 2000, in which they assessed the occurrence of apoptosis in human osteoarthritic cartilage demonstrated that chondrocyte apoptosis is a predominant feature in Osteoarthritis (OA) and OA lesional cartilage compared to normal and non-OA lesional cartilage respectively (Kim *et al*, 2000).

Previous studies have shown that SNAP induces apoptosis via the intrinsic mitochondrial pathway (Figueroa *et al*, 2006; Tamatani *et al*, 1998). Moreover, Intekhab-Alam (2006) has also shown activation of caspase-9 and -3, but not caspase-8 in C-20/A4 chondrocytes. SNAP induces apoptosis via promoting DNA damage with consequent elevation of p53 levels, activation of caspase 9 and 3, inhibition of activity of the Mitochondrial respiratory transport chain (in particular complex IV), breakdown of the mitochondrial membrane potential, up-regulation of the pro-apoptotic Bcl-2 protein Bax and mitochondrial pore opening accompanied by cytochrome c release (Tamatani *et al*, 1998; Maneiro *et al*, 2005; Figueroa *et al*, 2006). Consequently, based on the above evidence, it can be suggested that the NO donor, SNAP, may induce apoptosis through the intrinsic (mitochondrial) pathway in C-20/A4 chondrocytes.

Given that UCNI protected the chondrocytes from apoptotic cell death, as members of the CRF family predominantly, but not exclusively, mediate their autocrine/paracrine effects through CRF receptors (CRFR1 or CRFR2), (Grammatopoulos and Chrousos, 2002)the assumption could be made that this cytoprotection would be achieved through a CRF receptor mediated pathway. Indeed, there is evidence from other cell types to show that UCNI effects are blocked following the addition of the receptor antagonist α-helical $CRH_{(9-41)}$(Lawrence *et al*, 2005; Terui *et al*, 2001; Tu *et al*, 2007) and preliminary studies by Intekhab-Alam (2006) has suggested similar results in the C-20/A4 chondrocyte cell line (Intekhab-Alam, 2006).Despite these reports, the data, documented in

figure 3.2 showed that treatment of chondrocytes with the CRF receptor antagonist: α-helical $CRH_{(9-41)}$ in isolation did not induce chondrocyte apoptosis, neither was the protective effect of UCNI significantly inhibited following co-treatment of C-20/A4 cells with SNAP+UCNI+α-helical $CRH_{(9-41)}$. A diagrammatic representation of the data in figure 3.2 is illustrated in the flow cytometry histograms of figure 3.1, which shows a range of flow cytometry analysis of C-20/A4 cells following various treatments from a typical experiment. In the latter figure, it can be observed that treatment of C-20/A4 chondrocytes with SNAP resulted in ~32% apoptosis (R7, 7.82%; R9, 23.95%); and SNAP+UCNI resulted in ~15% (R7, 9.59%; R9, 5.53%) apoptotic cell death; whilst treatment of chondrocytes with SNAP+UCNI+α-helical $CRH_{(9-41)}$ resulted in ~ 18% (R7, 15%; R9, 3%) apoptosis. This data shows that UCNI reduces apoptosis previously induced by SNAP/NO; however the protective effects was not revoked when α-helical $CRH_{(9-41)}$ was added in conjunction with SNAP+UCNI. In addition, treatment of chondrocytes with α-helical $CRH_{(9-41)}$ alone did not induce apoptosis ~9% (R7, 4.35%; R9,4.64%) when compared to the control (untreated) chondrocytes ~ 8% (R7, 5.03%; R9, 2.54%). This would suggest that the chondroprotective effects of UCNI may be mediated through a non-CRFR dependent pathway possibly involving L-type calcium channels as previously demonstrated by Tao *et al*. The studies by Tao *et al*, showed that UCNI inhibits L-type calcium channels in ventricular cells which may have a consequence of preventing calcium overload by reducing intracellular calcium ions; a mechanism which has been implicated in the cardioprotective effects of UCNI. This inhibition of L-type calcium channels by UCNI was in a CRF receptor independent manner, which could occur via binding of UCNI to L-type calcium channels inhibiting activation, to reduce the entry of calcium into the cell that consequently, reduce calcium overload (Tao and Li, 2005a; Tao *et al*, 2004; Tao and Li, 2005b). Therefore, the findings in this study that the CRF receptor antagonist: α-helical $CRH_{(9-41)}$, did not induce apoptosis in the C-20/A4 chondrocytes, based on the findings from Tao *et al*, would suggests that UCNI may be acting through ion channels and consequently, α-helical $CRH_{(9-41)}$ would have no effect.

Alternatively, it is possible that the α-helical $CRH_{(9-41)}$ has lost its efficacy from long term storage. This discrepancy can be resolved by repeating these inhibition experiments with a fresh supply of α-helical $CRH_{(9-41)}$; however due to financial and time constraints these experiments could not be repeated.

4.3 *UCNI* mRNA in C-20/A4 chondrocytes

Following, the data in section 3.1 which demonstrated the anti-apoptotic effects of UCNI *in vitro*, experiments were also performed to confirm the endogenous expression of *UCNI* mRNA in C-20/A4 chondrocytes under basal conditions and to determine the nature of *UCNI* expression in human chondrocytes. The UCNI forward and reverse primers used for the detection of *UCNI* mRNA (see table 2. 1) were those used by Takahashi *et al*, 1998 for the detection of *UCNI* mRNA in the human brain. The sequence for the human *UCNI* mRNA transcript (GenBank accession no. NM_003353), comprises a nucleotide sequence which encodes for the *UCNI* pro-peptide (nucleotide 192-488, (296bp)) which is processed into a mature protein (nucleotide 363-482, (119bp)). The *UCNI* primer set used in this study includes a forward primer located at nucleotide 343-358 and a reverse at 470-488, generating the 146 bp product observed in figure 3.4. This RT-PCR amplicon therefore confirms that UCNI is synthesised by C-20/A4 chondrocytes as a precursor protein, and this pro-peptide is cleaved proteolytically by convertases to yield the 40 amino acid mature peptide. This is in keeping with the proposed synthesis of UCNI in other tissues including regions of the human brain (e.g. in the hypothalamus, cerebral cortex, pons, thalamus and cerebellum), foetal membranes and placenta (Takahashi *et al*, 1998; Petraglia *et al*, 1996).

Given the endogenous mRNA expression of the *UCNI* pro-peptide and other members of the Urocortin family (*Stresscopin Related peptide* (*UCNII*) and *Stresscopin* (*UCNIII*)) which have also been shown to be chondroprotective albeit less effectively than UCNI, the results from the studies with α-helical $CRH_{(9-41)}$ are even more curious. The endogenous mRNA expression of members of the CRF family of peptides (*UCNI, SRP* and *SCP*) in the C-20/A4 chondrocytes suggests a possible function of these peptides within chondrocyte. One such role is their cytoprotective effects against apoptosis as shown in figure 3.2 of this thesis and also previous work in the C-20/A4 chondrocytes (Pesta, 2007; Intekhab-Alam, 2006).

Consequently, one would expect the expression of CRF receptors to which these peptides could bind and mediate their functions. RT-PCR studies were consequently performed for all known functional forms of human CRFR and other postulated targets for UCNI.

4.4 Urocortin I receptor/target expression:

In keeping with CRF receptor mediated pathways for UCNI chondroprotection, reverse transcriptase-PCR (RT-PCR) studies were performed to identify potential CRF receptors and K_{ATP} channel subunits based on reports from Brar *et al* 1999, Brar *et al* 2000 and Lawrence *et al* 2002; which showed that UCNI protection against ischaemia is achieved by activation of such targets in cardiac myocytes.

In relation to *CRF* receptor mRNA expression in the C-20/A4 chondrocytes, the RT-PCR data in figure 3.6, demonstrates that the C-20/A4 chondrocytes express the mRNA for the only functional CRFR1 isoform: *CRFR1*α (Zmijewski and Slominski, 2010) and a *CRFR2* receptor which was verified by further RT-PCR and sequence analysis as CRFR2β (figure 3.7), the largest of the CRFR2 isoforms containing 438 amino acids; although the predominant CRFR2 isoform expressed in the human peripheral tissues is CRFR2α (Chen *et al*, 2005; Dautzenberg and Hauger, 2002). The sequence analysis data for the mRNA expression of *CRFR1*α is detailed in section 3.3.1.1, *CRFR2* in section 3.3.1.2 and *CRFR2*β in section 3.3.2.1. Interestingly, the *CRFR2*β isoform mRNA has also been found in osteoclasts (personal communication with Lawrence, 2011). While no PCR products were generated for the *CRFR2*α (239 bp) and *CRFR2*γ (212 bp) in figure 3.7 suggesting the mRNA expression of such CRFR2 isoforms in the C-20/A4 chondrocytes, the RT-PCR for CRFR2γ mRNA expression requires further optimization to confirm that only CRFR2β mRNA is expressed. This is due to the presence non-specific PCR products which are visible on the gel image of figure 3.7 for *CRFR2*γ. As previously mentioned, the *CRFR1*α contains 13 exons following alternative splicing of exon 6, which forms the first intracellular loop (see figure 1.8) (Grammatopoulos and Chrousos, 2002). The *CRFR2*β contains exons 1,2, 5-15 (see figure 3.8). Although, the CRFR2 isoforms vary in their N-terminus (due to alternative splicing) and tissue distribution, no pharmacological differences in ligand binding exists between the CRFR2 variants (Dautzenberg and Hauger,

2002), however, in adenylate cyclase activation studies, UCNI and other CRF related peptides preferentially activate CRFR2β than either CRFR2α or CRFR2γ (Grammatopoulos and Chrousos, 2002; Parkes *et al*, 2001). Consequently, it is thought that the exons 1 and 2 which are absent in both CRFR2α or CRFR2γ are important in ligand –receptor recognition and interaction (Grammatopoulos and Chrousos, 2002). To the best of our knowledge, the chondrocytes are the only known cell type which express both *CRFR1* and *CRFR2* mRNA simultaneously.

Indeed, the observation in C-20/A4 chondroctyes that UCNI exerted greater protection than UCNII and UCNIII against apoptotic cell death (Pesta, 2007) could be attributed to the fact that UCNI can bind and activate both CRFR1 and CRFR2 receptors (Grammatopoulos and Chrousos, 2002), whilst UCNII and UCNIII are exclusive ligands for CRFR2 (Grammatopoulos and Chrousos, 2002; Koob and Heinrichs, 1999). Therefore, this would suggest that the chondroprotective effects of UCNI may be mediated through both CRFR1 and CRFR2 receptors, whilst UCNII and UCNIII employ CRFR2 only. However, as UCNI has a higher affinity for CRFR2 than CRFR1 receptors (Dautzenberg and Hauger, 2002) it can be postulated that the CRFR2 receptor may play a greater role in UCNI mediated chondroprotection.

Figure.3.8 and 3.9 illustrates the products obtained from amplification for the pore forming *Kir6.1* and *Kir6.2* subunits of the K_{ATP} channels. The expected product sizes of 312 bp and 249 bp respectively and sequence analysis data (sections 3.4.1.1 and 3.4.2.1, respectively) confirms the mRNA expression of both the *Kir6.1* and *Kir6.2* subunits by C-20/A4 chondrocytes. Although the Kir6.x pore forming subunits, 6.1 and 6.2 are ubiquitously expressed in many tissue types, the Kir6.1 subunit, is showed to be predominantly expressed in the inner mitochondrial membrane, thus constituting the mitoK_{ATP} channel (Seino and Miki, 2003; Seino, 1999). Conversely, knockout mice studies of the K_{ATP} channel subunits indicates that the Kir6.2 is largely the Kir6.x pore forming subunit composing the sacrcolemmal K_{ATP} channels (Seino and Miki, 2003; Burke *et al*, 2008; Tao and Li, 2005b). In relation to the potential formation of functional K_{ATP} channels by the C-20/A4 chondrocyte cell line, the mRNA expression of the regulatory subunit, the Sulfonyl Urea Receptor (SUR) for these Kir channels were also investigated by

RT-PCR. The data in figure 3.10 and sequence analysis data in sections 3.4.3.1.1and 3.4.3.1.2 shows the initial experiments for *SUR1* and *SUR2* mRNA expression by the C-20/A4 cell line; and indicates that both a *SUR1* and *SUR2* regulatory sub unit is expressed by these chondrocytes.

As previously mentioned, the SUR2 regulatory subunit exists in two predominant isoforms resulting from alternative splicing; SUR2A and SUR2B, which share a 97% amino acid homology differing only at the C-terminal exon, exon 38 (Yokoshiki *et al*, 1998) which encodes for 42 amino acids. As a consequence, the *SUR2A* mRNA has a C-terminus exon denoted 38A whilst the *SUR2B* employs the alternatively spliced exon 38B (Shi *et al*, 2005; Seino and Miki, 2003). Previous RT-PCR studies have indicated that the *SUR2A* gene found primarily in the heart and skeletal muscle whereas the *SUR2B* variant is ubiquitously expressed (Seino and Miki, 2003; Seino, 1999).

In considering the exon composition of *SUR2A* and *SUR2B*, primer pairs were designed towards the non-identical exons of these receptors (38A and 38B) and further RT-PCR studies performed in an aim to establish the specific isoforms being expressed in the C-20/A4 cell line. The results for these experiments are shown in figure 3.11 with sequencing data in sections 3.4.4.1.1 to 3.4.4.1.3. Interestingly, the latter figure demonstrates that the chondrocytes expressed mRNA for S*UR2A* and *SUR2B*, lanes 1-2 and lanes 7-8 respectively. Further alternative splicing of the SUR2A isoforms is known to exist resulting in two such transcript variants which have been identified and characterised human tissues namely: SUR2A delta 14 (SUR2-A-Δ-14) and SUR2A delta 17 (SUR2A-Δ-17) which are generated from deletion of exon 14 and 17 respectively (Shi *et al*, 2005; Chutkow *et al*, 1999; Aguilar-Bryan *et al*, 1998). Subsequent assessment of the SUR2A transcript variant expressed by C-20/A4 chondrocytes shown also in figure 3.11, reveals that the *SUR2A-Δ-14* variant (lanes 4-5) exists at the mRNA level. Presently, this variant has only been detected in the heart tissue in mouse (Chutkow *et al*, 1999; Burke *et al*, 2008).

Additionally, work by Chutkow *et al* in 1999, also showed that K_{ATP} channel re-constituted with the SUR2A-Δ-14 subunit failed to generate currents in electrophysiological studies thus deeming this subunit not functional. Although,

they were unclear as to why this K_{ATP} channel was non-functional, these studies indicated that exon 14 is essential for the formation of functional K_{ATP} channels as it is constitutes a segment of amino acid sequence for the cytoplasmic NBD1 domain of the SUR subunit (see figure 1.11) (Chutkow *et al*, 1999) which is involved in regulating K_{ATP} channel activity (Burke *et al*, 2008) . Based on these findings, it can be confirmed that the functional *SUR2* regulatory subunit that is expressed at the mRNA by the C20/A4 chondrocytes is *SUR2B*. Having established that the C-20/A4 chondrocytes express the mRNA for *Kir6.1*, *Kir6.2*, *SUR1*, and*SUR2B* subunits it is suggested that these cells are capable of expressing functional K_{ATP} channels. The mRNA expression of *Kir6.1* subunit by the C-20/A4 human chondrocyte cell line is comparable to research findings which demonstrated that the chondrocytes from normal and OA cartilage expressed the pore forming subunit, Kir6.1 and functional K_{ATP} channels. The protein for the Kir6.1 subunit was identified in all four layers of normal articular cartilage (see figure 1.1) but predominantly in the superficial and middle layer, whilst Kir6.1 expression was altered in OA cartilage where it was only detected in the superficial layer (Mobasheri *et al*, 2007).

Accordingly, in an attempt to investigate UCNI regulation ofthe CRF receptors and K_{ATP} channels subunits, C-20/A4 chondrocytes was treated with SNAP and exogenous UCNI to determine their effect on the expression levels of some of the potential targets (*CRFR1*α, *CRFR2*β and *Kir6.1*) for UCNI. qPCR studies were conducted and the relative quantification of gene expression analysed by the Comparative C_q ($2^{-\Delta\Delta C_q}$) method to establish if their expression is regulated by UCNI. The Comparative C_q method quantifies changes in gene expression as a relative fold change in expression levels between the treated and calibrator sample. The calibrator is the reference sample to which all other samples are compared and is given a value of 1 which denotes “no change”; in most instances the untreated sample is the calibrator (Wong and Medrano, 2005); herein the control (untreated) samples for *CRFR1*α, *CRFR2*β and *Kir6.1* were used as the calibrator samples. The calculations for the determination of changes in gene expression by this method were detailed in section 3.5. The statistical approach for the analysis of the qPCR data was to subject the ΔCq of the control and treated samples to an students unpaired T-test to determine the significant of the changes

in gene expression (Yuan *et al*, 2006), and values where $p<0.05$ was considered statistically significant. qPCR was conducted using one-step RT-qPCR and a total of three independent experiments (the minimum number of repeats required in order to scientifically determine the statistical significance of data) was performed for each gene (*GAPDH*, *CRFR1*α, *CRFR2*β and *Kir6.1*).

Within each experiment conducted the control, UCNI, SNAP and SNAP+UCNI samples were performed in triplicates. The reference gene used as an internal control for normalising mRNA for qPCR studies was *GAPDH*. This was based on previous work by Petsa (2007), which demonstrated that the mRNA expression of GAPDH was stable in C-20/A4 chondrocytes and does not vary under experimental conditions. Additionally, studies on the human chondrocyte cell line, C-28/I2, an immortalised chondrocyte cell line derived from a mature cartilage sample (a 15 yr old donor), recommended *GAPDH* as suitable reference gene in their investigation of chondroprotective agents by qPCR (Toegel *et al*, 2007). However, the qPCR data generated in tables 3.1-3.12 demonstrates that the mRNA synthesis of *GAPDH* varied under experimental conditions. Though qPCR is a very robust technique, it is also very sensitive and minor variations in PCR components and cycling conditions can affect the amount of PCR product produced. The quantification of mRNA in this thesis was performed using one-step RT-qPCR; and although it is suggested that the one-step RT-qPCR method may minimise experimental variation since both the reverse transcription and qPCR occurs in the same tube, the fact the starting material which is mRNA rather than cDNA degrades rapidly, can affect the RNA concentration. Additionally, the structure of the RNA can cause variation in qPCR as RNA secondary structures may interfere with the PCR reaction (Wong and Medrano, 2005; Bustin *et al*, 2009). For the reasons mentioned above a two-step qPCR system would have been more advantageous for qPCR studies since it is suggested to be more sensitive and reproducible than one-step RT-qPCR (Wong and Medrano, 2005).

Statistical analysis of the qPCR data shows that treatment of C-20/A4 chondrocytes with UCNI only, SNAP only and SNAP+UCNI all resulted statistically significant ($p>0.05$) change in the mRNA expression of *CRFR1*α (section 3.5.1), *CRFR2*β (section 3.5.2) when compared to the calibrator (control *CRFR1*α and *CRFR2*β samples respectively); as determined by the students unpaired T-test.

This therefore suggests that UCNI regulation of CRF receptors in the C-20/A4 chondrocytes does not require *de novo* mRNA synthesis of the CRF receptors and thus the peptide may be utilising the receptors present to mediate its anti-apoptotic effects. Several studies have also documented down-regulation of CRF receptors *in vivo* and *in vitro*. Findings by Heldwein *et al*, demonstrated *in vivo* that administration of the bacterial endotoxin lipopolysaccharide (LPS) resulted in a down-regulation of *CRFR2*β mRNA expression in the rat heart. This down-regulation is potentially mediated via NO generation following the release of inflammatory cytokines (e.g. TNFα and IL-1β) from LPS exposure (Heldwein *et al*, 1997; Finkel *et al*, 1992). To test their hypothesis of proinflammatory mediators' regulation of CRFR2β, they conducted studies on the effects of IL-1α, TNFα and UCNI administration on *CRFR2*β mRNA expression in mouse heart. The results demonstrated that these cytokines and UCNI which were administered singly and not in combination, down-regulated *CRFR2*β expression. Based on their findings they suggested that cytokines, endotoxins and other inflammatory mediators regulate *CRFR2* mRNA expression indirectly by enhancing *UCNI* mRNA expression and release *in vivo* which then down-regulates *CRFR2*β expression (Coste *et al*, 2001). Studies by Kageyama group in 2000 and 2005, is also in broad agreement as they also demonstrated that UCNI decreased CRFR2β expression in the aortic smooth muscle cells (Kageyama *et al*, 2005; Kageyama *et al*, 2000).

It may postulated that the down-regulation of *CRFR2* mRNA expression will result in a reduced amount of ligand binding sites and mediated activity that may serve to limit the time course of *CRFR2* agonists (such as UCNI) during prolonged stress in order to restore tissue homeostasis (Kageyama *et al*, 2000). A decrease of *CRFR1* mRNA expression has also been documented following treatment of rat anterior pituitary cells with CRF (Moriyama *et al*, 2005; Dautzenberg and Hauger, 2002) and this down-regulation of the *CRFR* mRNA may occur via internalisation and receptor degradation and suppression of further receptor synthesis (via inhibition of mRNA translation) (Moriyama *et al*, 2005; Kageyama *et al*, 2000; Dautzenberg and Hauger, 2002).

In keeping with UCNI regulation of receptor and K_{ATP} channel targets, the qPCR data in section 3.5.3 for the relative expression of *Kir6.1* mRNA indicates that

treatment of C-20/A4 chondrocytes with UCNI, SNAP and SNAP+UCNI resulted in no statistically significant ($p>0.05$) change in *Kir6.1* mRNA expression levels when compared to the calibrator. The K_{ATP} channels have been previously implicated in the cardioprotective mechanisms of UCNI against cell death (Lawrence *et al*, 2002; Lawrence *et al*, 2004). However, the observation that stimulation of chondrocytes with UCNI resulted in no significant change in *Kir6.1*mRNA expression is in contrast to findings by Lawrence *et al* in 2002, which showed that cardiac myocytes exposed to exogenous UCNI resulted in an increased expression of*Kir6.1* mRNA and protein (Lawrence *et al*, 2002). Lawrence *et al,* (2002) also demonstrated enhanced expression of Kir6.1in the intact heart during ischaemia/reperfusion. Furthermore, they showed that ischaemia/reperfusion injury causes damage to the cardiac myocyte mitochondrial membrane and that the cardioprotective mechanism of UCNI against ischaemia/reperfusion injury may be a result of preventing mitochondrial damage and therefore cell death. This was partly achieved by opening of mitochondrial Kir6.1 K_{ATP} channels, inhibition of a calcium independent phospholipase A_2 and its' metabolite, Lysophosphatidylcholine- LPC, and Protein Kinase C epsilon (PKCε) activation all localised to the cardiac myocyte mitochondria (Lawrence *et al*, 2004; Lawrence *et al*, 2003; Kuizon *et al*, 2009). Again, similar to the *CRF* receptor qPCR findings of sections 3.5.1 and 3.5.2, the qPCR data for the relative expression of *Kir6.1* mRNA expression following SNAP and SNAP+UCNI treatment would suggest that *de novo* synthesis of this potential UCNI target is not required for mediating the chondroprotective effects against apoptosis.

Additionally, as previously mentioned, it is believed that the activity of K_{ATP} channels can be regulated by G-protein coupled receptors directly or via Protein Kinase A or C stimulation. The SUR regulatory subunit is said to be the target for direct stimulation of the Gα subunit of the GPCR and thus suggests that the SUR regulatory subunits could be directly activated by the binding of UCNI to its' receptor. Moreover, the Kir6.1 protein is said to contain two PKA phosphorylation sites and seven for PKC. Conversely, the Kir6.2 contains two and five phosphorylation sites for PKA and PKC respectively. Protein Kinase A and C dependent phosphorylation sites also exist on the SUR regulatory subunits; for instance SUR1 contains four sites for PKA and multiple sites have been identified

for PKC in humans (Seino, 1999; Seino and Miki, 2003). In the heart, as mentioned, where UCNI has been shown to activate the epsilon isoform of PKC and this is at least partially responsible for its cardioprotective effects, although it is unknown whether this particular isoform can phosphorylate Kir6.1 or SURs(Lawrence *et al*, 2004). However, PKC activation by UCNI may be another mechanism by which UCNI modulates K_{ATP} channel activity in C-20/A4 cells possibly by phosphorylation of Kir6.1 or SURs considering that phosphorylation sites exits in these K_{ATP} channel subunits.

In an attempt to determine the possible functional involvement of K_{ATP} channels in UCNI chondroprotection as previously implicated in cardiac myocytes (Lawrence *et al*, 2004), chondrocytes were treated with a pharmacological K_{ATP} channel opener, Diazoxide. The pharmacological agent, Diazoxide is a K_{ATP} channel opener with a high affinity for the mitochondrial K_{ATP} channels (Suzuki *et al*, 2003). It is well established that the site of action of K_{ATP} channel openers and blockers (KCO's and KCB's respectively) are via interaction with the SURx regulatory subunits of the K_{ATP} channels (Shi *et al*, 2005; Moreau *et al*, 2005). Diazoxide has been implicated to activate K_{ATP} channels via interaction with the transmembrane segments TM6-11 of TMD1 and the NBD1 of the SUR subunit (see figure 1.11A) (Shi *et al*, 2005).

The preliminary flow cytometry data shown in figure 3.12 indicates that concurrent treatment of chondrocytes with SNAP and Diazoxide reduces apoptosis induced by SNAP. This may occur as a result of activation of the mitoK_{ATP} channels and subsequent prevention of calcium overload and mitochondrial damage (Lawrence *et al*, 2003; Tao and Li, 2005a; Jahangir and Terzic, 2005). Whilst the data requires further confirmation, it does suggest that the K_{ATP} channels may be involved in UCNI reduction of apoptosis in chondrocytes as in the heart. Although the existence of Kir6.x and SURx subunits that can form functional K_{ATP} channels in the C-20/A4 chondrocyte cell line was demonstrated by RT-PCR and sequence analysis of the generated PCR amplicons, the exact molecular formation of K_{ATP} channels in these C-20/A4 chondrocytes were not inferred. It is believed that Diazoxide activates K_{ATP} channels by interacting with SUR1 and *SUR2B* but not SUR2A regulatory subunits (Shi *et al*, 2005; Isomoto *et al*, 1996). Additionally, the Kir6.1 pore forming subunit has been shown to be activated by SUR1and SUR2B

and not *SUR2A* (Aguilar-Bryan *et al*, 1998). Therefore, if the Kir6.x and SURx subunits are expressed at the protein level in the C-20/A4 chondrocytes, then the Kir6.1 pore forming subunit could preferentially associate with SUR1 or SUR2B regulatory subunit to compose functional K_{ATP} channels.

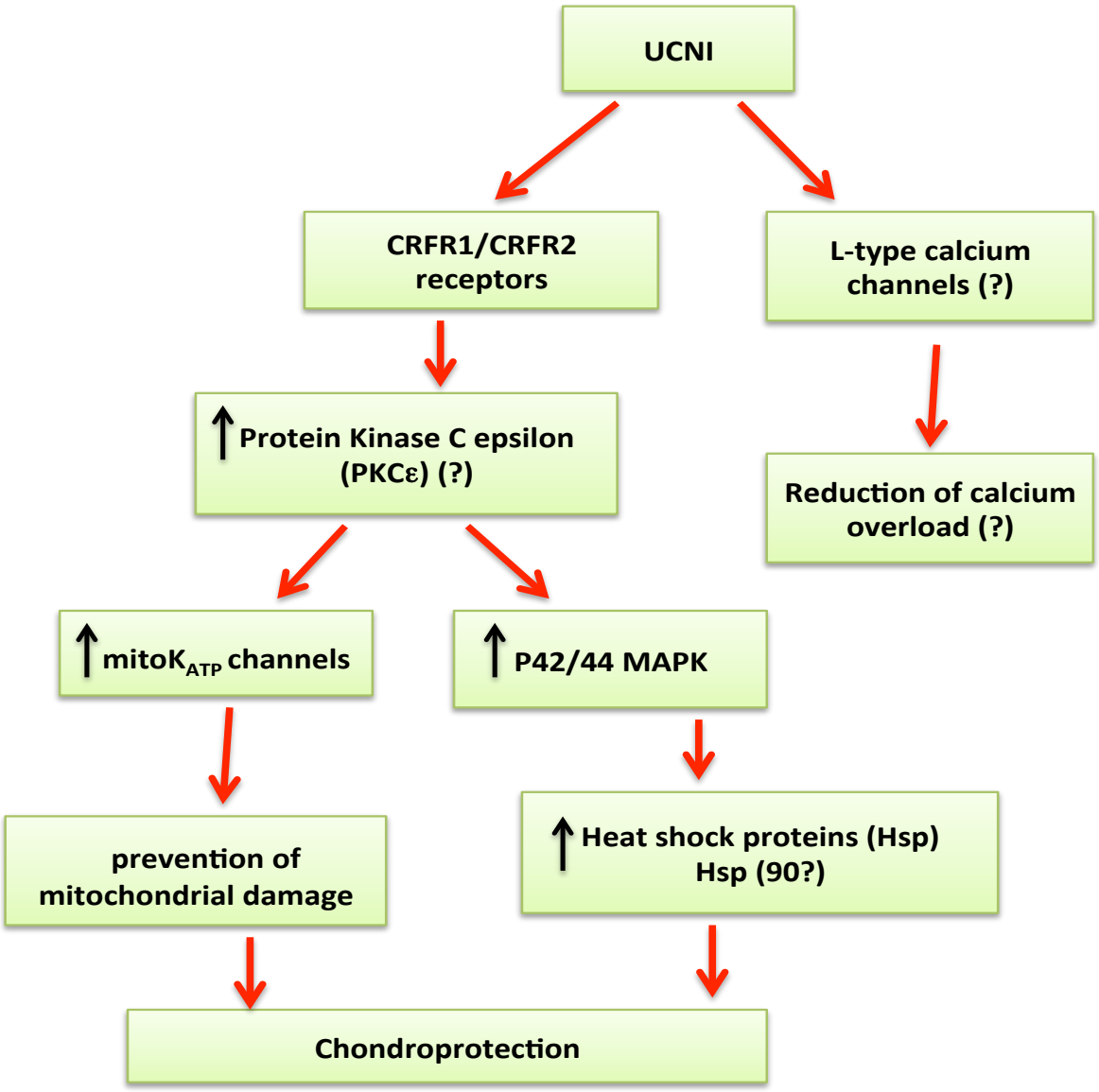

Figure 4.1: The potential mechanisms of UCNI's chondroprotective effects against apoptosis in the C-20/A4 chondrocytes.
UCNI may mediate their effects through ligation to CRF receptors or by inhibiting L-type calcium channels. Activation of the CRF receptors may result in PKC activation and subsequent P42/P44 MAPK and K_{ATP} channels mediated pathways. The UCNI mediated protection via P42/44 MAPK may involve induced protein expression of heat shock protein (hsp) 90, whilst activation of the mitoK$_{ATP}$ channels prevents mitochondrial damage through maintenance of the mitochondrial membrane potential. UCNI inhibition of L-type calcium channels may reduce calcium entry into the cell and thus calcium overload. The black arrows imply activation.

4.5 Conclusions and Future Work

Having confirmed the cytoprotective effects of UCNI against SNAP induced apoptosis in the C-20/A4 chondrocyte cell line by flow cytometry, the research in this thesis has gone to further identify possible receptors and/or target molecules involved in the chondroprotective mechanism.

Reverse Transcriptase-Polymerase Chain Reaction (RT-PCR) studies indicated that *UCNI*, *CRFR1*α and *CRFR2*β mRNA is endogenously expressed by the C-20/A4 chondrocyte cell line providing a viable cell surface receptor dependant pathway for *UCNI* mediated chondroprotection. This suggests that, in C-20/A4 cells, UCNI may act in an autocrine/paracrine manner through either CRFR. Indeed, Intekhab-Alam (2006) has shown that treatment with a CRFR antagonist resulted in cell death, suggesting that UCNI also acts as a growth factor for C-20/A4 cells. In both animal models of cardiac ischaemia/reperfusion and in the human heart exposed to the I/R that accompanies bypass surgery, UCNI expression is increased, and UCNI expressing cells, unlike UCNI negative cells, are viable (Knight *et al*, 2008; Scarabelli *et al*, 2004).

Furthermore, the increased expression of endogenous *UCNI* mRNA following SNAP treatment suggests an autocrine/paracrine mode of action for this cytoprotective peptide in chondrocytes although the importance of this mechanism may be called in question based upon the lack of inhibition of the cytoprotective effect following αhCRH$_{(9\text{-}41)}$ treatment. For reason discussed earlier however, this work requires further confirmation.

qPCR studies demonstrated that stimulation of chondrocytes with SNAP/NO and UCNI alone and in combination resulted in no statistically significant change ($p>0.05$) in *CRFR1* and *CRFR2* mRNA expression. This suggests thatinC-20/A4 chondrocytes, UCNI regulation of the CRF receptor expression does not require *de novo* mRNA and protein synthesis. Additionally, RT-PCR also demonstrated the mRNA expression of K_{ATP} channel subunits (*Kir6.1*, *Kir6.2*, *SUR1* and *SUR2B*) that can constitute functional K_{ATP} channels in the C-20/A4 chondrocytes.

Our preliminary experiments also indicated that the Kir6.1 channel opener, Diaxoxide, is also cytoprotective, though further studies with both channel openers and inhibitors are required to confirm this. However, based on these preliminary

pharmacological studies performed, it is possible that the Kir6.1 mitoK_{ATP} channels may also comprise a mechanism by which UCNI may exert its effects, perhaps by preventing mitochondrial damage; although the mRNA and protein expression of the Kir6.1 subunit to the mitochondria remains controversial (Lawrence *et al*, 2002). Nevertheless, if the Kir6.1 subunit is located at the inner mitochondrial membrane to constitute a mitoK_{ATP} and SNAP/NO induces apoptosis via the mitochondrial pathway then opening of the Kir6.1 mitoK_{ATP} channel following SNAP and UCNI alone and in combination further supports the hypothesis that the Kir6.1 mitoK_{ATP} channel represents a possible protective mechanism in chondroprotection.

Other signalling mechanisms for UCNI chondroprotection may also exist in the C-20/A4 chondrocyte cell line. Indeed, previous studies have indicated that the P42/P44 MAP Kinase pathways may be involved in mediating UCNI protection as there was a significant increase in P42/P44 MAP Kinase following exposure to exogenous UCNI (Intekhab-Alam, 2006). In cardiac myocytes the P42/44 MAP Kinases were suggested to mediate UCNI cardioprotection possibly by inducing the protein expression of heat shock protein (hsp) 90, therefore hsp 90 may also be implicated in UCNI chondroprotection (see figure 4.1) (Brar *et al*, 2002).

Another alternative mechanism for UCNI chondroprotection may be via L-type calcium channels as discussed earlier. Therefore further work to be undertaken includes: further investigation in the effects of Diazoxide and pharmacological inhibitors (e.g. the mitochondrial K_{ATP} channel blocker 5-Hdroydecanoate; 5-HD) on the levels of apoptosis in chondrocytes and the significance of the K_{ATP} channels (in particular the Kir6.1 mitoK_{ATP} channel) in preventing cell death. Additionally, western blot studies could be performed on subcellular fractions to confirm the localisation of Kir6.1 protein expression to the mitochondria in C-20/A4 chondrocytes.

Following qPCR experiments that indicated UCNI regulation of CRF receptor and Kir6.1 subunit at the mRNA level, further studies can be conducted to determine whether the mRNA is translated into protein since not all mRNA which is detected is translated to functional protein (Bustin *et al*, 2009). The changes in protein expression of the CRF receptors and K_{ATP} channels subunits could also be investigated following treatment with SNAP/NO and UCNI alone and in

combination to determine any change in protein expression following exposure to these treatments.

The regulation of the SUR regulatory subunits (*SUR1* and *SUR2B*) by UCNI could also be investigated by qPCR to determine any changes in their mRNA expression following treatment of chondrocytes with SNAP/NO and UCNI. The existence of the protein expression for the SUR subunits detected at the mRNA level could also be examined by performing western blot analysis. The identification of Kir6.x and SURx proteins in the C-20/A4 chondrocytes would thus indicate that functional K_{ATP} channels would exist in this cell line. Furthermore, changes in protein expression of the SUR subunits following SNAP/NO and UCNI treatment can then be determined.

Since both SNAP/NO and UCNI act at the mitochondrial level, it would also be of interest to investigate the effects of UCNI on the anti and pro-apoptotic members of the Bcl2 family, a mechanism that has not been studied in other models of UCNI mediated cytoprotection. As shown in the heart, the phosphorylation of protein kinase C in the prevention of chondrocyte apoptotic cell death could also be investigated. These studies would indicate the possible G-protein and CRF receptor signalling pathway activated (see figure 1.7) to mediate UCNI chondroprotection. The investigation of L-type calcium channels in C-20/A4 chondrocytes by Reverse transcriptase PCR (RT-PCR) and inhibition studies could be performed to confirm the existence of a non-CRF receptor mediated UCNI protection in chondrocytes.

Consequently, if UCNI serves as a possible protective mechanism against NO induced apoptosis, identifying the exact intracellular effectors molecules which underlying this chondroprotection could provide avenues for the development of therapy which can inhibit cell death in OA.

Chapter 5: References

5 References

ABRAMSON, S. B. 2008. Osteoarthritis and nitric oxide. *Osteoarthritis Cartilage,* 16 Suppl 2**,** S15-20.

ABRAMSON, S. B. & YAZICI, Y. 2006. Biologics in development for rheumatoid arthritis: relevance to osteoarthritis. *Adv Drug Deliv Rev,* 58**,** 212-25.

ABUIRMEILEH, A., LEVER, R., KINGSBURY, A. E., LEES, A. J., LOCKE, I. C., KNIGHT, R. A., CHOWDREY, H. S., BIGGS, C. S. & WHITTON, P. S. 2007. The corticotrophin-releasing factor-like peptide urocortin reverses key deficits in two rodent models of Parkinson's disease. *Eur J Neurosci,* 26**,** 417-23.

ADAMS, J. M. & CORY, S. 2001. Life-or-death decisions by the Bcl-2 protein family. *Trends Biochem Sci,* 26**,** 61-6.

ADAMS, S. L., PALLANTE, K. M., NIU, Z., LEBOY, P. S., GOLDEN, E. B. & PACIFICI, M. 1991. Rapid induction of type X collagen gene expression in cultured chick vertebral chondrocytes. *Exp Cell Res,* 193**,** 190-7.

AGUILAR-BRYAN, L., CLEMENT, J. P. T., GONZALEZ, G., KUNJILWAR, K., BABENKO, A. & BRYAN, J. 1998. Toward understanding the assembly and structure of KATP channels. *Physiol Rev,* 78**,** 227-45.

AIGNER, T., HAAG, J., MARTIN, J. & BUCKWALTER, J. 2007. Osteoarthritis: aging of matrix and cells--going for a remedy. *Curr Drug Targets,* 8**,** 325-31.

AIGNER, T., SOEDER, S. & HAAG, J. 2006. IL-1beta and BMPs--interactive players of cartilage matrix degradation and regeneration. *Eur Cell Mater,* 12**,** 49-56; discussion 56.

ANTONSSON, B. & MARTINOU, J. C. 2000. The Bcl-2 protein family. *Exp Cell Res,* 256**,** 50-7.

ARAI, M., ASSIL, I. Q. & ABOU-SAMRA, A. B. 2001. Characterization of three corticotropin-releasing factor receptors in catfish: a novel third receptor is predominantly expressed in pituitary and urophysis. *Endocrinology,* 142**,** 446-54.

BALE, T. L. & VALE, W. W. 2004. CRF and CRF receptors: role in stress responsivity and other behaviors. *Annu Rev Pharmacol Toxicol,* 44**,** 525-57.

BELL, R. S., BOURRET, L. A., BELL, D. F., GEBHARDT, M. C., ROSENBERG, A., BERREY, H. B., TREADWELL, B. V., TOMFORD, W. W. & MANKIN, H. J. 1988. Evaluation of fluorescein diacetate for flow cytometric determination of cell viability in orthopaedic research. *J Orthop Res,* 6**,** 467-74.

BIRCHFIELD, P. C. 2001. Osteoarthritis overview. *Geriatr Nurs,* 22**,** 124-30; quiz 130-1.

BLANCO, F. J., GUITIAN, R., VAZQUEZ-MARTUL, E., DE TORO, F. J. & GALDO, F. 1998. Osteoarthritis chondrocytes die by apoptosis. A possible pathway for osteoarthritis pathology. *Arthritis Rheum,* 41**,** 284-9.

BLANCO, F. J., OCHS, R. L., SCHWARZ, H. & LOTZ, M. 1995. Chondrocyte apoptosis induced by nitric oxide. *Am J Pathol,* 146**,** 75-85.

BLOCK, J. A., INEROT, S. E., GITELIS, S. & KIMURA, J. H. 1991. Synthesis of chondrocytic keratan sulphate-containing proteoglycans by human chondrosarcoma cells in long-term cell culture. *J Bone Joint Surg Am,* 73**,** 647-58.

BRAR, B. K., JONASSEN, A. K., STEPHANOU, A., SANTILLI, G., RAILSON, J., KNIGHT, R. A., YELLON, D. M. & LATCHMAN, D. S. 2000. Urocortin protects against ischemic and reperfusion injury via a MAPK-dependent pathway. *J Biol Chem,* 275**,** 8508-14.

BRAR, B. K., STEPHANOU, A., OKOSI, A., LAWRENCE, K. M., KNIGHT, R. A., MARBER, M. S. & LATCHMAN, D. S. 1999. CRH-like peptides protect cardiac myocytes from lethal ischaemic injury. *Molecular and Cellular Endocrinology,* 158**,** 55-63.

BRAR, B. K., RAILSON, A., STEPHANOU, A., KNIGHT, R. A., & LATCHMAN, D. S. 2002. Urocortin increases the expression of heat shock protein 90 in rat cardiac myocytes in a MEK1/2- dependent manner. *Journal of Endocrinology*, 172, 283-93.

BRYAN, J., MUNOZ, A., ZHANG, X., DUFER, M., DREWS, G., KRIPPEIT-DREWS, P. & AGUILAR-BRYAN, L. 2007. ABCC8 and ABCC9: ABC transporters that regulate K+ channels. *Pflugers Arch,* 453**,** 703-18.

BUCKWALTER, J. A. & MANKIN, H. J. 1998. Articular cartilage: tissue design and chondrocyte-matrix interactions. *Instr Course Lect,* 47**,** 477-86.

BUCKWALTER, J. A. & MARTIN, J. A. 2006. Osteoarthritis. *Advanced Drug Delivery Reviews,* 58**,** 150-167.

BURKE, M. A., MUTHARASAN, R. K. & ARDEHALI, H. 2008. The sulfonylurea receptor, an atypical ATP-binding cassette protein, and its regulation of the KATP channel. *Circ Res,* 102**,** 164-76.

BUSTIN, S. A., BENES, V., GARSON, J. A., HELLEMANS, J., HUGGETT, J., KUBISTA, M., MUELLER, R., NOLAN, T., PFAFFL, M. W., SHIPLEY, G. L., VANDESOMPELE, J. & WITTWER, C. T. 2009. The MIQE guidelines: minimum information for publication of quantitative real-time PCR experiments. *Clin Chem,* 55**,** 611-22.

CARLSON, K. W., NAWY, S. S., WEI, E. T., SADEE, W., FILOV, V. A., REZSOVA, V. V., SLOMINSKI, A. & QUILLAN, J. M. 2001. Inhibition of mouse melanoma cell proliferation by corticotropin-releasing hormone and its analogs. *Anticancer Res,* 21**,** 1173-9.

CATALANO, R. D., KYRIAKOU, T., CHEN, J., EASTON, A. & HILLHOUSE, E. W. 2003. Regulation of corticotropin-releasing hormone type 2 receptors by multiple promoters and alternative splicing: identification of multiple splice variants. *Mol Endocrinol,* 17**,** 395-410.

CEPOI, D., SUTTON, S., ARIAS, C., SAWCHENKO, P. & VALE, W. W. 1999. Ovine genomic urocortin: cloning, pharmacologic characterization, and distribution of central mRNA. *Molecular Brain Research,* 68**,** 109-118.

CHANALARIS, A., LAWRENCE, K. M., STEPHANOU, A., KNIGHT, R. D., HSU, S. Y., HSUEH, A. J. & LATCHMAN, D. S. 2003. Protective effects of the urocortin homologues stresscopin (SCP) and stresscopin-related peptide (SRP) against hypoxia/reoxygenation injury in rat neonatal cardiomyocytes. *J Mol Cell Cardiol,* 35**,** 1295-305.

CHANALARIS, A., LAWRENCE, K. M., TOWNSEND, P. A., DAVIDSON, S., JAMSHIDI, Y., STEPHANOU, A., KNIGHT, R. D., HSU, S. Y., HSUEH, A. J. & LATCHMAN, D. S. 2005. Hypertrophic effects of urocortin homologous peptides are mediated via activation of the Akt pathway. *Biochem Biophys Res Commun,* 328**,** 442-8.

CHEN, A., PERRIN, M., BRAR, B., LI, C., JAMIESON, P., DIGRUCCIO, M., LEWIS, K. & VALE, W. 2005. Mouse corticotropin-releasing factor receptor type 2alpha gene: isolation, distribution, pharmacological characterization and regulation by stress and glucocorticoids. *Mol Endocrinol,* 19**,** 441-58.

CHEN, R., LEWIS, K. A., PERRIN, M. H. & VALE, W. W. 1993. Expression cloning of a human corticotropin-releasing-factor receptor. *Proc Natl Acad Sci U S A,* 90**,** 8967-71.

CHENG, A. X., LOU, S. Q., ZHOU, H. W., WANG, Y. & MA, D. L. 2004. Expression of PDCD5, a novel apoptosis related protein, in human osteoarthritic cartilage. *Acta Pharmacol Sin,* 25**,** 685-90.

CHI, S. S., RATTNER, J. B. & MATYAS, J. R. 2004. Communication between paired chondrocytes in the superficial zone of articular cartilage. *J Anat,* 205**,** 363-70.

CHUBINSKAYA, S. & KUETTNER, K. E. 2003. Regulation of osteogenic proteins by chondrocytes. *Int J Biochem Cell Biol,* 35**,** 1323-40.

CHUTKOW, W. A., MAKIELSKI, J. C., NELSON, D. J., BURANT, C. F. & FAN, Z. 1999. Alternative splicing of sur2 Exon 17 regulates nucleotide sensitivity of the ATP-sensitive potassium channel. *J Biol Chem,* 274**,** 13656-65.

COIMBRA, I. B., JIMENEZ, S. A., HAWKINS, D. F., PIERA-VELAZQUEZ, S. & STOKES, D. G. 2004. Hypoxia inducible factor-1 alpha expression in human normal and osteoarthritic chondrocytes. *Osteoarthritis Cartilage,* 12**,** 336-45.

COSTE, S. C., HELDWEIN, K. A., STEVENS, S. L., TOBAR-DUPRES, E. & STENZEL-POORE, M. P. 2001. IL-1alpha and TNFalpha down-regulate

CRH receptor-2 mRNA expression in the mouse heart. *Endocrinology,* 142**,** 3537-45.

DAUTZENBERG, F. M. & HAUGER, R. L. 2002. The CRF peptide family and their receptors: yet more partners discovered. *Trends Pharmacol Sci,* 23**,** 71-7.

DIEPPE, P. A. & LOHMANDER, L. S. 2005. Pathogenesis and management of pain in osteoarthritis. *The Lancet,* 365**,** 965-973.

DONALDSON, C. J., SUTTON, S. W., PERRIN, M. H., CORRIGAN, A. Z., LEWIS, K. A., RIVIER, J. E., VAUGHAN, J. M. & VALE, W. W. 1996. Cloning and characterization of human urocortin. *Endocrinology,* 137**,** 2167-70.

FEKETE, E. M. & ZORRILLA, E. P. 2007. Physiology, pharmacology, and therapeutic relevance of urocortins in mammals: Ancient CRF paralogs. *Frontiers in Neuroendocrinology,* 28**,** 1-27.

FELSON, D. T., LAWRENCE, R. C., DIEPPE, P. A., HIRSCH, R., HELMICK, C. G., JORDAN, J. M., KINGTON, R. S., LANE, N. E., NEVITT, M. C., ZHANG, Y., SOWERS, M., MCALINDON, T., SPECTOR, T. D., POOLE, A. R., YANOVSKI, S. Z., ATESHIAN, G., SHARMA, L., BUCKWALTER, J. A., BRANDT, K. D. & FRIES, J. F. 2000. Osteoarthritis: new insights. Part 1: the disease and its risk factors. *Ann Intern Med,* 133**,** 635-46.

FERNANDEZ-MORENO, M., REGO, I., CARREIRA-GARCIA, V. & BLANCO, F. J. 2008. Genetics in osteoarthritis. *Curr Genomics,* 9**,** 542-7.

FERNANDEZ-SOLA, J., PREEDY, V. R., LANG, C. H., GONZALEZ-REIMERS, E., ARNO, M., LIN, J. C., WISEMAN, H., ZHOU, S., EMERY, P. W., NAKAHARA, T., HASHIMOTO, K., HIRANO, M., SANTOLARIA-FERNANDEZ, F., GONZALEZ-HERNANDEZ, T., FATJO, F., SACANELLA, E., ESTRUCH, R., NICOLAS, J. M. & URBANO-MARQUEZ, A. 2007. Molecular and cellular events in alcohol-induced muscle disease. *Alcohol Clin Exp Res,* 31**,** 1953-62.

FIGUEROA, S., OSET-GASQUE, M. J., ARCE, C., MARTINEZ-HONDUVILLA, C. J. & GONZALEZ, M. P. 2006. Mitochondrial involvement in nitric oxide-induced cellular death in cortical neurons in culture. *J Neurosci Res,* 83**,** 441-9.

FINGER, F., SCHORLE, C., ZIEN, A., GEBHARD, P., GOLDRING, M. B. & AIGNER, T. 2003. Molecular phenotyping of human chondrocyte cell lines T/C-28a2, T/C-28a4, and C-28/I2. *Arthritis Rheum,* 48**,** 3395-403.

FINKEL, M. S., ODDIS, C. V., JACOB, T. D., WATKINS, S. C., HATTLER, B. G. & SIMMONS, R. L. 1992. Negative inotropic effects of cytokines on the heart mediated by nitric oxide. *Science,* 257**,** 387-9.

FLEIGE, S. & PFAFFL, M. W. 2006. RNA integrity and the effect on the real-time qRT-PCR performance. *Mol Aspects Med,* 27**,** 126-39.

GENTLES, A. J. & KARLIN, S. 1999. Why are human G-protein-coupled receptors predominantly intronless? *Trends Genet,* 15**,** 47-9.

GERSTENFELD, L. C., KELLY, C. M., VON DECK, M. & LIAN, J. B. 1990. Comparative morphological and biochemical analysis of hypertrophic, non-hypertrophic and 1,25(OH)2D3 treated non-hypertrophic chondrocytes. *Connect Tissue Res,* 24**,** 29-39.

GEWIES, A. 2003. ApoReview - Introduction to Apoptosis. *www.celldeath.de/encyclo/aporev/aporev.htm*1-26.

GOGGS, R., CARTER, S. D., SCHULZE-TANZIL, G., SHAKIBAEI, M. & MOBASHERI, A. 2003. Apoptosis and the loss of chondrocyte survival signals contribute to articular cartilage degradation in osteoarthritis. *The Veterinary Journal,* 166**,** 140-158.

GOLDRING, M. B. 2000. The role of the chondrocyte in osteoarthritis. *Arthritis Rheum,* 43**,** 1916-26.

GOLDRING, M. B., BIRKHEAD, J. R., SUEN, L. F., YAMIN, R., MIZUNO, S., GLOWACKI, J., ARBISER, J. L. & APPERLEY, J. F. 1994. Interleukin-1 beta-modulated gene expression in immortalized human chondrocytes. *J Clin Invest,* 94**,** 2307-16.

GOLDRING, M. B., SANDELL, L. J., STEPHENSON, M. L. & KRANE, S. M. 1986. Immune interferon suppresses levels of procollagen mRNA and type II collagen synthesis in cultured human articular and costal chondrocytes. *J Biol Chem,* 261**,** 9049-55.

GRAMMATOPOULOS, D. K. & CHROUSOS, G. P. 2002. Functional characteristics of CRH receptors and potential clinical applications of CRH-receptor antagonists. *Trends in Endocrinology and Metabolism,* 13**,** 436-444.

GRAMMATOPOULOS, D. K., DAI, Y., RANDEVA, H. S., LEVINE, M. A., KARTERIS, E., EASTON, A. J. & HILLHOUSE, E. W. 1999. A novel spliced variant of the type 1 corticotropin-releasing hormone receptor with a deletion in the seventh transmembrane domain present in the human pregnant term myometrium and fetal membranes. *Mol Endocrinol,* 13**,** 2189-202.

GROSS, A., MCDONNELL, J. M. & KORSMEYER, S. J. 1999. BCL-2 family members and the mitochondria in apoptosis. *Genes Dev,* 13**,** 1899-911.

GYSLING, K., FORRAY, M. I., HAEGER, P., DAZA, C. & ROJAS, R. 2004. Corticotropin-releasing hormone and urocortin: redundant or distinctive functions? *Brain Res Brain Res Rev,* 47**,** 116-25.

HAQ, I., MURPHY, E. & DACRE, J. 2003. Osteoarthritis. *Postgrad Med J,* 79**,** 377-83.

HASHIMOTO, S., SETAREH, M., OCHS, R. L. & LOTZ, M. 1997. Fas/Fas ligand expression and induction of apoptosis in chondrocytes. *Arthritis Rheum,* 40**,** 1749-55.

HASHIMOTO, S., TAKAHASHI, K., AMIEL, D., COUTTS, R. D. & LOTZ, M. 1998. Chondrocyte apoptosis and nitric oxide production during experimentally induced osteoarthritis. *Arthritis Rheum,* 41**,** 1266-74.

HAUGER, R. L., GRIGORIADIS, D. E., DALLMAN, M. F., PLOTSKY, P. M., VALE, W. W. & DAUTZENBERG, F. M. 2003. International Union of Pharmacology. XXXVI. Current status of the nomenclature for receptors for corticotropin-releasing factor and their ligands. *Pharmacol Rev,* 55**,** 21-6.

HAUGER, R. L., RISBROUGH, V., BRAUNS, O. & DAUTZENBERG, F. M. 2006. Corticotropin releasing factor (CRF) receptor signaling in the central nervous system: new molecular targets. *CNS Neurol Disord Drug Targets,* 5**,** 453-79.

HAYES, A. J., DOWTHWAITE, G. P., WEBSTER, S. V. & ARCHER, C. W. 2003. The distribution of Notch receptors and their ligands during articular cartilage development. *J Anat,* 202**,** 495-502.

HELDWEIN, K. A., DUNCAN, J. E., STENZEL, P., RITTENBERG, M. B. & STENZEL-POORE, M. P. 1997. Endotoxin regulates corticotropin-releasing hormone receptor 2 in heart and skeletal muscle. *Mol Cell Endocrinol,* 131**,** 167-72.

HERAUD, F., HERAUD, A. & HARMAND, M. F. 2000. Apoptosis in normal and osteoarthritic human articular cartilage. *Ann Rheum Dis,* 59**,** 959-65.

HILLHOUSE, E. W. & GRAMMATOPOULOS, D. K. 2002. Role of stress peptides during human pregnancy and labour. *Reproduction,* 124**,** 323-9.

HILLHOUSE, E. W. & GRAMMATOPOULOS, D. K. 2006. The molecular mechanisms underlying the regulation of the biological activity of corticotropin-releasing hormone receptors: implications for physiology and pathophysiology. *Endocr Rev,* 27**,** 260-86.

HORTON, W. E., JR., CLEVELAND, J., RAPP, U., NEMUTH, G., BOLANDER, M., DOEGE, K., YAMADA, Y. & HASSELL, J. R. 1988. An established rat cell line expressing chondrocyte properties. *Exp Cell Res,* 178**,** 457-68.

HSU, S. Y. & HSUEH, A. J. 2001. Human stresscopin and stresscopin-related peptide are selective ligands for the type 2 corticotropin-releasing hormone receptor. *Nat Med,* 7**,** 605-11.

HUANG, Y., YAO, X. Q., LAU, C. W., CHAN, Y. C., TSANG, S. Y. & CHAN, F. L. 2004. Urocortin and cardiovascular protection. *Acta Pharmacol Sin,* 25**,** 257-65.

HUNZIKER, E. B., QUINN, T. M. & HAUSELMANN, H. J. 2002. Quantitative structural organization of normal adult human articular cartilage. *Osteoarthritis Cartilage,* 10**,** 564-72.

IMPERATORE, A., FLORIO, P., TORRES, P. B., TORRICELLI, M., GALLERI, L., TOTI, P., OCCHINI, R., PICCIOLINI, E., VALE, W. & PETRAGLIA, F. 2006. Urocortin 2 and urocortin 3 are expressed by the human placenta, deciduas, and fetal membranes. *Am J Obstet Gynecol,* 195**,** 288-95.

INAGAKI, N., INAZAWA, J. & SEINO, S. 1995. cDNA sequence, gene structure, and chromosomal localization of the human ATP-sensitive potassium channel, uKATP-1, gene (KCNJ8). *Genomics,* 30**,** 102-4.

INTEKHAB-ALAM, N. 2006. *Mechanisms of chondrocyte death in Osteoarthritis.* PhD thesis, University of Westminster.

ISOMOTO, S., KONDO, C., YAMADA, M., MATSUMOTO, S., HIGASHIGUCHI, O., HORIO, Y., MATSUZAWA, Y. & KURACHI, Y. 1996. A novel sulfonylurea receptor forms with BIR (Kir6.2) a smooth muscle type ATP-sensitive K+ channel. *J Biol Chem,* 271**,** 24321-4.

JAHANGIR, A. & TERZIC, A. 2005. K(ATP) channel therapeutics at the bedside. *J Mol Cell Cardiol,* 39**,** 99-112.

KAGEYAMA, K., GAUDRIAULT, G. E., BRADBURY, M. J. & VALE, W. W. 2000. Regulation of corticotropin-releasing factor receptor type 2 beta messenger ribonucleic acid in the rat cardiovascular system by urocortin, glucocorticoids, and cytokines. *Endocrinology,* 141**,** 2285-93.

KAGEYAMA, K., HANADA, K. & SUDA, T. 2005. Regulation of corticotropin-releasing factor receptor type 2[beta] mRNA by mitogen-activated protein kinases in aortic smooth muscle cells. *Regulatory Peptides,* 126**,** 223-231.

KIM, H. A. & BLANCO, F. J. 2007. Cell death and apoptosis in osteoarthritic cartilage. *Curr Drug Targets,* 8**,** 333-45.

KIM, H. A., LEE, Y. J., SEONG, S. C., CHOE, K. W. & SONG, Y. W. 2000. Apoptotic chondrocyte death in human osteoarthritis. *J Rheumatol,* 27**,** 455-62.

KIM, J. S., PARK, Z. Y., YOO, Y. J., YU, S. S. & CHUN, J. S. 2005. p38 kinase mediates nitric oxide-induced apoptosis of chondrocytes through the inhibition of protein kinase C zeta by blocking autophosphorylation. *Cell Death Differ,* 12**,** 201-12.

KNIGHT, R. A., CHEN-SCARABELLI, C., YUAN, Z., MCCAULEY, R. B., DI REZZE, J., SCARABELLI, G. M., TOWNSEND, P. A., LATCHMAN, D., SARAVOLATZ, L., FAGGIAN, G., MAZZUCCO, A., CHOWDREY, H. S., STEPHANOU, A. & SCARABELLI, T. M. 2008. Cardiac release of urocortin precedes the occurrence of irreversible myocardial damage in the rat heart exposed to ischemia/reperfusion injury. *FEBS Lett,* 582**,** 984-90.

KOOB, G. F. & HEINRICHS, S. C. 1999. A role for corticotropin releasing factor and urocortin in behavioral responses to stressors. *Brain Research,* 848**,** 141-152.

KOSTICH, W. A., CHEN, A., SPERLE, K. & LARGENT, B. L. 1998. Molecular identification and analysis of a novel human corticotropin-releasing factor (CRF) receptor: the CRF2gamma receptor. *Mol Endocrinol,* 12**,** 1077-85.

KRUIDERING, M. & EVAN, G. I. 2000. Caspase-8 in apoptosis: the beginning of "the end"? *IUBMB Life,* 50**,** 85-90.

KUHN, K., D'LIMA, D. D., HASHIMOTO, S. & LOTZ, M. 2004. Cell death in cartilage. *Osteoarthritis Cartilage,* 12**,** 1-16.

KUIZON, E., PEARCE, E. G., BAILEY, S. G., CHEN-SCARABELLI, C., YUAN, Z., ABOUNIT, K., MCCAULEY, R. B., SARAVOLATZ, L., FAGGIAN, G., MAZZUCCO, A., TOWNSEND, P. A. & SCARABELLI, T. M. 2009. Mechanisms of action and clinical implications of cardiac urocortin: a journey from the heart to the systemic circulation, with a stopover in the mitochondria. *Int J Cardiol,* 137**,** 189-94.

LATCHMAN, D. S. 2002. Urocortin. *The International Journal of Biochemistry & Cell Biology,* 34**,** 907-910.

LAWRENCE, K. M., CHANALARIS, A., SCARABELLI, T., HUBANK, M., PASINI, E., TOWNSEND, P. A., COMINI, L., FERRARI, R., TINKER, A., STEPHANOU, A., KNIGHT, R. A. & LATCHMAN, D. S. 2002. K(ATP) channel gene expression is induced by urocortin and mediates its cardioprotective effect. *Circulation,* 106**,** 1556-62.

LAWRENCE, K. M., KABIR, A. M., BELLAHCENE, M., DAVIDSON, S., CAO, X. B., MCCORMICK, J., MESQUITA, R. A., CARROLL, C. J., CHANALARIS, A., TOWNSEND, P. A., HUBANK, M., STEPHANOU, A., KNIGHT, R. A., MARBER, M. S. & LATCHMAN, D. S. 2005. Cardioprotection mediated by urocortin is dependent on PKCepsilon activation. *Faseb J,* 19**,** 831-3.

LAWRENCE, K. M., SCARABELLI, T. M., TURTLE, L., CHANALARIS, A., TOWNSEND, P. A., CARROLL, C. J., HUBANK, M., STEPHANOU, A., KNIGHT, R. A. & LATCHMAN, D. S. 2003. Urocortin protects cardiac myocytes from ischemia/reperfusion injury by attenuating calcium-insensitive phospholipase A2 gene expression. *FASEB J,* 17**,** 2313-5.

LAWRENCE, K. M., TOWNSEND, P. A., DAVIDSON, S. M., CARROLL, C. J., EATON, S., HUBANK, M., KNIGHT, R. A., STEPHANOU, A. & LATCHMAN, D. S. 2004. The cardioprotective effect of urocortin during ischaemia/reperfusion involves the prevention of mitochondrial damage. *Biochemical and Biophysical Research Communications,* 321**,** 479-486.

LEDERIS, K., LETTER, A., MCMASTER, D., MOORE, G. & SCHLESINGER, D. 1982. Complete amino acid sequence of urotensin I, a hypotensive and corticotropin-releasing neuropeptide from Catostomus. *Science,* 218**,** 162-5.

LEWIS, K., LI, C., PERRIN, M. H., BLOUNT, A., KUNITAKE, K., DONALDSON, C., VAUGHAN, J., REYES, T. M., GULYAS, J., FISCHER, W., BILEZIKJIAN, L., RIVIER, J., SAWCHENKO, P. E. & VALE, W. W. 2001. Identification of urocortin III, an additional member of the corticotropin-releasing factor (CRF)

family with high affinity for the CRF2 receptor. *Proc Natl Acad Sci U S A,* 98**,** 7570-5.

LIN, Z., WILLERS, C., XU, J. & ZHENG, M. H. 2006. The chondrocyte: biology and clinical application. *Tissue Eng,* 12**,** 1971-84.

LIVAK, K. J. & SCHMITTGEN, T. D. 2001. Analysis of relative gene expression data using real-time quantitative PCR and the 2(-Delta Delta C(T)) Method. *Methods,* 25**,** 402-8.

LOESER, R. F., SADIEV, S., TAN, L. & GOLDRING, M. B. 2000. Integrin expression by primary and immortalized human chondrocytes: evidence of a differential role for alpha1beta1 and alpha2beta1 integrins in mediating chondrocyte adhesion to types II and VI collagen. *Osteoarthritis Cartilage,* 8**,** 96-105.

LOO, D. T. & RILLEMA, J. R. 1998. Measurement of cell death. *Methods Cell Biol,* 57**,** 251-64.

LOPEZ-ARMADA, M. J., CARAMES, B., LIRES-DEAN, M., CILLERO-PASTOR, B., RUIZ-ROMERO, C., GALDO, F. & BLANCO, F. J. 2006. Cytokines, tumor necrosis factor-alpha and interleukin-1beta, differentially regulate apoptosis in osteoarthritis cultured human chondrocytes. *Osteoarthritis Cartilage,* 14**,** 660-9.

LORENZ, H. & RICHTER, W. 2006. Osteoarthritis: Cellular and molecular changes in degenerating cartilage. *Progress in Histochemistry and Cytochemistry,* 40**,** 135-163.

LORENZO, P., BAYLISS, M. T. & HEINEGARD, D. 1998. A novel cartilage protein (CILP) present in the mid-zone of human articular cartilage increases with age. *J Biol Chem,* 273**,** 23463-8.

LOTZ, M., BLANCO, F. J., VON KEMPIS, J., DUDLER, J., MAIER, R., VILLIGER, P. M. & GENG, Y. 1995. Cytokine regulation of chondrocyte functions. *J Rheumatol Suppl,* 43**,** 104-8.

LOTZ, M., HASHIMOTO, S. & KUHN, K. 1999. Mechanisms of chondrocyte apoptosis. *Osteoarthritis and Cartilage,* 7**,** 389-391.

LUKASHEV, M. E. & WERB, Z. 1998. ECM signalling: orchestrating cell behaviour and misbehaviour. *Trends Cell Biol,* 8**,** 437-41.

MAGNE, D., VINATIER, C., JULIEN, M., WEISS, P. & GUICHEUX, J. 2005. Mesenchymal stem cell therapy to rebuild cartilage. *Trends Mol Med,* 11**,** 519-26.

MAJNO, G. & JORIS, I. 1995. Apoptosis, oncosis, and necrosis. An overview of cell death. *Am J Pathol,* 146**,** 3-15.

MANEIRO, E., LOPEZ-ARMADA, M. J., DE ANDRES, M. C., CARAMES, B., MARTIN, M. A., BONILLA, A., DEL HOYO, P., GALDO, F., ARENAS, J. & BLANCO, F. J. 2005. Effect of nitric oxide on mitochondrial respiratory activity of human articular chondrocytes. *Ann Rheum Dis,* 64**,** 388-95.

MARTEL-PELLETIER, J., BOILEAU, C., PELLETIER, J.-P. & ROUGHLEY, P. J. 2008. Cartilage in normal and osteoarthritis conditions. *Best Practice & Research Clinical Rheumatology,* 22**,** 351-384.

MATSUKI, K., SASHO, T., NAKAGAWA, K., TAHARA, M., SUGIOKA, K., OCHIAI, N., OGINO, S., WADA, Y. & MORIYA, H. 2008. RGD peptide-induced cell death of chondrocytes and synovial cells. *J Orthop Sci,* 13**,** 524-32.

MCHUGH, P. & TURINA, M. 2006. Apoptosis and necrosis: a review for surgeons. *Surg Infect (Larchmt),* 7**,** 53-68.

MOBASHERI, A., GENT, T. C., NASH, A. I., WOMACK, M. D., MOSKALUK, C. A. & BARRETT-JOLLEY, R. 2007. Evidence for functional ATP-sensitive (KATP) potassium channels in human and equine articular chondrocytes. *Osteoarthritis and Cartilage,* 15**,** 1-8.

MONTECUCCHI, P. C. & HENSCHEN, A. 1981. Amino acid composition and sequence analysis of sauvagine, a new active peptide from the skin of Phyllomedusa sauvagei. *Int J Pept Protein Res,* 18**,** 113-20.

MOREAU, C., PROST, A.-L., DERAND, R. & VIVAUDOU, M. 2005. SUR, ABC proteins targeted by KATP channel openers. *Journal of Molecular and Cellular Cardiology,* 38**,** 951-963.

MORIYAMA, T., KAGEYAMA, K., KASAGI, Y., IWASAKI, Y., NIGAWARA, T., SAKIHARA, S. & SUDA, T. 2005. Differential regulation of corticotropin-releasing factor receptor type 1 (CRF1 receptor) mRNA via protein kinase A and mitogen-activated protein kinase pathways in rat anterior pituitary cells. *Mol Cell Endocrinol,* 243**,** 74-9.

MURAMATSU, Y., FUKUSHIMA, K., IINO, K., TOTSUNE, K., TAKAHASHI, K., SUZUKI, T., HIRASAWA, G., TAKEYAMA, J., ITO, M., NOSE, M., TASHIRO, A., HONGO, M., OKI, Y., NAGURA, H. & SASANO, H. 2000. Urocortin and corticotropin-releasing factor receptor expression in the human colonic mucosa. *Peptides,* 21**,** 1799-809.

NISHIKIMI, T., MIYATA, A., HORIO, T., YOSHIHARA, F., NAGAYA, N., TAKISHITA, S., YUTANI, C., MATSUO, H., MATSUOKA, H. & KANGAWA, K. 2000. Urocortin, a member of the corticotropin-releasing factor family, in normal and diseased heart. *Am J Physiol Heart Circ Physiol,* 279**,** H3031-9.

NOTOYA, K., JOVANOVIC, D. V., REBOUL, P., MARTEL-PELLETIER, J., MINEAU, F. & PELLETIER, J. P. 2000. The induction of cell death in human osteoarthritis chondrocytes by nitric oxide is related to the production of prostaglandin E2 via the induction of cyclooxygenase-2. *J Immunol,* 165**,** 3402-10.

OKAWARA, Y., MORLEY, S. D., BURZIO, L. O., ZWIERS, H., LEDERIS, K. & RICHTER, D. 1988. Cloning and sequence analysis of cDNA for corticotropin-releasing factor precursor from the teleost fish Catostomus commersoni. *Proc Natl Acad Sci U S A,* 85**,** 8439-43.

OKI, Y. & SASANO, H. 2004. Localization and physiological roles of urocortin. *Peptides,* 25**,** 1745-9.

OKOSI, A., BRAR, B. K., CHAN, M., D'SOUZA, L., SMITH, E., STEPHANOU, A., LATCHMAN, D. S., CHOWDREY, H. S. & KNIGHT, R. A. 1998. Expression and protective effects of urocortin in cardiac myocytes. *Neuropeptides,* 32**,** 167-171.

PARKES, D. G. & MAY, C. N. 2000. Urocortin: A Novel Player in Cardiac Control. *News Physiol Sci,* 15**,** 264-268.

PARKES, D. G., WEISINGER, R. S. & MAY, C. N. 2001. Cardiovascular actions of CRH and urocortin: an update. *Peptides,* 22**,** 821-7.

PERRIN, M. H., GRACE, C. R., RIEK, R. & VALE, W. W. 2006. The three-dimensional structure of the N-terminal domain of corticotropin-releasing factor receptors: sushi domains and the B1 family of G protein-coupled receptors. *Ann N Y Acad Sci,* 1070**,** 105-19.

PESTA, A. 2007. *The effect of matrix components and the urocortin family of peptides on chondrocyte survival* PhD, University of Westminster.

PETRAGLIA, F., FLORIO, P., GALLO, R., SIMONCINI, T., SAVIOZZI, M., DI BLASIO, A. M., VAUGHAN, J. & VALE, W. 1996. Human placenta and fetal membranes express human urocortin mRNA and peptide. *J Clin Endocrinol Metab,* 81**,** 3807-10.

PETSA, A. 2007. *The Effect of Matrix components and the Urocortin family of peptides on chondrocyte survival.* PhD thesis, University of Westminster.

PFAFFL, M. W. 2001. A new mathematical model for relative quantification in real-time RT-PCR. *Nucleic Acids Res,* 29**,** e45.

PISARCHIK, A. & SLOMINSKI, A. T. 2001. Alternative splicing of CRH-R1 receptors in human and mouse skin: identification of new variants and their differential expression. *FASEB J,* 15**,** 2754-6.

POOLE, A. R., KOBAYASHI, M., YASUDA, T., LAVERTY, S., MWALE, F., KOJIMA, T., SAKAI, T., WAHL, C., EL-MAADAWY, S., WEBB, G., TCHETINA, E. & WU, W. 2002. Type II collagen degradation and its regulation in articular cartilage in osteoarthritis. *Ann Rheum Dis,* 61 Suppl 2**,** ii78-81.

POOLE, C. A. 1997. Articular cartilage chondrons: form, function and failure. *J Anat,* 191 (Pt 1)**,** 1-13.

PROSKURYAKOV, S. Y., KONOPLYANNIKOV, A. G. & GABAI, V. L. 2003. Necrosis: a specific form of programmed cell death? *Exp Cell Res,* 283**,** 1-16.

REYES, T. M., LEWIS, K., PERRIN, M. H., KUNITAKE, K. S., VAUGHAN, J., ARIAS, C. A., HOGENESCH, J. B., GULYAS, J., RIVIER, J., VALE, W. W. & SAWCHENKO, P. E. 2001. Urocortin II: a member of the corticotropin-releasing factor (CRF) neuropeptide family that is selectively bound by type 2 CRF receptors. *Proc Natl Acad Sci U S A,* 98**,** 2843-8.

ROACH, H. I., AIGNER, T., SODER, S., HAAG, J. & WELKERLING, H. 2007. Pathobiology of osteoarthritis: pathomechanisms and potential therapeutic targets. *Curr Drug Targets,* 8**,** 271-82.

ROUGHLEY, P. J. 2001. Articular cartilage and changes in arthritis: noncollagenous proteins and proteoglycans in the extracellular matrix of cartilage. *Arthritis Res,* 3**,** 342-7.

RUIZ-ROMERO, C., LOPEZ-ARMADA, M. J. & BLANCO, F. J. 2005. Proteomic characterization of human normal articular chondrocytes: a novel tool for the study of osteoarthritis and other rheumatic diseases. *Proteomics,* 5**,** 3048-59.

SANDELL, L. J. & AIGNER, T. 2001. Articular cartilage and changes in arthritis. An introduction: cell biology of osteoarthritis. *Arthritis Res,* 3**,** 107-13.

SCAFFIDI, C., FULDA, S., SRINIVASAN, A., FRIESEN, C., LI, F., TOMASELLI, K. J., DEBATIN, K. M., KRAMMER, P. H. & PETER, M. E. 1998. Two CD95 (APO-1/Fas) signaling pathways. *EMBO J,* 17**,** 1675-87.

SCARABELLI, T. M., PASINI, E., FERRARI, G., FERRARI, M., STEPHANOU, A., LAWRENCE, K., TOWNSEND, P., CHEN-SCARABELLI, C., GITTI, G., SARAVOLATZ, L., LATCHMAN, D., KNIGHT, R. A. & GARDIN, J. M. 2004. Warm blood cardioplegic arrest induces mitochondrial-mediated cardiomyocyte apoptosis associated with increased urocortin expression in viable cells. *J Thorac Cardiovasc Surg,* 128**,** 364-71.

SCHMITTGEN, T. D. & LIVAK, K. J. 2008. Analyzing real-time PCR data by the comparative C(T) method. *Nat Protoc,* 3**,** 1101-8.

SCHOEFFTER, P., FEUERBACH, D., BOBIRNAC, I., GAZI, L. & LONGATO, R. 1999. Functional, endogenously expressed corticotropin-releasing factor receptor type 1 (CRF1) and CRF1 receptor mRNA expression in human neuroblastoma SH-SY5Y cells. *Fundam Clin Pharmacol,* 13**,** 484-9.

SCHULTZ, D. R. & HARRINGTON, W. J., JR. 2003. Apoptosis: programmed cell death at a molecular level. *Semin Arthritis Rheum,* 32**,** 345-69.

SCHULZE-OSTHOFF, K., FERRARI, D., LOS, M., WESSELBORG, S. & PETER, M. E. 1998. Apoptosis signaling by death receptors. *Eur J Biochem,* 254**,** 439-59.

SEINO, S. 1999. ATP-sensitive potassium channels: a model of heteromultimeric potassium channel/receptor assemblies. *Annu Rev Physiol,* 61**,** 337-62.

SEINO, S. & MIKI, T. 2003. Physiological and pathophysiological roles of ATP-sensitive K+ channels. *Prog Biophys Mol Biol,* 81**,** 133-76.

SHI, N.-Q., YE, B. & MAKIELSKI, J. C. 2005. Function and distribution of the SUR isoforms and splice variants. *Journal of Molecular and Cellular Cardiology,* 39**,** 51-60.

SKELTON, K. H., OWENS, M. J. & NEMEROFF, C. B. 2000. The neurobiology of urocortin. *Regul Pept,* 93**,** 85-92.

SLOMINSKI, A., ROLOFF, B., CURRY, J., DAHIYA, M., SZCZESNIEWSKI, A. & WORTSMAN, J. 2000. The skin produces urocortin. *J Clin Endocrinol Metab,* 85**,** 815-23.

SLOMINSKI, A., WORTSMAN, J., PISARCHIK, A., ZBYTEK, B., LINTON, E. A., MAZURKIEWICZ, J. E. & WEI, E. T. 2001. Cutaneous expression of corticotropin-releasing hormone (CRH), urocortin, and CRH receptors. *Faseb J,* 15**,** 1678-93.

SPINA, M., MERLO-PICH, E., CHAN, R. K., BASSO, A. M., RIVIER, J., VALE, W. & KOOB, G. F. 1996. Appetite-suppressing effects of urocortin, a CRF-related neuropeptide. *Science,* 273**,** 1561-4.

STENZEL-POORE, M. P., HELDWEIN, K. A., STENZEL, P., LEE, S. & VALE, W. W. 1992. Characterization of the genomic corticotropin-releasing factor (CRF) gene from Xenopus laevis: two members of the CRF family exist in amphibians. *Mol Endocrinol,* 6**,** 1716-24.

SUDA, T., KAGEYAMA, K., SAKIHARA, S. & NIGAWARA, T. 2004. Physiological roles of urocortins, human homologues of fish urotensin I, and their receptors. *Peptides,* 25**,** 1689-1701.

SUZUKI, M., SAITO, T., SATO, T., TAMAGAWA, M., MIKI, T., SEINO, S. & NAKAYA, H. 2003. Cardioprotective effect of diazoxide is mediated by activation of sarcolemmal but not mitochondrial ATP-sensitive potassium channels in mice. *Circulation,* 107**,** 682-5.

TAKACS-BUIA, L., IORDACHEL, C., EFIMOV, N., CALOIANU, M., MONTREUIL, J. & BRATOSIN, D. 2008. Pathogenesis of osteoarthritis: chondrocyte replicative senescence or apoptosis? *Cytometry B Clin Cytom,* 74**,** 356-62.

TAKAHASHI, K., TOTSUNE, K., MURAKAMI, O. & SHIBAHARA, S. 2004. Urocortins as cardiovascular peptides. *Peptides,* 25**,** 1723-1731.

TAKAHASHI, K., TOTSUNE, K., SONE, M., MURAKAMI, O., SATOH, F., ARIHARA, Z., SASANO, H., IINO, K. & MOURI, T. 1998. Regional Distribution of Urocortin-like Immunoreactivity and Expression of Urocortin mRNA in the Human Brain. *Peptides,* 19**,** 643-647.

TAKAHASHI, L. K. 2001. Role of CRF(1) and CRF(2) receptors in fear and anxiety. *Neurosci Biobehav Rev,* 25**,** 627-36.

TAKIGAWA, M., TAJIMA, K., PAN, H. O., ENOMOTO, M., KINOSHITA, A., SUZUKI, F., TAKANO, Y. & MORI, Y. 1989. Establishment of a clonal human chondrosarcoma cell line with cartilage phenotypes. *Cancer Res,* 49**,** 3996-4002.

TAMATANI, M., OGAWA, S., NIITSU, Y. & TOHYAMA, M. 1998. Involvement of Bcl-2 family and caspase-3-like protease in NO-mediated neuronal apoptosis. *J Neurochem,* 71**,** 1588-96.

TAO, J. & LI, S. 2005a. Effects of urocortin via ion mechanisms or CRF receptors? *Biochemical and Biophysical Research Communications,* 336**,** 731-736.

TAO, J. & LI, S. 2005b. Urocortin: A cardiac protective peptide? *Biochemical and Biophysical Research Communications,* 332**,** 923-926.

TAO, J., XU, H. E., YANG, C., LIU, C.-N. & LI, S. 2004. Effect of urocortin on L-type calcium currents in adult rat ventricular myocytes. *Pharmacological Research,* 50**,** 471-476.

TERUI, K., HIGASHIYAMA, A., HORIBA, N., FURUKAWA, K. I., MOTOMURA, S. & SUDA, T. 2001. Coronary vasodilation and positive inotropism by urocortin in the isolated rat heart. *J Endocrinol,* 169**,** 177-83.

THENET, S., BENYA, P. D., DEMIGNOT, S., FEUNTEUN, J. & ADOLPHE, M. 1992. SV40-immortalization of rabbit articular chondrocytes: alteration of differentiated functions. *J Cell Physiol,* 150**,** 158-67.

THUONG-GUYOT, M., DOMARLE, O., POCIDALO, J. J. & HAYEM, G. 1994. Effects of fluoroquinolones on cultured articular chondrocytes flow cytometric analysis of free radical production. *J Pharmacol Exp Ther,* 271**,** 1544-9.

TOEGEL, S., HUANG, W., PIANA, C., UNGER, F. M., WIRTH, M., GOLDRING, M. B., GABOR, F. & VIERNSTEIN, H. 2007. Selection of reliable reference genes for qPCR studies on chondroprotective action. *BMC Mol Biol,* 8**,** 13.

TU, H., KASTIN, A. J. & PAN, W. 2007. Corticotropin-releasing hormone receptor (CRHR)1 and CRHR2 are both trafficking and signaling receptors for urocortin. *Mol Endocrinol,* 21**,** 700-11.

USHMOROV, A., RATTER, F., LEHMANN, V., DROGE, W., SCHIRRMACHER, V. & UMANSKY, V. 1999. Nitric-oxide-induced apoptosis in human leukemic lines requires mitochondrial lipid degradation and cytochrome C release. *Blood,* 93**,** 2342-52.

VALE, W., SPIESS, J., RIVIER, C. & RIVIER, J. 1981. Characterization of a 41-residue ovine hypothalamic peptide that stimulates secretion of corticotropin and beta-endorphin. *Science,* 213**,** 1394-7.

VALE, W., VAUGHN, J. & PERRIN, M. 1997. Corticotropin-releasing factor (CRF) family of ligands and their receptors. *The Endocrinoligist,* 7**,** S3-S9.

VAUGHAN, J., DONALDSON, C., BITTENCOURT, J., PERRIN, M. H., LEWIS, K., SUTTON, S., CHAN, R., TURNBULL, A. V., LOVEJOY, D., RIVIER, C. & ET AL. 1995. Urocortin, a mammalian neuropeptide related to fish urotensin I and to corticotropin-releasing factor. *Nature,* 378**,** 287-92.

WANG, J. & LI, S. 2007. Corticotropin-releasing factor family and its receptors: tumor therapeutic targets? *Biochem Biophys Res Commun,* 362**,** 785-8.

WANG, L., VERBRUGGEN, G., ALMQVIST, K. F., ELEWAUT, D., BRODDELEZ, C. & VEYS, E. M. 2001. Flow cytometric analysis of the human articular chondrocyte phenotype in vitro. *Osteoarthritis Cartilage,* 9**,** 73-84.

WONG, M. L. & MEDRANO, J. F. 2005. Real-time PCR for mRNA quantitation. *Biotechniques,* 39**,** 75-85.

WROBLEWSKI, F. & LADUE, J. S. 1955. Lactic dehydrogenase activity in blood. *Proc Soc Exp Biol Med,* 90**,** 210-3.

YOKOSHIKI, H., SUNAGAWA, M., SEKI, T. & SPERELAKIS, N. 1998. ATP-sensitive K+ channels in pancreatic, cardiac, and vascular smooth muscle cells. *Am J Physiol,* 274**,** C25-37.

YUAN, J. S., REED, A., CHEN, F. & STEWART, C. N., JR. 2006. Statistical analysis of real-time PCR data. *BMC Bioinformatics,* 7**,** 85.

ZHAO, L., DONALDSON, C. J., SMITH, G. W. & VALE, W. W. 1998. The structures of the mouse and human urocortin genes (Ucn and UCN). *Genomics,* 50**,** 23-33.

ZIEGLER, U. & GROSCURTH, P. 2004. Morphological features of cell death. *News Physiol Sci,* 19**,** 124-8.

ZMIJEWSKI, M. A. & SLOMINSKI, A. T. 2010. Emerging role of alternative splicing of CRF1 receptor in CRF signaling. *Acta Biochim Pol,* 57**,** 1-13.